Terms and Conditions of Use of Digitised Theses from Trinity College Library Dublin

Copyright statement

All material supplied by Trinity College Library is protected by copyright (under the Copyright and Related Rights Act, 2000 as amended) and other relevant Intellectual Property Rights. By accessing and using a Digitised Thesis from Trinity College Library you acknowledge that all Intellectual Property Rights in any Works supplied are the sole and exclusive property of the copyright and/or other IPR holder. Specific copyright holders may not be explicitly identified. Use of materials from other sources within a thesis should not be construed as a claim over them.

A non-exclusive, non-transferable licence is hereby granted to those using or reproducing, in whole or in part, the material for valid purposes, providing the copyright owners are acknowledged using the normal conventions. Where specific permission to use material is required, this is identified and such permission must be sought from the copyright holder or agency cited.

Liability statement

By using a Digitised Thesis, I accept that Trinity College Dublin bears no legal responsibility for the accuracy, legality or comprehensiveness of materials contained within the thesis, and that Trinity College Dublin accepts no liability for indirect, consequential, or incidental, damages or losses arising from use of the thesis for whatever reason. Information located in a thesis may be subject to specific use constraints, details of which may not be explicitly described. It is the responsibility of potential and actual users to be aware of such constraints and to abide by them. By making use of material from a digitised thesis, you accept these copyright and disclaimer provisions. Where it is brought to the attention of Trinity College Library that there may be a breach of copyright or other restraint, it is the policy to withdraw or take down access to a thesis while the issue is being resolved.

Access Agreement

By using a Digitised Thesis from Trinity College Library you are bound by the following Terms & Conditions. Please read them carefully.

I have read and I understand the following statement: All material supplied via a Digitised Thesis from Trinity College Library is protected by copyright and other intellectual property rights, and duplication or sale of all or part of any of a thesis is not permitted, except that material may be duplicated by you for your research use or for educational purposes in electronic or print form providing the copyright owners are acknowledged using the normal conventions. You must obtain permission for any other use. Electronic or print copies may not be offered, whether for sale or otherwise to anyone. This copy has been supplied on the understanding that it is copyright material and that no quotation from the thesis may be published without proper acknowledgement.

The identification of novel peptides using phage display with the potential for use in breast cancer therapy.

A thesis submitted to Trinity College Dublin for the degree of Doctor of Philosophy

2011

by Christina Siebke

<u>Declaration</u>

I declare that this thesis has not been submitted as an exercise for a degree at this or any other University. This thesis is based entirely on my own work. I agree that the Library may lend or copy this thesis upon request.

Christina Siebke

Summary

Breast cancer is a leading cause of cancer-related mortality in women. Current treatments for breast cancer include surgery, radiotherapy, chemotherapy and hormone therapy. The recent development of Herceptin has added a new category of treatments available for breast cancer, in the form of monoclonal antibodies which are aimed at targeting specific proteins which are over-expressed or altered in cancer. However there remains a need for the development of more specifically targeted breast cancer treatments. This project aimed to use phage-peptide display libraries to identify novel peptides that could bind specifically to breast tumour cells. Phage-peptide display libraries consist of genetically modified bacteriophage (phage) which have been engineered to express a vast array of different peptides on their surface. The display of these peptides on the phage surface allows for interaction with other proteins. By incubating a target protein of interest with a phage library, peptides with binding affinity to the target protein can be isolated and amplified. This step can be repeated numerous times to allow for the identification of peptides with high binding affinity for the target protein and this process is termed bio-panning.

Three main approaches were employed to identify peptides specific for breast cancer cells. Firstly, bio-panning was carried out on live breast cells *in vitro* which led to the identification of a number of highly selected peptides. A second approach combined *in vivo* and *in vitro* bio-panning with the aim of identifying peptides with tumour-homing abilities. A small set of peptides were reproducibly identified from these two bio-panning approaches, which had high affinity for breast tumour cells as demonstrated by immuno-fluorescent cytology, enzyme-linked immunosorbent assays and flow cytometry. However these peptides also had high affinity for non-tumour cells and did not demonstrate tumour or tissue specificity. A third approach was pursued to identify peptides which could specifically bind

breast tumour cells. This involved purifying a group of proteins known to be associated with tumour antigens. Heat shock protein-70 (HSP70) represents a family of proteins that are known to be associated with peptide complexes (HSP70-PC's) containing tumour antigens within tumour cells. HSP70-PC's purified from breast tumour cells were therefore used in a bio-panning experiment to identify peptides that could bind with high affinity and specificity to breast tumour antigens. The result was the successful identification of a set of peptides capable of binding tumour-derived HSP70-PC's (termed HSP70-PC recognizers). One of these peptides, called cISTc, was further characterized and was shown to localize to the same areas as HSP70 in patient breast tumour tissues but was less abundant or absent in the other tumour tissues tested when compared to HSP70. This peptide may therefore have potential for use as a breast tumour biomarker.

Tumour antigens can arise from over- or altered expression of normal proteins, which can allow for an immune response against a cancer. Therefore identification of novel tumour antigens and methods of stimulating anti-tumour immune responses are essential for the generation of novel therapeutic agents for use in cancer immunotherapy. Tumour antigen mimic epitopes (mimotopes) are small molecules, often peptides, which are capable of eliciting specific anti-tumour immune responses. The HSP70-PC recognizer peptides identified earlier bind to putative breast tumour antigens. Therefore any peptide capable of binding to these recognizers may be a molecular mimic of the original tumour antigen. Mirror image phage display was employed whereby the newly identified HSP70-PC recognizers were used as bait in a new bio-panning experiment to identify peptides that may be molecular mimics (or mirror images) of the original tumour antigens. This mirror image phage display methodology led to the identification of three novel breast tumour mimotopes called TNT, LAP and LSS, which are capable of stimulating a human immune response *in vitro*. Therefore these mimotopes may have potential for use in future cancer immunotherapy.

For my parents
Heinz & Brigitte Siebke

Acknowledgements

Conferences & presentations

2008: 4th All-Ireland Cancer Conference held by the Ireland-Northern Ireland-National Cancer Institute Cancer Consortium at the Four Seasons Hotel, Dublin 4.

Poster presentation.

2007: EMBO Practical Course on: Tissue Microarrays and Image Analysis at the Conway Institute, University College Dublin, Dublin 4.

Oral presentation and practical skills workshop.

2007: 5th International Cancer Conference of St. James's Hospital at the Shelbourne Hotel, Dublin 2.

Attended.

Table of contents

List of tables

Chapter 5: Generation and characterization of putative tumour antigen mimic peptides

List of figures

Chapter 5: Generation and characterization of putative tumour antigen mimic peptides

List of abbreviations

A	Alanine
ADP	Adenosine diphosphate
APC	Antigen-presenting cell
ATP	Adenosine triphosphate
BSA	Bovine serum albumin
C	Cysteine
CAR	Chimeric antigen receptor
C.I.	Confidence interval
CNA	Copy number alteration
D	Aspartic acid
DAB	3,3'-diaminobenzidine tetrahydrochloride
DAPI	4',6-diamidino-2-phenylindole
DC	Dendritic cells
DNA	Deoxyribonucleic acid
DPBS	Dulbecco's phosphate buffered saline
DSBR	Double-strand break repair
DTT	Dithiothreitol
E	Glutamic acid
E.coli	*Escherichia coli*
ECD	N-(3-dimethylaminopropyl)-N′-ethylcarbodiimide hydrochloride
EGFR	Epidermal growth factor receptor
ELISA	Enzyme linked immunosorbent assay
ER	Oestrogen receptor
F	Phenylalanine
Fab'	Fragment antigen binding
FDA	Food and Drug Administration
FITC	Fluorescein isothiocyanate
FFPE	Formalin-fixed paraffin embedded
FPLC	Fast purification liquid chromatography
G	Glycine

GM-CSF	Granulocyte macrophage colony stimulating factor
H	Histidine
H&E	Hematoxylin & eosin
HAMA	Human anti-mouse antibodies
HEPES	4-(2-hydroxyethyl)-1-piperazineethanesulfonic acid
HER-2	Human epidermal growth factor receptor 2
HPV	Human papillomavirus
hr	Human recombinant
HSP	Heat shock protein
HSP70-PC	Heat shock protein 70-peptide complexes
I	Isoleucine
IDO	Indolamine-2,3-dioxygenase
IFN	Interferon
IL	Interleukin
K	Lysine
L	Leucine
LPS	Lipopolysaccharide
M	Methionine
MALDI-TOF	Matrix-assisted laser desorption/ionization-time of flight
MHC	Major histocompatability complex
MRI	Magnetic resonance imaging
mRNA	Messenger RNA
miRNA	Micro RNA
MT	Microtiter
MUC	Mucin
MW	Molecular weight
N	Asparagine
NCRI	National Cancer Registry Ireland
NK	Natural killer cell
NKT	Natural killer T cell
P	Proline
PAP	Prostatic acid phosphatase

PBMC	Peripheral blood mononuclear cells
PBS	Phosphate-buffered saline
PCR	Polymerase chain reaction
PET	Positron emission tomography
PFA	Paraformaldehyde
PR	Progesterone receptor
Q	Glutamine
R	Arginine
RNA	Ribonucleic acid
S	Serine
scFv	Single chain fragment variable
SDS-PAGE	Sodium dodecyl sulphate polyacrylimide gel electrophoresis
SEREX	Serological analysis of recominbant cDNA expression libraries
SERPA	Serological proteome analysis
SNP	Single-nucleotide polymorphism
SPECT	Single-photon emission computed tomography
ssDNA	Single stranded DNA
T	Threonine
TAA	Tumour-associated antigen
TBS	Tris-buffered saline
TCR	T cell receptor
TGF-β	Transforming growth factor-β
TMA	Tissue microarray
TMB	3,3',5,5' tetramethylbenzidine
TNF-α	Tumour necrosis factor-α
TLR9	Toll-like receptor 9
Treg	Regulatory T cell
TSA	Tumour-specific antigen
V	Valine
W	Trytophan
WHO	World Health Organization
Y	Tyrosine

Chapter 1:

General Introduction

1.1 Cancer prevalence.

Cancer is a leading cause of death worldwide and accounted for 7.4 million deaths in 2004, according the World Health Organization (WHO, 2009). The main types leading to overall cancer mortality were lung, stomach, colorectal, liver and breast cancer. In men, lung cancer was the most frequent cause of cancer related mortality, whereas breast cancer was the leading cause in women (WHO, 2009). These trends also hold true for Ireland where, according to the National Cancer Registry Ireland (NCRI, 2009), lung cancer accounted for 22% of cancer-related deaths in men and breast cancer accounted for 17.5% of cancer-related deaths in women in 2006. Our research interest is currently focused on breast cancer due to its increasing prevalence and high rates of cancer-related mortality in women.

1.2 Causes of cancer.

Approximately 5-10% of all cancers are attributed to inherited genetic defects, whereas 90-95% are attributed to environmental factors and lifestyle (Anand et al., 2008). Cancer-related deaths can be attributed to tobacco usage (25-30%), diet (30-35%), infections (15-20%) while the remainder are related to multiple other factors including radiation, exercise, stress and environmental pollutants (Anand et al., 2008). Cancer is caused by genetic alterations in oncogenes and tumour suppressor genes and the development of cancer usually requires multiple genetic alterations.

1.2.1 Oncogenes and tumour suppressors.

Oncogenes encode proteins that consist of transcription factors, growth factor receptors, signal transducers and apoptosis regulators including c-MYC, epidermal growth factor receptor (EGFR), RAS and BCL-2, respectively (Croce, 2008). Translocations and mutations in oncogenes are believed to be initiators of oncogenesis with amplification usually occurring during disease progression (Croce, 2008). EGFR, a transmembrane protein with tyrosine kinase activity, is an example of an oncogene in which mutations or deletions of the ligand-binding domain can result in constitutive activation of the receptor leading to continuous cell growth and tumourigenesis (Croce, 2008).

Tumour suppressors are proteins with roles in cell cycle regulation, regulation of apoptosis or DNA repair and include p53 (Green and Kroemer, 2009), pRb (Classon and Harlow, 2002) and BRCA. Mutations or deletions resulting in loss of protein function can contribute to tumourigenesis. Approximately 5% of breast cancers are caused by inherited defects in tumour suppressors *BRCA1* and *BRCA2*. Germ line mutations in these genes can result in truncation or inactivation of the proteins and these mutations increase the risk of developing breast cancer by up to 80% and 50%, respectively (O'Donovan and Livingston, 2010). These proteins have critical functions in the double-strand break repair (DSBR) of DNA by homologous recombination and loss of protein function is known to result in genomic instability (O'Donovan and Livingston, 2010).

1.2.2 Genetic alterations in cancer cells.

Somatic genetic mutations are present in all cancer cells and can include base substitutions, small insertions or deletions termed "indels", rearrangements or copy number

alterations. For example, the COLO-829 melanoma cell line was identified as having 33,345 somatic base substitutions, 66 indels and 37 rearrangements (Pleasance et al., 2009). Mutations that confer a growth advantage which lead to oncogenesis have been termed "driver mutations" and mutations which have no such effect are termed "passenger mutations". The analysis of somatic mutations in cancer genomes has led to the identification of approximately 400 cancer genes (Pleasance et al., 2009).

A recent study by Ding et al (Ding et al., 2010) examined the genetic changes in a patient with basal-like breast cancer. DNA taken from the primary tumour, a brain metastasis and a xenograft derived from the primary tumour were analyzed and found to contain in total 50 novel somatic point mutations and indels in coding sequences, RNA genes and splice sites. Point mutations can be missense (codes for a different amino acid), nonsense (codes for a stop) or silent (codes for the same amino acid) and the majority of point mutations (28/50) in this study were missense mutations. One example of a missense mutation present in all three tumours was in *CSMD1* (A409S). *CSMD1* encodes a protein of unknown function but was recently identified as a novel candidate tumour suppressor due to the fact that 50% of breast cancers carry deletions in this gene which are associated with poor prognosis (Kamal et al., 2010). An indel (1bp insertion in exon 4) in *TP53* caused a frameshift mutation (Q167fs) in the DNA binding domain of p53 resulting in a truncated protein (Ding et al., 2010). p53 is a known tumour suppressor and 50% of all cancers have mutations in *TP53* (Green and Kroemer, 2009).

In addition to the 50 somatic mutations detected, Ding et al (Ding et al., 2010) also identified 28 large deletions, 6 inversions and 7 translocations. Copy number alterations (CNAs) were evident with a total of 516.5Mb amplified and 342.5Mb deleted in the primary tumour. One example of a CNA was the deletion on chromosome 4 of 46,462bp which removed the last 10 exons of *FBXW7*. FBXW7 is an ubiquitin ligase which targets several

4

proteins with roles in the regulation of cell growth and division, including cyclin E and MYC, for ubiquitin-mediated degradation (Welcker and Clurman, 2008). Mutations in FBXW7 are found in 6% of all cancers and loss of function contributes to tumourigenesis (Welcker and Clurman, 2008). Most CNAs in the primary tumour were also present in the metastasis and xenograft, however the latter two tumours also showed an increase in CNA's presumably associated with disease progression. The genomic instability observed in cancer can result in increased mutation rates, thus an individual cancer can display considerable heterogeneity.

A recent study by Moelans et al (Moelans et al., 2010) analyzed gene copy number changes in 20 breast cancer-related genes in 104 invasive breast cancers and identified c-*MYC* gene amplification in 48% of patients and *HER-2* in 28% of patients. HER-2 is another member of the EGFR family of proteins with roles in signal transduction leading to cell growth. c-*MYC* and *HER-2* amplifications were associated with a high mitotic index, with *HER-2* amplifications correlated with high histological grade while c-*MYC* amplifications were associated with large tumour size. In addition, *HER-2*/*MYC* co-amplified tumours were significantly larger than tumours with either of these amplifications.

Over-expression of oncogenes can be caused by translocations resulting in fusion genes which put the oncogene under the control of a strong promoter. One of the first examples of a translocation resulting in a fusion gene involved in cancer development was the discovery in 1983 (Battey et al., 1983) in Burkitt's lymphoma where translocation of the c-*MYC* oncogene from chromosome 8 to chromosome 14 resulted in its fusion to a highly active immunoglobulin promoter. c-MYC is an important transcription factor which regulates a number of cellular processes including cell cycle progression, cell growth, differentiation and apoptosis. Aberrant expression of c-*MYC* is known to be common in a large number of human malignancies, including breast cancer (Gonzalez and Hurley, 2010).

MicroRNAs (miRNA's) are conserved small non-coding RNA's, approximately 22 nucleotides in length, that can regulate gene expression post-transcriptionally by binding to messenger RNA's (mRNA's) and preventing their translation or resulting in their degradation. Over 700 human miRNA's have been identified, some of which have been implicated in tumourigenesis. Two examples of miRNA's implicated in breast cancer are miR-125a, a predicted tumour suppressor by its interaction with *HER-2* transcripts and miR-21, a possible oncogenic miRNA suggested to interact with transcripts from a number of tumour suppressor genes (O'Day and Lal, 2010).

1.2.3 Infectious agents and cancer.

Several infectious agents, most notably viruses, contribute to 15-20% of malignancies worldwide and these include human papillomaviruses (cervical cancer), human polyomaviruses (brain tumours), Epstein-Barr virus (lymphoma), Kaposi's sarcoma herpesvirus (Kaposi's sarcoma), hepatitis B and C viruses (liver cancer), human T-cell leukemia virus-1 (T-cell leukaemia) and *H. pylori* (gastric carcinoma) (Pagano et al., 2004). The human papillomavirus (HPV), for example, is a non-enveloped double-stranded DNA virus which infects basal epithelial cells of the skin and mucosa. There are over 100 different genotypes with a dozen of them considered "high risk" as they can cause cancer. HPV-16 and HPV-18 are the most virulent and cause approximately 70% of cervical cancers. Cervical cancer is caused by persistent infection with a high risk HPV which results in the integration of viral sequences into human DNA. The viral E6 and E7 proteins interact with tumour suppressors, p53 and pRb, promoting tumour growth and inhibiting apoptosis (de Martel and Franceschi, 2009).

1.3 Tumour antigen and biomarker discovery.

The mutation, over-expression or altered modification of oncoproteins in cancer cells can indicate disease and therefore be useful tools as cancer biomarkers. In addition, they provide possible sites for therapeutic targeting. Tumour antigens can be divided into two broad classes; tumour-specific or tumour-associated antigens (TSA's and TAA's, respectively). TSA's derive from proteins bearing a unique mutation or fusion resulting in the production of an antigen recognized as foreign by the immune system, whereas TAA's can be derived from over-expressed proteins or proteins present in altered form or location. Table 1.1 describes the different types of currently identified tumour antigens.

In 1977 Shiku et al (Shiku et al., 1977) discovered that sera from melanoma patients could react with antigens present on melanoma cells but also with normal cells. Since then a large number of auto-antibodies have been discovered which have aided the discovery of novel tumour antigens (reviewed (Reuschenbach et al., 2009; Tan et al., 2009)). A meta-analysis by Reuschenbach et al (Reuschenbach et al., 2009) showed that an average of 14% of cancer patients produce humoral responses against tumour antigens. The frequency of auto-antibody production was higher against certain antigens including HER-2 with nearly 27% of breast cancer patients producing HER-2 specific auto-antibodies compared to only 2% in healthy individuals. In 1991, T cells derived from a melanoma patient were shown to react with tumour-derived antigens and led to the identification of the MAGE-1, the first known tumour antigen to be recognized by T cells (van der Bruggen et al., 1991). Since then a large number of antigens recognized by T cells have been identified (reviewed (Renkvist et al., 2001).

Table 1.1 Types and examples of known tumour antigens.

Class	Type	Example	Tumour type
Tumour-associated antigens	Cancer-testis antigens	MAGE	Multiple, including breast carcinoma
		BAGE	Multiple, including breast carcinoma
		GAGE	Multiple, including breast carcinoma
		NY-ESO-1	Multiple, including breast carcinoma
	Differentiation antigens	MART-1	Melanoma
		GP100	Melanoma
		Prostate-specific antigen (PSA)	Prostate carcinoma
		TRP-1	Melanoma
	Over-expressed antigens	Carcinoembryonic antigen (CEA)	Multiple, including breast carcinoma
		HER-2	Multiple, including breast carcinoma
		MUC-1	Multiple, including breast carcinoma
		Survivin	Multiple, including breast carcinoma
Tumour-specific antigens	Mutation antigens	p53	Multiple, including breast carcinoma
		RAS	Multiple, including breast carcinoma
		β-catenin	Melanoma
		CDK-4	Melanoma
	Fusion antigens	BCR-ABL	Chronic myelogenous leukemia
	Viral antigens	E6 & E7 (HPV)	Cervical cancer

Ref; (Mocellin et al., 2004; Pejawar-Gaddy and Finn, 2008; Renkvist et al., 2001; Reuschenbach et al., 2009).

Serological analysis of tumour antigens by recominbant cDNA expression cloning (SEREX), serological proteome analysis (SERPA) and protein microarrays are current tools being used to identify novel tumour antigens from patient sera. SEREX involves extracting mRNAs from a tumour, synthesizing corresponding double-stranded cDNAs, inserting them into the λ phage genome and infecting *E. coli*. Recombinant proteins are subsequently expressed during the lytic phase of infection, transferred onto nitrocellulose membrane and incubated with autologous serum (from the same patient). Reactive clones are then isolated and corresponding cDNAs are sequenced (Desmetz et al., 2009). One of the first tumour antigens identified using SEREX was NY-ESO-1 (Table 1.1) whose expression is normally restricted to the testis and ovary. This antigen is expressed in multiple cancers, including breast cancer (Chen et al., 1997). One drawback of SEREX is the inability to analyze post-translationally modified proteins.

SERPA involves the separation of equivalent quantities of protein extracted from cell cultures or tumours by two-dimensional gel electrophoresis. Proteins are transferred onto membranes and probed with sera from cancer patients or healthy individuals. Proteins reactive specifically with the cancer sera are subsequently identified by mass spectrometry. Autoantibodies against heat shock protein 60 (HSP60) were recently identified in 32.6% of ductal carcinomas of the breast using SERPA (Desmetz et al., 2009). One drawback of SERPA is the requirement for sufficient amounts of cellular protein for visualization on the gels and mass spectrometry analysis.

Protein microarrays employ the use of purified or recombinant proteins, peptides or tumour lysates which are spotted onto microarrays and incubated with patient sera. A protein microarray containing 5,005 human proteins purified from insect cells was screened with sera from 30 ovarian cancer patients and 30 age-matched healthy individuals (Hudson et al.,

2007). Ninety-four antigens showed enhanced reactivity to patient sera over control sera. Lamin A/C, SSRP1 and RALBP1 were identified as potential novel ovarian biomarkers.

In addition to identifying antigens which are recognized by antibodies, antigens recognized by T cells are equally important but have been more difficult to identify. The first method, as with MAGE-1, is the purification of tumour-reactive T cells and the identification of interacting proteins. One difficulty with this approach is the low number of purified reactive T cells available. The second approach has been to elute peptides presented on the surface of tumour cells and identify them using mass spectrometry (Lemmel and Stevanovic, 2003). Drawbacks of this approach include the large quantity of cellular peptides expressed on the cell surface and the difficulty in purifying and identifying the tumour-specific peptides. The third approach utilizes bioinformatics to predict potential T cell epitopes (Rammensee et al., 1999).

1.4 Phage display and cancer.

In 1985 the method for displaying peptides on the surface of the M13 bacteriophage (phage display) was established (Smith, 1985). This is achieved by inserting DNA encoding small random peptides into the genes encoding either the major (pVIII) or minor (pIII) phage coat protein and these peptides are then expressed in 2700 or 5 copies, respectively (Sergeeva et al., 2006). A phage-peptide display library consists of billions of individual phage clones each displaying a different peptide. Phage libraries can be used to identify peptides capable of binding any target of interest in a process called "bio-panning" which is outlined in FIG. 1.1. Originally this technology was used to map epitope-binding sites of antibodies *in vitro* (Sergeeva et al., 2006) but it is now a powerful tool in identifying tumour-targeting peptides by bio-panning tumour proteins and cells *in vitro* and *in vivo* (reviewed (Deutscher, 2010)).

10

Overview of bio-panning

1. Immobilize target of interest.
2. Incubate with phage display library.
3. Wash away unbound phage.
4. Elute target-bound phage.
5. Amplify eluted phage in host *E.coli*.
6. Purify phage.
7. Repeat steps 1-6 numerous times to increase the numbers of phage displaying target-binding peptides.
8. Sequence final enriched phage pool to identify target-specific peptides.

Amplify + repeat

Sequence
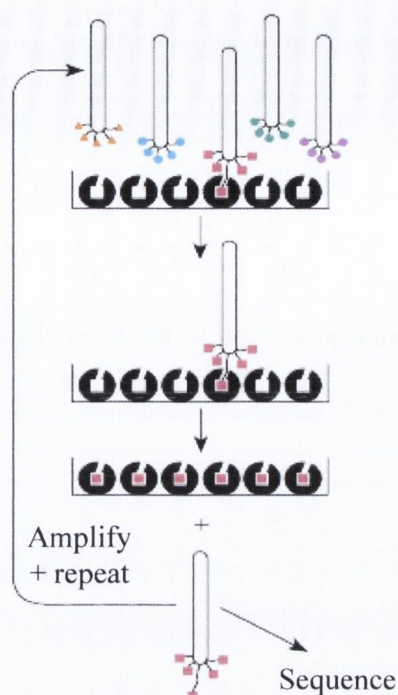
FIG.1.1 Overview of bio-panning using M13 phage-peptide display libraries.

In 1996, Renata Pasqualini and Erkki Ruoslahti documented the first ever *in vivo* bio-panning experiment where they identified peptides capable of homing to the brain and kidneys of mice (Pasqualini and Ruoslahti, 1996). This was followed by the identification of peptides that home to various other organs including the lungs, prostate and breast, which led to the subsequent identification of a number of organ-specific markers such as membrane dipeptidase, IL-11 receptor (Pasqualini et al., 2002) and aminopeptidase P (Trepel et al., 2002), respectively. Since then it has been shown that blood and lymph vessels in tumours differ from those in normal tissue and a number of tumour-homing peptides have been identified using *in vivo* phage bio-panning (Ruoslahti, 2002). These homing peptides gave rise to the identification of tumour-specific molecular markers or "vascular zip codes". One peptide called RGD-4C was shown to bind the $\alpha v \beta 3$ and $\alpha v \beta 5$ integrins, which are over-

expressed in some tumour vasculature (Ruoslahti, 2002). These integrins are now known to be markers of angiogenesis, the growth of new blood vessels which is essentially absent from most adult tissues except in cases of tissue damage (Ruoslahti, 2002). A peptide which specifically binds to tumour lymphatics, LyP-1, has been identified (Laakkonen et al., 2004) and more recently a number of peptides capable of binding to lymphatics in prostate tumours and pre-malignant lesions have also been identified (Zhang et al., 2006).

1.5 Cancer immunology.

In 1909 Paul Ehrlich suggested that the immune system could respond to tumour cells and this was later developed by Burnet and Thomas into the theory of immunosurveillance which states that the immune system can recognize malignant cells as foreign and eliminate them (Dunn et al., 2004). It was shown using numerous studies in knock-out mice that interferons (IFN's), perforin and lymphocytes were essential for tumour immunity (Dunn et al., 2004). This theory was supported in humans by evidence that transplant patients, who require immunosuppressive drugs to prevent graft rejection, had much higher rates of cancer than healthy individuals (Finn, 2008). Additionally clinical findings of spontaneous regressions of melanoma, gastrointestinal, lung and breast cancers lent further support to this theory (Srinivasan, 2008). The subsequent identification of both humoral and cellular immune responses in cancer patients further validated this theory. The theory of immunosurveillance has since been furthered developed into the concept of immunoediting. Immunoediting is defined by the three "E's"; elimination, equilibrium and escape (Dunn et al., 2006; Dunn et al., 2004) and is summarized in FIG. 1.2.
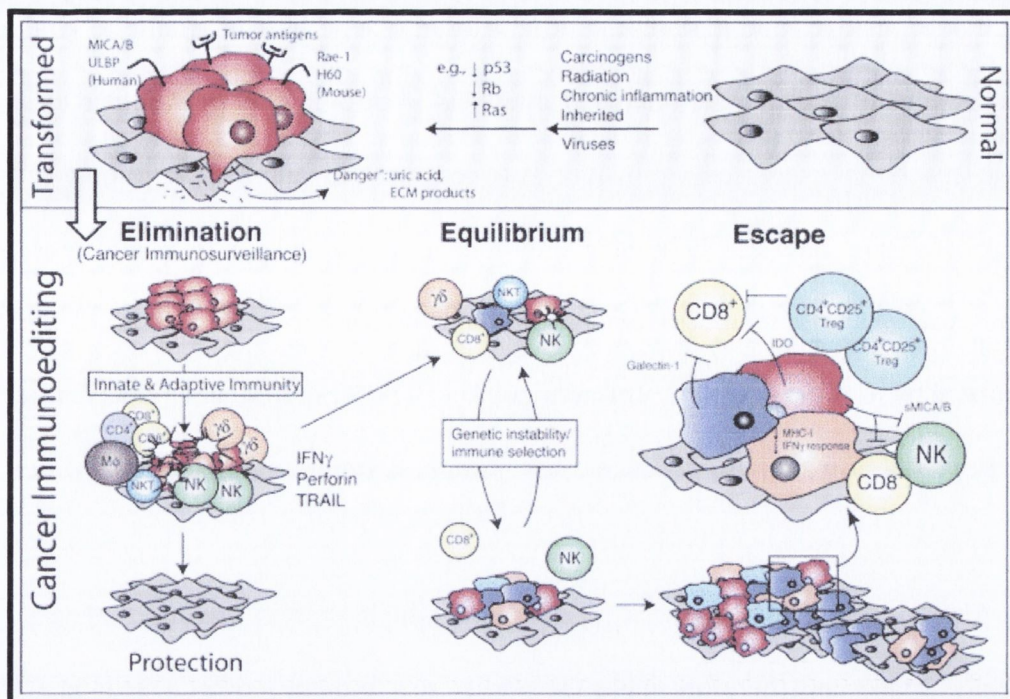
FIG.1.2 The three E's of cancer immunoediting. Taken from (Schreiber, 2005).

The first step of immunoediting is elimination which encompasses the original theory of immunosurveillance involving recognition of tumours by the innate (NK, NKT and macrophages) and/or adaptive (CD4+ and CD8+ T cells) immune systems resulting in tumour clearance. In the event that not all tumour cells are destroyed, a small number of tumour cells may persist in a stage termed equilibrium. During this stage, tumour cells may be continually bombarded by the immune system and are therefore not able to fully establish but may persist for many years. Immune escape is the final stage which allows the development of the tumour and can arise due to immune exhaustion, inhibition or the emergence of tumour variants established by mutation.

Most cells in the body express the Major Histocompatability Complex (MHC) Class I on their cell surface and proteins produced endogenously are routinely processed into peptides and presented on the cell surface by MHC Class I molecules for recognition by CD8+ T cells (Mittendorf et al., 2007). The peptides presented by MHC Class I molecules are usually

13

between 8-10 residues and the presentation of foreign peptides (for example, viral antigens or TSA's) results in lymphocyte-mediated cytolysis (Schroter, 2008). Another class of MHC, MHC Class II, is expressed exclusively on professional antigen-presenting cells (APC's) (Mittendorf et al., 2007). APC's have important roles in phagocytosis and present peptides (approximately 12-25 residues) of extracellular origin on MHC Class II molecules for recognition by CD4+ T cells (Schroter, 2008). CD4+ T cells can induce antigen-specific antibody production and also produce other immuno-stimulatory molecules (Mittendorf et al., 2007).

Dendritic cells (DC's) are a type of APC which express both MHC Class I and II on their cell surface and therefore have the ability to stimulate both CD8+ and CD4+ T cell activity (Weiner et al., 2009). Dying tumour cells, tumour proteins or peptides can be taken up by DC's and presented on either MHC Class I or II or both (Finn, 2008). If the DC's are activated by an appropriate danger signal (Fong and Engleman, 2000), they can induce both humoral and cellular immune responses (Finn, 2008). Some tumours may be recognized by innate immune cells including macrophages, NK and NKT cells, which can result in immediate tumour cell destruction. Innate immune activity can also result in the stimulation of subsequent adaptive responses. A model of tumour elimination by the immune system is shown in FIG.1.3.

Mechanisms of tumour escape often involve mutations affecting the cell surface expression of immunogenic proteins with 40-90% of human tumours showing full or partial loss of MHC Class I cell surface expression (Dunn et al., 2004). Tumours have since been shown to evade the immune system by producing immunosuppressive molecules such as transforming growth factor β (TGF-β), soluble FAS ligand or indolamine-2,3-dioxygenase (IDO) (Finn, 2008). Both TGF-β and FAS can induce T cell death in a process usually reserved for preventing auto-immunity and IDO is an enzyme that promotes tolerance to self-

14

antigens (Lu and Finn, 2007). Regulatory T cells (Tregs) are a subset of CD4+ T cells that are also involved in ensuring immune tolerance to self antigens, but have been shown to be present in higher concentrations in tumours, including breast cancer (Anderson, 2009). Tregs can suppress immune responses by producing immuno-suppressive cytokines including TGF-β and IL-10 (Finn, 2008).
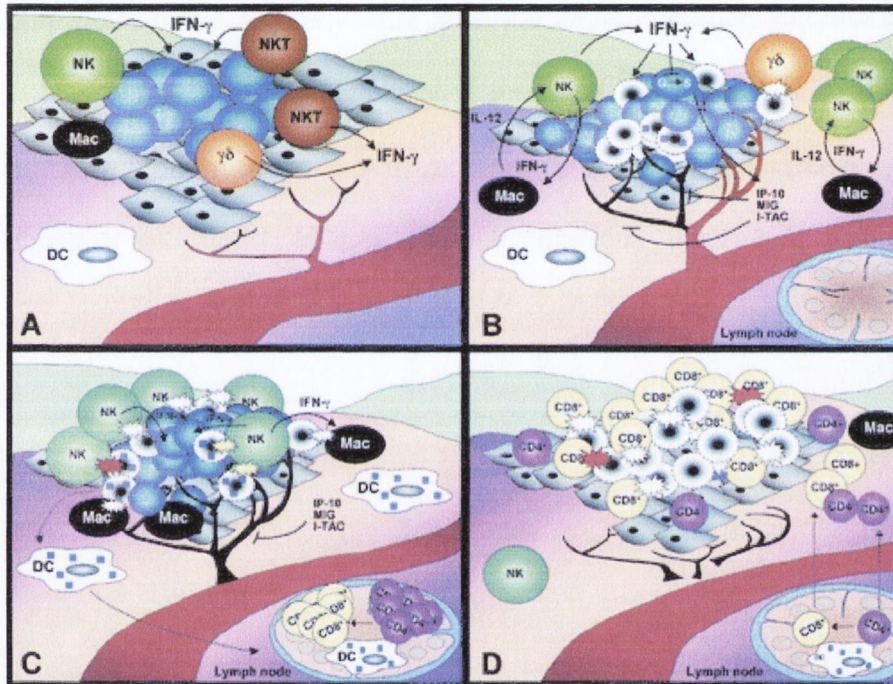
FIG.1.3 Model for tumour elimination by the immune system. Taken from (Dunn et al, 2004). Panel A represents the initiation of the response, where innate immune cells recognize and attack a tumour (blue). In panel B, IFN-γ produced by the innate immune cells starts a cascade of innate immune reactions that result in some tumour cell death (white). In panel C, the innate immune responses trigger the adaptive response wherein dead tumour cells are ingested by DCs, which migrate to the draining lymph node and present antigen to naive CD4+ and CD8+ T cells. In panel D, tumour-specific CD4+ and CD8+ T cells home to the tumour along a chemokine gradient where they recognize and destroy tumor cells expressing the tumour antigens.

1.6 Heat shock proteins (HSP) and cancer.

HSP's are ubiquitous in nature and are comprised of highly conserved chaperone proteins with functions in protein stability, folding, degradation and transport, in addition to roles in the regulation of apoptosis (Galluzzi et al., 2009). Originally identified as being upregulated by heat shock, they are now known to be upregulated by virtually any type of stress with roles in maintaining cell survival. HSP's are classified into families by size, for example HSP70 are a group of HSP's all approximately 70kDa in size. The HSP70 family is the best characterized and all members are known to contain an N-terminal nucleotide binding domain and a C-terminal substrate binding domain which are separated by a short hydrophobic linker (Evans et al., 2010). When bound to ATP the substrate binding domain is in a low-affinity conformation, however upon ATP hydrolysis to ADP, substrate binding affinity is enhanced. Members of the HSP70 family include; HSP72 and heat shock cognate 70 (HSC70) which are present in the cytosol and nucleus, glucose regulated protein 78 (GRP78) present in the endoplasmic reticulum and mtHSP70 located in the mitochondria (Evans et al., 2010).

A key discovery of the roles of HSP's in cancer came from the work of Pramod Srivastava who demonstrated that autologous tumour-derived HSP preparations, comprised of either the HSP70 or HSP90 family, could inhibit tumour growth, reduce metastases and prolong the life span of mice induced with a variety of different cancers (Tamura et al., 1997). Furthermore, HSP's purified from a given cancer could confer protective immunity specific to that cancer, whereas HSP's purified from normal tissues could not (Przepiorka and Srivastava, 1998). It was later discovered that peptides associated with the HSP's were responsible for the tumour-specific immunity, and that HSP's alone could not induce the same response (Przepiorka and Srivastava, 1998).

16

HSP70 and HSP90 are believed to transport immunogenic peptides to the cell surface for presentation by MHC Class I (Przepiorka and Srivastava, 1998) and have been shown to elicit CD8+ cytotoxic T cell activity (Srivastava et al., 1998). Furthermore, HSP's have been shown to directly bind APC's via a dedicated receptor, CD91, which results in uptake of the HSP complexes and re-presentation of their associated peptides on both MHC Class I and II molecules (Srivastava, 2002). This interaction has been shown to directly activate DC's and promote both CD4+ and CD8+ anti-tumour responses (Pejawar-Gaddy and Finn, 2008). Therefore in addition to HSP's presenting tumour antigens, they also have potent adjuvant properties. HSP's alone (without associated peptides) have been shown to activate innate immune responses by their interaction with APC's which subsequently produce pro-inflammatory cytokines and chemokines and upregulate MHC Class I on their cell surface (Chen and Cao, 2010).

The upregulation of the *HSP* genes during stress is induced by the transcription factor heat shock factor 1 (HSF1), however the activity of HSF1 can be "hijacked" in cancer cells and over-expression of HSP's can be found in many cancers including breast cancer (Calderwood, 2010). Over-expression of HSP70 is thought to confer a growth advantage by blocking both caspase-dependent and caspase-independent apoptotic pathways (Evans et al., 2010). Over-expression of HSP70 and HSP90 has been shown in several tumours and are associated with increased resistance to chemotherapeutics and poor prognosis (Galluzzi et al., 2009). Therefore HSP's are a double-edged sword, on one side their ability to present tumour antigens both intracellularly to the cell surface and extracellularly to APC's can result in adaptive and innate anti-tumour immune responses, whereas intracellular over-expression of HSP's can be detrimental due their anti-apoptotic effects.

1.7 Cancer treatment and immunotherapy.

Current treatments for cancer include surgery, radiotherapy, chemotherapy and hormonal therapy. Major drawbacks of current cancer therapies are their side effects and low tumour specificity. In fact most chemotherapy agents don't preferentially locate to tumour sites, and in some cases as little as 5-10% of the drugs reach the tumour when compared to normal organs (Alessi et al., 2004). Therefore there is a requirement for more targeted therapies and the development of tumour homing molecules which would enable the targeting of therapeutic agents specifically to tumour cells.

Cancer immunotherapy is key area undergoing current research with the goal of developing cancer vaccines. The aim of cancer immunotherapy is to use a patients own immune system to fight cancer. There are two main types of immunotherapy; passive immunotherapy which involves the use of an antibody, usually a monoclonal antibody, or an immunological component made outside the body to treat a disease and active immunotherapy which aims to activate a patients own immune system which could lead to better immune responses and the possibility of inducing immunological memory. A number of cancer vaccines and targeting agents recently approved or in current development are listed in Table 1.2.

Table 1.2 Cancer vaccines and therapies in current use or clinical trials.

Therapy type	Name	Component	Cancer type	Status	Reference
Monoclonal antibodies	Herceptin (trastuzumab)	Humanized monoclonal anti-HER-2 antibody	Breast (HER2+)	Approved	(Weiner et al., 2009)
	Avastin (bevaizumab)	Murine human chimeric monoclonal anti-VEGF antibody	Colorectal, lung & breast	Approved	(Weiner et al., 2009)
scFv	-	Patient-specific scFv + GM-CSF	Melanoma	Phase I	(McCormick et al., 2008)
Homing peptides	Cilengitide	Cyclized RGD pentapeptide	Brain	Phase I	(MacDonald et al., 2008)
	NGR- hTNF	NGR peptide-TNF-α fusion peptide	Liver	Phase II	(Santoro et al., 2010)
Allogeneic	GVAX	Prostate cell lines; LN-CaP + PC-3 + GM-CSF	Prostate	Phase III	(Simons and Sacks, 2006)
	Melacine	Tumor lysates derived from two melanoma cell lines + DETOX adjuvant	Melanoma	Approved in Canada	(Srinivasan, 2008)
HSP-PC's	Oncophage	Autologous tumour-derived HSP70-PC's & HSP90-PC's	Kidney	Approved in Russia	(Srivastava et al., 2009)
Anti-idiotype antibody	Abagovomab	Monoclonal anti-idiotype antibody mimics CA-125	Ovarian	Phase II	(Sabbatini et al., 2010)
Mimotopes	-	Oxidized mannan-MUC-1	Breast	Phase III	(Apostolopoulos et al., 2006)
	E75	HER-2 peptide + GM-CSF	Breast	Phase I/II	(Patil et al., 2010)
DNA vaccine	-	GM-CSF DNA + gp100 + tyrosinase	Melanoma	Phase I/II	(Perales et al., 2008)
Viral vaccine	Gardasil	HPV L1 virus-like particles + aluminum adjuvant	Cervical	Approved	(Shi et al., 2007)
DC's	Provenge (Sipuleucel-T)	Autologous DC's + PAP + GM-CSF	Prostate	Approved	(Higano et al., 2009)
	-	LPS-activated DC's + killed COLO829 melanoma cells	Melanoma	Phase I/IIa	(Palucka et al., 2010)

1.7.1 Passive immunotherapy.

1.7.1.1 Monoclonal antibodies.

The most recent developments in current clinical use have come in the form of passive immunotherapy with monoclonal antibodies. A number of humanized or chimeric monoclonal antibodies are now approved for use in oncology. One example is trastuzumab (Herceptin) which is used in the treatment of breast cancers over-expressing HER-2. Trastuzumab is derived from a murine antibody called 4D5 which was identified from a series of antibodies directed against the HER-2 receptor (Kruser and Wheeler, 2010). 4D5 was selected for further development as it demonstrated inhibition of tumour growth, whereas some antibodies caused enhanced tumour proliferation (Riemer et al., 2004). HER-2 is over-expressed in 25-30% of primary breast cancers and trastuzumab is currently used a monotherapy for early stage breast cancer and is used in conjunction with chemotherapy for metastatic breast cancer (Kruser and Wheeler, 2010).

The mechanism of action of trastuzumab is still unknown, although several hypotheses have been put forward to explain its action. These include the internalization of the HER-2 receptor following trastuzumab binding resulting in cell cycle arrest or apoptosis, or antibody-dependent cellular cytotoxicity mediated by NK cells (Kruser and Wheeler, 2010). A study by Taylor et al (Taylor et al., 2007) showed that 29% of cancer patients tested had anti-HER-2 antibodies prior to trastuzumab treatment but this increased to 56% during treatment. This demonstrates that an active immune response can also be induced by trastuzumab. Both intrinsic and acquired resistance pose problems for trastuzumab therapy, with reportedly only 11-26% of patients showing a response to monotherapy (Kruser and Wheeler, 2010). When used in combination with chemotherapy acquired resistance develops after 5-9 months

20

(Kruser and Wheeler, 2010). Again the mechanisms remain to be fully elucidated but masking of the HER-2 epitope by MUC-4 or over-expression of the other EGFR family members has been implicated (Kruser and Wheeler, 2010).

Several monoclonal antibodies have been used as vehicles for targeting drugs, radionuclides or toxins to tumours. One example in current clinical use is gemtuzumab ozogamicin, a humanized monoclonal antibody conjugated to a calicheamicin toxin directed against CD33 for use in acute myeloid leukemia (Weiner et al., 2009). A number of studies employing combination therapies of monoclonal antibodies and chemotherapeutics are underway (Schlotter et al., 2008).

1.7.2 Tumour targeting agents.

1.7.2.1 Antibody fragments.

Smaller components used for tumour targeting have been derived from monoclonal antibodies including fragment antigen binding (Fab') and single chain fragment variable (scFv), which have the advantage of their smaller size enabling better penetration into tumour tissue, in addition to rapid blood clearance, reduced kidney damage and reduced production costs (Staneloudi et al., 2007). In particular scFv, identified by phage display libraries, have recently been successfully used in preclinical models to target chemotherapy drugs (Cheng and Allen, 2010) and photosensitizing agents to tumour cells (Staneloudi et al., 2007). McCormick et al (McCormick et al., 2008) cloned tumour-derived antibody variable regions derived from patients with non-Hodgkin's lymphoma and used a plant virus expression system to produce large amounts of patient-specific scFv. They administered patient-specific scFv with or without GM-CSF and nearly 50% of patients showed antigen-specific immune

21

responses. This demonstrates that in addition the targeting ability of scFv, they also have potential for active immunotherapy.

1.7.2.2 Tumour-homing peptides.

Two peptides that home to tumour vasculature, RGD-4C which binds to $\alpha v \beta 3$ and $\alpha v \beta 5$ integrins and NGR which binds to aminopeptidase N (Ruoslahti, 2002) have been extensively studied in animal models. Treatment of tumour-bearing animals with the peptides coupled to doxorubicin was more effective and less toxic than doxorubicin alone (Ruoslahti, 2002). A similar study showed that the peptides fused to apoptosis-inducing peptide moieties resulted in reduced tumour growth and prolonged survival (Laakkonen and Vuorinen, 2010).

RGD-4C and NGR and their derivatives, are currently being evaluated in clinical studies and trials for the drug targeting of cytotoxins and other therapeutic agents in a number of different cancers (Laakkonen and Vuorinen, 2010). For example, NGR coupled to human tumour necrosis factor-α showed activity and low toxicity in a recent study with patients suffering from advanced hepatocellular carcinoma (Santoro et al., 2010). Tumour-homing peptides are also under clinical investigation for *in vivo* cancer imaging and localization (Lee et al., 2010). For example, the RGD peptide has been coupled to radionuclides for use in positron emission tomography (PET) and single-photon emission computed tomography (SPECT). In addition, the RGD peptide has been tagged with magnetic iron oxide nanoparticles for use in magnetic resonance imaging (MRI) and quantum dots for optical imaging (Lee et al., 2010).

1.7.3 Active Immunotherapy.

1.7.3.1 Allogeneic cancer vaccines.

One of the first types of vaccines tested against tumours were allogeneic vaccines, consisting of either whole tumour cells or tumour lysates. One advantage of this type of vaccine is the potential induction of immune responses against multiple tumour antigens. Melacine consists of a lysate derived from two melanoma cell lines in combination with an adjuvant and has shown clinical responses in phase I and II trials and has been licensed in Canada for the treatment of stage IV melanoma (Srinivasan, 2008). One method of enhancing allogeneic whole tumour cell vaccines is to engineer the tumour cells to express immuno-stimulatory cytokines. One such example is GVAX which is composed of two prostate cancer cell lines engineered to express granulocyte macrophage-colony stimulating factor (GM-CSF), a potent DC activator. GVAX is in phase III trials in patients with advanced prostate cancer (Patel and Simons, 2010).

1.7.3.2 HSP vaccines

As mentioned earlier, HSP's chaperone antigenic peptides to the cell surface for presentation by MHC Class I and can also directly present these antigens to APC's through interaction with the CD91 receptor. Therefore vaccines based on HSP's are currently being developed. Autologous tumour-derived HSP preparations have shown excellent cure rates in early stage fibrosarcoma and lung cancer in animal models (Levey, 2008) and have progressed through human trials with the most recent consisting of two phase III trials for stage IV melanoma and renal cell carcinoma (Srivastava et al., 2009). The procedure involves

purification of HSP90- or HSP70-peptide complexes from surgically removed tumours from patients. The HSP-peptide complexes are then tested for quality, frozen in 25μg aliquots in saline until ready for use and then patients are immunized intradermally or subcutaneously. Immunizations are carried out once every week for the first four weeks, followed by every other week for as long as supplies last. Both trials showed some clinical benefit in early stage disease however the collective results did not meet the regulatory intention-to-treat criteria and therefore more trials are being pursued (Srivastava et al., 2009). However autologous tumour-HSP's (trade name Oncophage) are already approved in Russia for the treatment of kidney cancer and has received fast-track drug designation in America for the treatment of kidney cancer and gliomas (http://www.antigenics.com). A recent study showed that treatment with autologous tumour-derived HSP's in metastatic melanoma was feasible and safe, although immune responses were modest (Eton et al., 2010).

Apart from the use of autologous tumour-derived HSP's to boost anti-tumour immune responses, HSP's are now being investigated as new targets for cancer therapy as over-expression of HSP70 and HSP90 in many cancers is associated with poor prognosis. A chemical inhibitor of HSP90 called 17-allyl-amino-17-demethoxygeldanamycin is currently undergoing clinical trials (Galluzzi et al., 2009) and several types of molecules including peptides, polyamines, sulfoglycolipids and adenosines are being investigated as potential inhibitors of HSP70 (Evans et al., 2010; Galluzzi et al., 2009).

1.7.3.3 Anti-idiotype antibodies.

A limitation of passive immunotherapy with monoclonal antibodies, like trastuzumab, is the need for repeated administration in order to achieve anti-tumour activity, in addition to their high cost (Riemer and Jensen-Jarolim, 2007). An active immunization would therefore

24

be more desirable. One approach as mentioned earlier is the linkage of monoclonal antibodies to cytokines or toxins in an attempt to stimulate the adaptive immune system. Another method involves the use of anti-idiotype antibodies. The idiotype of an antibody is the determinant of antigen-binding specificity (Weiner et al., 2009). The immune network theory proposed by Jerne (Jerne, 1974) predicts that the immune system is made up of a network of interacting antibodies and lymphocytes and that interaction of these molecules regulates the immune response. In particular it states that for every antibody with a given idiotype, there is a counter-antibody with an anti-idiotype which can mimic the structure of the original antigen (Foon and Bhattacharya-Chatterjee, 2001). Some cancer patients were shown to develop anti-idiotype antibodies against administered therapeutic monoclonal antibodies (Weiner et al., 2009). Anti-idiotype antibodies can shorten the half-life of administered antibodies but are also capable of triggering an active immune response if they mimic the original tumour antigen (Weiner et al., 2009).

Anti-idiotype vaccines can be used to generate anti-anti-idiotype antibodies, which are capable of binding both the anti-idiotype antibody administered but also the original tumour antigen, in an attempt to increase immune responses and break tolerance (Foon and Bhattacharya-Chatterjee, 2001). Various anti-idiotype antibodies are currently undergoing clinical trials for melanoma, colorectal, breast and ovarian cancer (de Cerio et al., 2007). One example is abagovomab, a mouse-derived anti-idiotype monoclonal antibody that mimics CA-125 (also known as MUC-16) which is highly expressed in epithelial ovarian cancers. Abagovomab is currently in phase II trials with good preliminary clinical responses, although development of human anti-mouse antibodies (HAMA) is one current problem (Sabbatini et al., 2010).

1.7.3.4 Mimotopes.

An alternative to anti-idiotype antibodies is the use of tumour-antigen mimic epitopes or "mimotopes". Phage display has been used more recently to generate mimotopes by identifying peptides that bind to the epitope-binding sites of known anti-tumour antibodies. Several mimotopes of HER-2 have been generated by phage display using trastuzumab, which show similar functionality to the antibody (Jiang et al., 2005; Riemer et al., 2004). Mimotopes of CD20 have been identified in a similar manner using rituximab (Perosa et al., 2007), which is a monoclonal anti-CD20 antibody used in the treatment of lymphoma (Weiner et al., 2009).

Mimotopes have several advantages over anti-idiotype antibodies which include their ease of manufacture, low cost, high purity, high stability and they can be easily modified or linked to conjugates to enhance stability or immunogenicity (Knittelfelder et al., 2009). Mimic peptides have been used alone and in combination with other agents in a number of clinical trials for melanoma, breast, prostate, liver, lung and pancreatic cancer (Schroter, 2008). One example is the current use of a HER-2 mimotope in combination with GM-CSF in a phase II trial in breast cancer which showed low toxicity and indications of clinical responses, however one drawback appears to be the requirement of boosters in maintaining these responses (Patil et al., 2010).

1.7.3.5 DNA vaccines

DNA is detected by the innate immune system and can be taken up by DC's via toll-like receptor 9 (TLR9) (Stevenson et al., 2010). DNA vaccines have therefore been considered for cancer therapy. DNA encoding tumour antigens and cytokines can be injected into a tumour allowing for uptake by DC's, which can subsequently activate an immune

26

response (Stevenson et al., 2010). Naked DNA vaccines have been shown good results in mouse models but initial clinical results were disappointing, largely due to the volume of DNA required for efficacy in humans (Stevenson et al., 2010). The use of viral vectors can enhance efficacy by strongly attracting APC's (Liu et al., 2010). The most commonly modified viruses used as vectors are the retrovirus, adenovirus and adeno-associated virus, however drawbacks include strong anti-vector immune responses which limit repeated doses, safety concerns and high costs (Liu et al., 2010). Other strategies for DNA delivery include packaging with nanoparticles, microparticles or liposomes (Pejawar-Gaddy and Finn, 2008).

The ability of viruses to stimulate strong immune responses is particularly useful in the development of vaccines against virus-induced cancers. The recent breakthrough with Gardasil demonstrates that protective immunity can be established against HPV, the causative agent of cervical cancer (Shi et al., 2007).

1.7.4 Adoptive immunotherapy

1.7.4.1 T cell therapy

Adoptive immunotherapy involves the isolation of immune cells from patients, *ex vivo* stimulation and subsequent re-administration to the patient with the aim of generating an active immune response. Adoptive immunotherapy in cancer initially focused on the use of *ex vivo* expanded antigen-specific cytotoxic (CD8+) T cells to target tumours. A phase I trial by Yee et al (Yee et al., 2002) showed that adoptive transfer of CD8+ T cells specific for MART-1 and GP100 showed clinical responses in patients with stage IV melanoma. More recently adoptively transferred CD4+ T cells specific for NY-ESO-1 were administered to a patient with metastatic melanoma which resulted in clinical remission (Hunder et al., 2008).

Limitations of adoptive T cell therapies have included difficulty in purifying sufficient numbers of tumour-specific T cells, the time-consuming process of T cell expansion, priming and purification and the fact that T cells can be destroyed *in vivo* due to an immunosuppressive environment. Genetically modified polyclonal T cells are undergoing research with the aim of overcoming the low availability or absence of tumour-specific T cells. These include T cells engineered to express tumour-specific T cell receptors (TCRs) and chimeric antigen receptors (CARs) designed to express tumour-specific binding molecules and co-stimulatory molecules (Cartellieri et al., 2010). The efficacy of adoptive T cell therapy has been shown to be affected by the presence of immunosuppressive molecules in the tumour. High numbers of Tregs can significantly affect induction of tumour immunity and so therapies targeting Tregs have clinical value. Denileukin difitox (Ontak) is a fusion protein containing IL-2 and a portion of diphtheria toxin which binds the CD25 (IL-2 receptor) on Tregs, resulting in cell death (Anderson, 2009).

1.7.4.2 DC-vaccines.

DC's are positioned in peripheral tissues lining the surfaces of the body where they capture disease-causing antigens, after which they migrate to lymphoid organs where they can present these antigens to T cells and either induce immunity or tolerance (Steinman and Banchereau, 2007). In their steady state, in the absence of maturation stimuli, DC's induce tolerance to self or detected antigens (Steinman and Banchereau, 2007). However in the presence of a maturation signal, such as a pro-inflammatory cytokine (TNF-α), bacterial product (LPS) or apoptotic cell, they can induce active immune responses (Soruri and Zwirner, 2005).

28

DC's are often used in the *ex vivo* generation of antigen-specific T cells for adoptive T cell therapy but have themselves become promising candidates for cancer immunotherapy. DC's have the unique ability to stimulate both cellular and humoral immune responses (Steinman and Banchereau, 2007). Autologous DC's can be generated *ex vivo* using purified CD34+ bone marrow progenitor cells or CD14+ monocytes, the latter of which is used in most cases as they can be more easily purified in sufficient number from a relatively small volume of blood and the process is less invasive (Reichardt et al., 2004). CD14+ monocytes require incubation with two cytokines, granulocyte macrophage colony-stimulating factor (GM-CSF) and IL-4, in order to differentiate into DC's, followed by a maturation step (Soruri and Zwirner, 2005). The DC's are then loaded or "pulsed" with tumour peptides, tumour proteins, tumour cell lysates, tumour-derived mRNA or DNA or they can be fused with tumour cells and are subsequently re-administered to the patient to generate anti-tumour immune responses (Pejawar-Gaddy and Finn, 2008).

Early work in animal models showed firstly that purified DC's loaded with tumour peptides *ex vivo*, upon re-administration could induce cytotoxic T cell activity. Secondly DC's pulsed with tumor peptides could cure animals with small tumours (Soruri and Zwirner, 2005). This has led to a number of clinical trials utilizing DC's for cancer treatment. A recent study performed by Barth et al (Barth et al., 2010) used autologous DC's pulsed with tumour lysates in the treatment of colorectal cancer. Twenty-six patients underwent surgical resection of colorectal metastases and were subsequently treated with autologous tumour lysate-pulsed DC's. Although the detected immune responses were low, patients who developed tumour-specific T cell responses showed enhanced recurrence-free survival after five years.

A recent breakthrough has come in the form of Sipuleucel-T (Provenge) which is the first FDA-approved autologous cellular immunotherapy designed for use in metastatic prostate cancer. Sipuleucel-T consists of autologous peripheral blood mononuclear cells

29

which have been activated *in vitro* with a recombinant fusion protein composed of prostatic acid phosphatase (PAP), an antigen expressed in the majority of prostate adenocarcinomas, linked to GM-CSF (Higano et al., 2009).

1.8 Limitations to current approaches to cancer immunotherapy.

While great progress has been made in the treatment of cancer using classical therapies such as chemotherapy and radiation, there is a need to develop more therapies to enhance treatment and prolong survival of cancer patients. Cancer immunotherapy holds great promise in this area and the recent breakthroughs of Gardasil and Provenge have reinforced this. However current research and clinical trial data with immunotherapeutic agents has highlighted some limitations. For example, acquired resistance and toxicity of monoclonal antibodies in current clinical use have posed new problems in treatment. In addition, immunotherapies based on activating B and T cell responses have met with limited success in clinical trials. However along with the disappointments comes an increased understanding of the mechanisms of action of the immune system. For example, we now know that the conditions with which tumour antigens are introduced to the immune system or their "first impression" can determine subsequent immune responses and that the correct conditions are required to ensure active immune responses as opposed to the induction of immune tolerance. For example, we know that DC's can be potent immune activators or silencers and that inclusion of pro-inflammatory cytokines can significantly improve anti-tumour immune responses (Steinman and Banchereau, 2007).

Many years of cancer research have shown that there is no "magic bullet" for curing cancer, rather alternative approaches utilizing individualized cancer therapies have come back to the fore-front. Pejawar-Gaddy and Finn (Pejawar-Gaddy and Finn, 2008) described ideal

30

cancer vaccines as being composed of the "right" antigen, the "right" adjuvant and the "right" immune response. The identification of more tumour antigens and the development of methods designed to improve the immuno-stimulatory effect of these antigens would significantly benefit the field of cancer immunotherapy.

1.9 Preface to thesis.

Previous work in this lab by Arnaiz et al (Arnaiz et al., 2006) used phage-peptide display libraries to generate synthetic tumour antigen mimic peptides. This was achieved using a technique now termed "mirror image phage display" as depicted in FIG. 1.4. This concept is based initially on the identification of a peptide (recognizer peptide) that can bind to an unknown tumour antigen. This recognizer peptide is subsequently used as a target in a second bio-panning experiment resulting in the generation of a so-called mimic peptide. This technique is based on the hypothesis that a peptide capable of binding the recognizer could be a mirror image (molecular mimic) of the original tumour antigen.
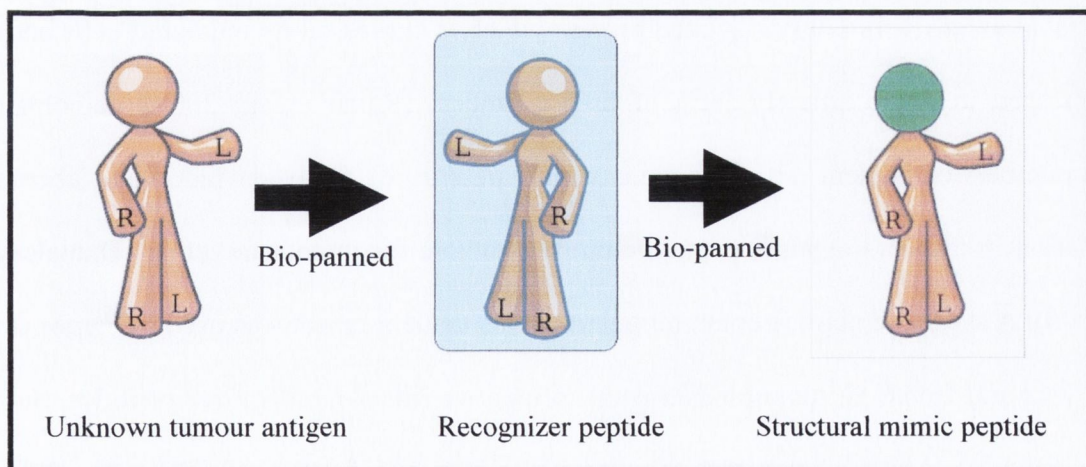
FIG. 1.4 Depiction of the concept of mirror image phage display.

The starting material for the original bio-panning experiments was purified HSP70-peptide complexes (HSP70-PC's) from the human breast carcinoma cell line MDA-MB-231. As HSP70 is known to be associated with tumour antigens when purified from tumour cells, it provides a rich reservoir of tumour antigens. Mirror image phage display was used to identify recognizers and mimics of antigens present in the HSP70-PC's. The mimic peptides were then assessed for their ability to stimulate immune responses *in vitro* by examining the ability of DC's pulsed with the mimic peptides to stimulate cytotoxic T cell activity, which can be measured by the production of interferon-γ. These experiments resulted in the identification of a number of recognizer and mimic peptides. One recognizer/mimic pair (TMG and DSP, respectively) displayed immuno-stimulatory ability and showed proof of principle that mirror image phage display could generate a true tumour antigen mimotope. A small pilot study involving the adoptive transfer of human immune effector cells primed by DC-loaded DSP mimic peptides into xenograft MDA-MB-231 tumours showed either tumour stabilization or a reduction in the tumour burden (James, T.C. and Bond, U., unpublished data).

This methodology has been further validated by James et al (James, T.C. and Bond, U., unpublished data) by the successful generation of synthetic mimic peptides of MUC-1. MUC-1 is an extensively *O*-glycosylated protein which is expressed by epithelial cells and is over-expressed in approximately 90% of breast cancers (Raina et al., 2009). It contains variable numbers of tandem repeat domains which are sites of *O*-glycosylation and aberrant glycosylation in tumours exposes peptide epitopes suitable for tumour targeting (Danielczyk et al., 2006). A synthetic peptide containing part of this tandem repeat was used by James et al (James, T.C. and Bond, U., unpublished data) to identify MUC-1 recognizer peptides. Some of these peptides showed homology to idiotype sequences of known MUC-1 antibodies. These MUC-1 recognizer peptides were subsequently used to generate MUC-1 mimic peptides using mirror image phage display.

1.10 Objectives of this study.

The overall aim of this project was to use unbiased approaches to discover novel breast tumour biomarkers and breast tumour mimotopes. The specific aims were to use phage-peptide display libraries to identify peptides (potential biomarkers) that specifically or differentially bind;

- Live breast tumour cells *in vitro*.

- Breast tumours *in vivo*.

- Breast tumour antigens associated with HSP70.

Finally the identified peptide biomarkers were used as targets for mirror image phage display to identify potential breast tumour mimotopes. The immuno-stimulatory ability of these mimotopes was tested *in vitro*.

Chapter 2:

Materials & Methods

2.1 Cell lines.

MCF-7 and MDA-MB-231 are tumourigenic breast epithelial cell lines derived from two patients with metastatic breast adenocarcinomas. MCF-12A is a non-tumourigenic breast epithelial cell line, derived from a patient with fibrocystic breast disease, which spontaneously immortalized in culture. All cell lines were grown in RPMI-1640 media containing 25mM 4-(2-hydroxyethyl)-1-piperazineethanesulfonic acid (HEPES) supplemented with 2mM L-Glutamine, 10% fetal calf serum and an antibiotic-antimycotic solution (Sigma A5955). MCF-12A media was also supplemented with 20ng/ml human epidermal growth factor, 0.01mg/ml human insulin and 500ng/ml hydrocortisone. Cells were grown at 37°C in 5% (v/v) carbon dioxide.

2.2 *In vitro* bio-panning on MCF-7 breast tumour cells using the PhD-C7C phage library.

The M13 phage peptide display library, PhD-C7C (New England Biolabs (NEB), E8120S), encodes cysteine-flanked random 7-mer peptides which are expressed on the minor coat protein (pIII) of the phage virion. Upon expression, the flanking cysteine residues spontaneously form a disulfide cross-link resulting in the display of cyclic peptides. The phage library was amplified once prior to use in all bio-panning experiments.

Approximately 10^5 MCF-7 tumour cells were seeded in 6-well dishes and grown to 50-70% confluency. Approximately $2x10^{11}$ pfu of the PhD-C7C phage peptide display library were added to the cells in 1ml of complete media and incubated for 1hr. Unbound phage were removed by washing with Dulbecco's Phosphate Buffered Saline (DPBS). Bound phage were eluted by incubation with the phage host strain *E. coli* K12 ER2738. A small amount of eluate

35

was kept for titration purposes and the remainder was amplified in *E. coli* as instructed by the manufacturer. The purified phage from this round (round 1) were used in a negative round of selection (round 2) by incubating the phage on non-tumour MCF-12A cells (10^6 cells) for 1hr and purifying the unbound phage from the supernatant. The phage were then used in four more rounds (rounds 3-6) of selective bio-panning on the MCF-7 tumour cells as per round 1, with one exception: the final round (round 6) elution was carried out in a two-step manner by incubation firstly with 1mM dithiothreitol (DTT) in DPBS for 10 min, followed by incubation with 0.2M glycine buffer pH 2.2 for 2 min, which was later neutralised with 1M Tris-HCl pH 9.1. Twenty-eight random individual phage clones were picked from the final round eluate and were amplified and sequenced as described in Section 2.4.

An additional independent *in vitro* bio-panning experiment was carried out in an identical manner but it included one additional round of negative selection (round 7), followed by two more rounds of selection on MCF-7 cells (rounds 8-9). The final round elution was performed in a two-step manner as before and forty-eight individual phage clones were randomly selected and amplified for sequencing.

2.3 *In vivo/ in vitro* combination bio-panning on MDA-MB-231 breast tumour cells using the PhD-C7C phage library.

All animal work was carried out in the "Scrubs" Isolation room in the Bio Resources Unit, Trinity College. Live animal experimentation, including injections and animal sacrifice, was performed by Dr. T.C. James (license reference number: B100/3897). Animal handling and day to day care was carried out by me and Dr. James. My personal authorization code for animal handling was M/CS1.

Two independent *in vivo/in vitro* combination bio-panning experiments were performed as follows. Approximately 10^7 sub-confluent MDA-MB-231 cells suspended in DPBS and Matrigel (Sigma, E1270) were injected into the upper left mammary pad of a 4 week old female nude mouse (Athymic Nude-Foxn1^{nu} supplied by Harlan U.K.). The tumour established after two weeks. Approximately 2×10^{11} pfu of the PhD-C7C library in 100µl DPBS were injected intravenously into the tail vein of the mouse. The phage were allowed to circulate for 30 min, after which time the animal was sacrificed. The tumour and liver were removed, washed in DPBS, cut into small pieces with razor blades and homogenized with glass beads. The phage that had localized in the tissues were rescued and amplified by incubation in *E. coli* K12 ER2738.

The phage purified from the tumour tissue (round 1) were then used in a subtractive round (round 2) of bio-panning by incubation on non-tumour MCF-12A cells (10^6 cells) for 1 hr, after which the unbound phage were re-purified. This was followed by a selective round (round 3) of bio-panning on the 10^5 MDA-MB-231 cells *in vitro* for 1hr. Unbound phage were removed by washing in DPBS and bound phage were eluted and amplified in *E. coli.* The phage were then used in another round (round 4) of *in vivo* selection in a mouse bearing an MDA-MB-231-induced tumour as before. Finally, the phage underwent two more rounds (rounds 5 & 6) of selective bio-panning on the MDA-MB-231 cells *in vitro*. The final elution was carried out firstly by incubating with 1mM DTT in DPBS, followed by 0.2M glycine buffer pH 2.2 which was later neutralised with 1M Tris-HCl pH 9.1. Random phage clones were picked from the final round eluates and amplified for sequencing.

2.4 PCR and DNA sequencing.

Bio-panning eluates were plated at a low density and well isolated phage colonies were selected and amplified in *E. coli* K12 ER2738. DNA was extracted using the sodium iodide method as per phage library manufacturer's instructions. PCR was performed to verify the presence of peptide inserts in the phage using the following primers; forward 5'-TGGTTGTTGTCATTGTCGGCG-3' and reverse 5'-GCCCTCATAGTTAGCGTAACG-3'. Subsequent M13 ssDNA sequencing was performed by GATC Biotech AG (Germany) using the following primer: 5'-CCCTCATAGTTAGCGTAACG-3'.

2.5 Peptide synthesis.

Peptides were synthesized by GL Biochem (Shanghai) Ltd., Peptron (South Korea) or Peptide 2.0 Inc. (U.S.A). All peptides were initially dissolved in dimethyl sulfoxide and further diluted in water and stored at -20°C or -70°C.

2.6 Peptide properties.

The properties of the peptides were analyzed using the online Innovagen peptide property calculator (http://www.innovagen.se/custom-peptide-synthesis/peptide-property-calculator/peptide-property-calculator.asp). The values range from 3 for the most hydrophilic to -3.4 for the most hydrophobic. Net charge is calculated as the sum of charged amino acids present in a sequence with values allocated as follows; D and E are -1 each, whereas K and R are +1 and H is +0.1.

2.7 Immuno-fluorescent cytology.

Approximately 10^4 cells were seeded in complete medium onto Nunc 8-chamber glass slides and grown to 50-90% confluency. Cells were washed thrice in PBS, fixed with 4% (w/v) paraformaldehyde in PBS (PFA/PBS), washed again and blocked overnight at 4°C in 1% (w/v) casein in PBS. The next day cells were washed in PBS and incubated with biotinylated peptides (at indicated concentrations) in 200μl of casein blocking buffer for 2 hr. Cells were washed thrice in PBS and incubated with ExtrAvidin-Cy3 (Sigma, E4142) at 1:100 in 200μl of blocking buffer for 2 hr. Cells were washed again, de-chambered and mounted in aqueous mounting medium containing DAPI (1μg/ml). Slides were examined using either a Nikon Eclipse E400 microscope or an Olympus confocal microscope, as indicated.

2.8 Enzyme linked immunosorbent assay (ELISA).

Soluble cell protein extracts were made using CelLytic M (Sigma, C2978) and protein concentrations were determined using Bradford reagent (Sigma, B6916) as per manufacturer's instructions. Soluble protein extracts or BSA were incubated in 0.1M sodium bicarbonate buffer, pH 8.6 at a concentration of 100μg/ml in sealed 96-well Maxisorp plates overnight at 4°C. Plates were washed thrice with TBS-T and blocked overnight at 4°C in 1% (w/v) casein in TBS. Following three washes in TBS-T, plates were incubated with biotinylated peptides at indicated concentrations in 100μl casein blocking buffer for 2 hr, followed by washing with TBS-T. Plates were then incubated with extravidin-peroxidase (Sigma, E2886) at a 1:3,000 dilution in 100μl casein blocking buffer for 2 hr. Plates were washed six times in TBS-T. 100μl of TMB (Sigma, T8655) was added to each well and the reaction was stopped by the addition of 50μl of H_2SO_4 after 5 min. Absorbance was read on a microplate reader at 450nm.

39

2.9 Flow cytometry.

Cells were washed in PBS, trypsinized, re-suspended in complete medium and aliquoted into sterile Eppendorf tubes (10^6 per tube). Supernatants were removed and cells were re-suspended in 200µl of plain medium containing 50µg/ml of biotinylated peptides in duplicate for 30 min. Cells were washed in PBS and fixed with 4% (w/v) PFA/PBS for 10 min and washed again in PBS. Cells were incubated with streptavidin-FITC (1:100) in 200µl PBS for 1hr, followed by washing with PBS. Cells were finally re-suspended in 500µl PBS. Fluorescence was analyzed on a Becton-Dickinson flow cytometer (5,000 events). Subsequent data analysis was performed using WinMDI version 2.8. The single cell population was gated and the green fluorescence detected is shown as FL1 log channel overlay graphs.

2.10 BLAST homology searches.

Homology to known proteins was examined using BLASTP version 2.2.24 (Altschul et al., 1997) with the PAM30 matrix and the human SwissProt database. As the input sequences are only 7-mer peptides it is not possible to obtain significant hits. Therefore the homology searches are included to provide an indication of homologous proteins and shared motifs but do not represent statistically significant matches.

2.11 Tissue pathology.

2.11.1 Immuno-fluorescent staining of patient tissue sections.

Formalin-fixed paraffin embedded (FFPE) patient tissue sections were obtained from Prof. Elaine Kay's lab, Department of Pathology, RCSI Education & Research Centre, Smurfit Building, Beaumont Hospital, Dublin 9 and were processed as follows;

1. De-paraffinized in Neo-Clear xylene substitute, 2 x 5 min.

2. Rehydrated in 100% absolute alcohol 2 x 5 min, followed by 95% absolute alcohol 1 x 5 min, 75% absolute alcohol 1 x 5 min and distilled H_20 2 x 10 min.

3. Underwent heat-induced antigen retrieval in 0.01M citric acid buffer, pH6.0 in a pressure cooker (maximum pressure for 1 min) and then allowed to cool to room temperature for 20 min.

4. Washed slides in cold tap water 3 x 5 min, followed by PBS for 5 min.

5. Incubated with 1% (w/v) casein/PBS blocking buffer overnight at 4°C.

6. Endogenous avidin and biotin were blocked using the Dako biotin blocking system (Dako, X0590).

7. Incubated with biotinylated peptides (1µg/ml) in 500µl blocking buffer for 1 hr.

8. Washed in PBS 3 x 10 min.

9. Incubated with extravidin-Cy3 1:100 in 500µl blocking buffer for 1 hr.

10. Washed in PBS 3 x 10 min.

11. Section mounted in anti-quench aqueous mounting media with DAPI (1µg/ml).

12. Viewed and photographed immediately using a Nikon E100 fluorescent microscope.

2.11.2 Immuno-fluorescent staining of tissue microarrays (TMA's).

Tissue microarrays (TMA-866) were purchased from Creative Biolabs. TMA-866 contains 48 tissue cores comprising 6 cores from 8 different tissue types; liver, lung, cerebrum, breast, prostate, intestine, kidney and epiploon/mesentery. Of the 6 cores from each tissue type, generally three cores are derived from tumour tissue and the other three from normal tissue. TMA's were processed in an identical manner as before (see Section 2.11.1) with two exceptions; sections were de-paraffinized in Neo-Clear xylene substitute for 4 x 20 min due to thicker wax coating and peptides were incubated at a concentration of 10µg/ml.

2.11.3 DAB staining of tissues and TMA's.

DAB (3,3'-diaminobenzidine tetrahydrochloride) staining was performed by our collaborators; Prof. Elaine Kay, consultant histopathologist, Dr. Tony O' Grady, chief medical scientist and Robert Cummins, senior medical scientist at the Department of Pathology, RCSI Education & Research Centre, Smurfit Building, Beaumont Hospital, Dublin 9. FFPE-tissue was incubated with biotinylated peptides (at indicated concentrations) and bound peptides were detected using an anti-biotin antibody (Leica Microsystems, AR0584). Staining with the peptides or with the anti-HSP70 antibody (Sigma, H5147) was detected using the Bond Polymer Refine Detection Kit (Leica Microsystems, DS9800) and visualized using DAB as the chromogen. Tissues were counterstained with hematoxylin. Bond Epitope Retrieval Solution 2 (Leica Microsystems, AR9640) was used for antigen retrieval in some cases as indicated.

2.12 Cellular heat shock protein 70-peptide complex (HSP70-PC) extraction.

Approximately 10^8 MDA-MB-231, MCF-7 and MCF-12A cells were lysed using CelLytic M reagent (Sigma, C2978) as instructed by the manufacturer and the protein concentrations were determined using Bradford reagent (Sigma, B6916). HSP70-PC's were subsequently purified from each cell line using soluble protein extracts of MDA-MB-231 (12.2mg), MCF-7 (12.6mg) and MCF-12A (13.9mg) cells and ADP-agarose (Sigma, A4398) affinity chromatography as previously described (Srivastava, 1997). HSP70-PC extracts were concentrated using centrifugal concentrators with a 10,000 molecular weight cut-off and final protein concentration was determined using Bradford reagent. Affinity-purified HSP70-PC's (approximately 5μg) were analyzed using sodium dodecyl sulphate polyacrylimide gel electrophoresis (SDS-PAGE). 12% SDS-PAGE gels were run and stained with Coomassie Brilliant Blue for 30min and allowed to de-stain overnight.

2.13 Western immuno-blotting.

Protein samples were separated by SDS-PAGE as above and were subsequently transferred to nitrocellulose membranes. Membranes were washed in TBS containing 0.05% (v/v) Tween-20 (TBS-T) thrice for 15 min and blocked in 5% (w/v) non-fat milk powder in TBS-T overnight at 4°C. Membranes were then washed in TBS-T and incubated with mouse anti-HSP70 monoclonal antibody (Sigma, H5147) at 1:5000 in blocking buffer for 2hr. Membranes were washed again and incubated with goat anti-mouse-IgG antibody-peroxidase (1:20,000) (Sigma, A9917) in blocking buffer for 2hr. Membranes were washed and developed with a chemiluminescent peroxidase substrate (Sigma, CPS160). The membrane was briefly drip-dried, placed in clean plastic membrane and exposed to light-sensitive film.

43

2.14 Matrix-assisted laser desorption/ionization-time of flight (MALDI-TOF) peptide mass fingerprinting.

Protein samples were separated by SDS-PAGE and stained with Coomassie Brilliant Blue as described in Section 2.12. Selected protein bands underwent in-gel trypsin digestion using the Trypsin Profile IGD Kit For In-Gel Digests (Sigma, PP0100), as per manufacturer's instructions with the following exception: reduction and alkylation of proteins was performed in-gel using the ProteoPrep Reduction and Alkylation Kit (Sigma, PROT-RA) after the gel pieces were de-stained but prior to digestion with trypsin. The final tryptic peptides were concentrated by SpeedVac and re-suspended in 0.5μl of 0.1% (v/v) trifluoroacetic acid. Analysis was performed by Gwen Manning using an Applied Biosystems 4800 Plus MALDI-TOF/TOF at the Mass Spectrometry Resource, Conway Institute of Biomolecular and Biomedical Research, University College Dublin.

2.15 HSP70-PC bio-panning strategy 1.

Cellular HSP70-PC's were purified through ADP-affinity chromatography as described earlier. Bio-panning was carried out in Nunc 96-well Maxisorp plates using the PhD-C7C library as instructed by the manufacturer with the following exceptions; washing buffer was TBS with 0.05% Tween-20 (TBS-T), blocking buffer was 1% (w/v) casein in TBS-T and elution buffer was 0.2M glycine buffer pH 2.2, neutralised with 1M Tris-HCl pH 9.1. Round 1 involved the application of 2×10^{11} pfu of PhD-C7C onto HSP70-PC's coated onto Maxisorp plates for 1hr. Unbound phage were removed by 20 washes with TBS-T and bound phage were eluted and amplified. One quarter of the amplified phage was used in the second round of panning, performed identically to round 1. The phage were then used in a

subtractive round (round 3) of panning by incubating the phage on plate-coated human recombinant HSP70 (ProSpec, HSP-170), in order to remove phage that can only bind to HSP70. Unbound phage were removed and amplified and used in three more rounds of selective bio-panning on the affinity purified HSP70-PC's, as before. Ten random phage clones from the final eluate were picked, amplified and sequenced as before.

2.16 HSP70-PC bio-panning strategy 2.

2.16.1 Column capture of HSP70-PC's and separation from co-purifying proteins.

HSP70-PC's were affinity-purified from MDA-MB-231 cells as described earlier. Protein concentration was determined using Bradford reagent and relative concentration of HSP70-PC's within the extract was approximated by comparing protein band density against known controls on an SDS-PAGE gel. Approximately 2μg of HSP70-PC's were incubated with a 10-fold excess of monoclonal anti-HSP70 antibody (Sigma, H5147) in TBS for 2hr at 4°C. 100μl of Protein A/G agarose (Pierce Ultralink 53132) was washed four times in TBS, added to the HSP70-PC-antibody complex and incubated at 4°C overnight. The next day the sample was spun gently to pellet the agarose and the unbound proteins were removed and kept. The agarose was washed in 40 column volumes of TBS. Agarose-bound proteins were eluted by boiling in protein sample buffer for 20 min. Samples were analyzed by SDS-PAGE as follows; half of the agarose-bound protein sample was run, along with 1/10 of the total unbound protein fraction. HSP70-PC extract (approx. 0.5μg HSP70-PC) was also run as a control, in addition to approx. 28μg (1μl) of anti-HSP70 antibody (approx. 4μg IgG) to show proteins present in the ascites fluid stock of antibody. Proteins were visualized by Coomassie staining as before.

45

2.16.2 HSP70-PC bio-panning method.

Affinity-purified HSP70-PC's (10μg) were incubated in 100μl of 0.1M NaHCO$_3$ pH 8.6 on a Maxisorp 96-well plate (Nunc) overnight at 4°C. The wells were then washed with TBS-T and blocked in 1% (w/v) casein in TBS overnight at 4°C. PhD-C7C phage library (2x10^{11} pfu) was added to the target wells in blocking solution and incubated for 1hr at room temperature. The wells were then washed twenty times with TBS-T and bound phage were eluted with 0.2M glycine buffer pH 2.2 which was immediately neutralised with 1M Tris-HCl pH 9.1. A small aliquot was kept for titration purposes and the remainder was amplified as instructed by the manufacturer.

The second round involved incubating affinity-purified HSP70-PC's (10μg, approx. 2μg actual HSP70-PC's) with a 10-fold excess of anti-HSP70 antibody (Sigma, H5147) for 2hr at room temperature and subsequently capturing the antibody-HSP70-PC complex on 100μl of Protein A/G agarose (Pierce Ultralink, 53132 and Santa Cruz, sc-2003) overnight at 4°C in TBS. The column was washed in TBS to remove unbound proteins and blocked with TBS containing BSA (5mg/ml). A quarter of the total amplified phage stock from round 1 was firstly pre-absorbed on antibody loaded-Protein A/G agarose and unbound phage were subsequently transferred to the HSP70-PC loaded column for 1hr at room temperature. Unbound phage were removed and the agarose was washed with 100 column volumes of TBS-T. Negative selection was performed by incubation with recombinant human HSP70 (100μg/ml) in 100μl TBS for 30 min at room temperature in order to remove phage binding only to HSP70 (and not to its associated peptides). This was followed by elution of remaining target-bound phage with 0.2M glycine buffer pH 2.2 (neutralised with 1M Tris-HCl pH 9.1). Glycine buffer-eluted phage were amplified as before in *E. coli* and used in the next round of panning.

Round 3 was carried out in the same manner as round 1 except that the phage (a quarter of the total amplified phage) were pre-incubated in a well coated with BSA in order to remove plastic- or BSA-binding phage before subsequent incubation on the HSP70-PC target coated wells. Rounds 4 and 5 were identical to round 2 except that the blocking solution was alternated and eluted phage were not amplified after round 5.

Bio-panning was extended to a total of 10 rounds performed in an identical manner to round 2 with the following exceptions; target-bound phage were eluted by incubation with 3mM ATP in TBS for 30min at room temperature. Incubation of HSP70-PC's with ATP is known to release the PC's associated with HSP70 (Srivastava, 1997). In addition, phage were purified but not amplified after rounds 7 and 10. Individual phage clones were picked, amplified and sequenced after rounds 4, 5, 6 and 10 in order to monitor phage enrichment during the experiment.

2.17 Peptide linkage to paramagnetic beads.

Batches of up to 1mg of synthetic peptides were linked via their carboxy-terminal to amino-coated paramagnetic beads (Kisker, PMSI-AM1.0-5) using N-(3-dimethylaminopropyl)-N'-ethylcarbodiimide hydrochloride (ECD, Sigma, 03449) at 10mg/ml in 0.1M phosphate buffer, pH 7.4. After 3hr, un-reacted material was removed by washing in PBS, and peptide-linked magnetic beads were re-suspended at concentration of 1mg/ml and stored in PBS at 4°C. A fraction of unlinked beads were re-suspended at the same density in PBS for use as a negative control in later experiments.

2.18 Peptide-bead linkage control experiment.

In order to ensure that peptides could be successfully linked to paramagnetic beads, two biotinylated peptides and one non-biotinylated control peptide were linked to amino-coated beads as described above. 50μl (50μg peptides) of peptide-linked beads and unlinked beads were blocked in triplicate in 1% (w/v) casein/PBS overnight at 4°C. Following washes in PBS, samples were incubated with extravidin-peroxidase (1:3,000) in blocking buffer for 1hr. Beads were then washed, transferred to a new tube and incubated with 100μl of TMB for 5 min and the reaction was stopped by adding 50μl of H_2SO_4. Supernatants were transferred to a 96-well plate and the absorbance was read at 450nm on a microplate reader.

2.19 HSP70-PC recognizer peptide binding assays.

Synthetic recognizer peptides were linked to amino-coated paramagnetic beads as described above. Recognizer-peptide linked beads (100μg) were blocked in 1% (w/v) casein/PBS for 1hr, washed with PBS three times and incubated with affinity purified HSP70-PC (approx. 1μg of HSP70-PC's) for 1hr. Unbound proteins were removed by washing thrice with PBS, followed by incubation with anti-HSP70 antibody at a 1:500 dilution in blocking buffer for 1hr. After three washes in PBS, an anti-mouse IgG-peroxidase conjugated antibody (Sigma, A9917) was added at 1:600 dilution in blocking buffer for 1hr. Following four washes in PBS, the beads were transferred to a fresh Eppendorf tube and incubated with 100μl of TMB (Sigma, T8655). After 5 min the reaction was stopped with 50μl of H_2SO_4 and the supernatants were transferred to a 96-well plate and the absorbance was read at 450nm on a microplate reader. Data plotted was a combination of three experiments. P values were determined using a paired student t-test.

48

2.20 Pull down of HSP70-PC recognizer peptide cellular binding partners.

HSP70-PC recognizer peptides were linked to amino-coated paramagnetic beads as described above. 100µg of peptide-linked beads or beads alone were blocked in 1% (w/v) casein in TBS for 2hr. Following washes with TBS, beads were each incubated with 2mg of MDA-MB-231 soluble protein extract in TBS for 1hr. Unbound proteins were removed and kept, after which the beads were washed twice in TBS, five times in TBS with 0.5M NaCl, followed thrice more with TBS. The last wash was performed using a small volume of TBS (30µl) which was kept to assess the efficiency of the washes. Beads were re-suspended in 30µl of TBS. Protein samples (1/20 of unbound, total last wash, total bound protein and 10µg affinity-purified HSP70-PC's) were boiled in protein sample buffer and analyzed by SDS-PAGE as before. Selected protein bands visualized by Coomassie-staining were excised, digested with trypsin and analyzed by MALDI-TOF peptide mass fingerprinting as in Section 2.14.

2.21 Identification of putative tumour antigen mimic peptides.

2.21.1 Bio-panning of the HSP70-PC recognizer peptides with the PhD-C7C phage library.

Synthetic recognizer peptides (AIP, SQE and cISTc) were linked to amino-coated paramagnetic beads (as described in section 2.17). 20µg of peptide-linked beads were blocked in 1% (w/v) casein in PBS overnight at 4°C. Following washes in TBS, the peptide-linked beads were incubated with 10^{11} pfu of PhD-C7C in blocking buffer for 1hr at room temperature. Beads were washed twice with TBS containing 0.5M NaCl, followed by three

49

washes in TBS. Phage bound to the peptides were eluted by incubation with respective free peptide (20μg) for 30 min. Phage eluates were amplified and purified as described by the manufacturer. Three more rounds of bio-panning were carried out exactly as the first round detailed above with the exception that a quarter of the total amplified phage from the previous round was used as input phage for the next round. In addition, round 4 consisted of a multi-step elution of bound phage with a variety of peptides (incubated at 20μg each for 30min) with regions of homology to the target peptide, followed by the target peptide itself. The first batch of phage sequencing was performed at this stage.

Following sequence analysis, eluted phage fractions were respectively pooled and amplified. Four more rounds of bio-panning were performed in the same manner as above with the following exceptions; buffer was changed to PBS, washes were performed using PBS with 0.05% Tween-20 rather than the high salt buffer, beads were transferred to a new tube prior to elution and bound phage were eluted with the target peptide only. Individual phage clones were picked from the final round (round 8) and sequenced.

2.21.2 Bio-panning of the HSP70-PC recognizer peptides with the PhD-12 phage library.

The PhD-12 phage library (NEB, E8110S) encodes random linear 12-mer peptides which are expressed on the surface of the M13 phage as with the PhD-C7C library. The PhD-12 library was used to identify any linear peptides capable of binding to the HSP70-PC recognizer peptides. 20μg of peptide-linked beads (AIP, SQE and cISTc) were blocked in 1% (w/v) casein in PBS overnight. Following washes in PBS, the peptide-linked beads were incubated with 10^{11} pfu of PhD-12 in blocking buffer for 1hr at room temperature. Beads were washed four times with PBS containing 0.05% Tween-20, followed by three washes in PBS. Phage bound to the peptides were eluted by incubation with respective free peptide (20μg) for

30 min. Phage eluates were amplified and purified as described by the manufacturer. Four rounds of bio-panning were performed in total with each round using one quarter of the amplified phage from the previous round. Random phage clones were picked from the final round (round 4) and sequenced.

2.22 Synthetic mimic peptide:HSP70-PC recognizer peptide binding assay.

Synthetic mimic peptides and a control peptide (alpha factor, WHWLQLKPGQPMY) were linked to amino-coated paramagnetic beads as before. 10μl (10μg peptide) of peptide-linked beads and beads alone were blocked in 1% (w/v) casein/PBS for 2hr and, following washes in PBS, were incubated with 1μg of biotinylated HSP70-PC recognizer peptides for 30 min. Following washes in PBS and PBS with 0.05% (v/v) Tween-20, beads were incubated with extravidin-peroxidase (1:1000) in blocking buffer for 30 min. Following washes in PBS, beads were transferred to a new tube and incubated with 100μl TMB for 5 min. The reaction was stopped by adding 50μl of H_2SO_4 and the supernatants transferred to a 96-well plate. Absorbance was read at 450nm on a microplate reader. P values were determined using a paired student t-test.

2.23 *In vitro* immune stimulation assay.

2.23.1 Purification of peripheral blood mononuclear cells and monocytes from buffy coat packs.

Buffy coat packs were obtained from the Irish Blood Transfusion Service, St. James's Street, Dublin 8. Peripheral blood mononuclear cells (PBMC's) were purified from the buffy

51

coat using Ficoll gradient centrifugation. Monocytes were purified from the PBMC's using positive selection with CD14+ Microbeads (MACS, 130-050-201) and MACS separation unit and columns (MiniMacs kit, 130-090-312) as per manufacturer's instructions.

2.23.2 Cell culture and generation of dendritic cells (DC's).

The purified CD14+ cells were split into two batches. One half of the CD14+ cells were re-suspended in Gibco medium (Invitrogen) supplemented with recombinant human granulocyte macrophage colony stimulating factor (GM-CSF, 60ng/ml) and recombinant human IL-4 (150ng/ml) to allow differentiation into DC's. The other half of CD14+ cells were incubated with Gibco medium alone for later use. The CD14- PBMC's were stored in RPMI-1640 media containing 25mM HEPES supplemented with 2mM L-Glutamine, 10% fetal calf serum and an antibiotic-antimycotic solution. Cells were incubated in 6-well plates at 37°C in 5% (v/v) carbon dioxide and medium was replaced every 3 days. Differentiation of the CD14+ cells into DC's was monitored by visualization of the cells under an inverted phase contrast microscope and was complete after 6 days. Photos were taken using a Nikon camera mounted on a Nikon E400 inverted microscope.

2.23.3 Loading of mimic peptides onto DC's.

DC's were removed from the 6-well plates by scrapping, transferred to an Eppendorf tube, washed in Gibco medium and incubated with lipopolysaccharide (LPS, 1μg/ml) and tumour necrosis factor-α (TNF-α, 50ng/ml) in 200μl of Gibco medium overnight. The next day, the supernatant was removed and stored at -70°C for subsequent IL-12 assays. DC's were then washed in Gibco medium and 10^5 cells were each incubated with either 200μl of

Gibco medium alone or with medium containing each of the mimic peptides (25μg/ml) overnight. The next day DC's were washed in Gibco medium to remove any remaining free peptides and were re-suspended in Gibco medium supplemented with human recombinant IL-2 (25ng/ml).

2.23.4 *In vitro* immune assay.

The peptide-loaded DC's were seeded at $3x10^4$ cells per well in triplicate in a V-bottomed 96-well plate. The CD14- PBMC's were washed, re-suspended in Gibco medium supplemented with human recombinant IL-2 and $3x10^5$ cells were added to each well. This represents the start of the assay (Day 0). Media was replaced every 2-3 days and stored at -70°C for subsequent interferon-γ assays.

Also on Day 0, the second batch of CD14+ cells were supplemented with recombinant human GM-CSF and recombinant human IL-4 as before to begin the differentiation into DC's. On Day 6, differentiation into DC's was complete and the cells were removed by scrapping, washed and re-suspended in 200μl of Gibco medium containing TNF-α (50ng/ml) overnight. The next day, DC's were washed again and incubated with either 200μl of Gibco medium alone or medium containing the mimic peptides (25μg/ml) overnight. The next day (Day 8), DC's were washed and re-suspended in Gibco medium supplemented with human recombinant IL-2. This second batch of peptide-loaded DC's was then added to the primed PBMC's (second stimulation) at $3x10^4$ cells per well. Medium was replaced every 3 days and stored at -70°C. The last time-point was taken on Day 17.

2.23.5 Cytokine assays.

2.23.5.1 IL-12 assays.

Maturation of the DC's was analyzed by measuring levels of secreted IL-12 present in the supernatant taken after overnight incubation with LPS and TNF-α for the first batch of DC's and after the overnight incubation with TNF-α for the second batch of DC's. Levels of IL-12 were detected by a human IL-12 sandwich ELISA kit (Peprotech, 900-K96) as per manufacturer's instructions and IL-12 concentrations were determined by comparison with an IL-12 standard curve.

2.23.5.2 Interferon-γ assays.

The ability of the mimic peptides to induce an immune response *in vitro* was examined by analyzing the levels of interferon-γ secreted by T cells present in the PBMC's upon stimulation by the peptide-loaded DC's. Samples were taken at days 3, 6, 8, 11, 14 and 17. Levels of interferon-γ produced were determined using a human interferon-γ sandwich ELISA kit (Peprotech, 900-K27) as per manufacturer's instructions. P values were determined using a paired student t-test.

Chapter 3:

Generation and characterization of breast tumour cell surface-binding peptides.

3.1 Introduction.

Most of the current cancer therapies, such as the wide range of chemotherapeutics, work by killing rapidly dividing cells non-specifically (Schliemann and Neri, 2007). Some of the more recent research developments have looked to enhance treatment and reduce the side effects of this therapy by targeting the tumour cells more specifically. The most recent notable successes in this area for breast cancer treatment have come in the form of the monoclonal antibodies, Herceptin (approved in 1998) and Avastin (approved in 2004) (Wu and Senter, 2005). However there is a need for more targeting agents and indeed the identification of more TAA's, in order to enlarge the repertoire of available treatments for breast cancer.

Whole tumour cell targeting agents have great potential for use in the diagnosis (tumour imaging or pathology) and treatment (delivery of a cytotoxic payload to tumour cells) of cancer. Numerous different agents are being investigated for use in tumour cell-targeting and these include monoclonal antibodies, single chain antibody fragments and peptides. The latter is of specific interest to us because peptides can be synthesized readily, relatively cheaply and in extremely high purity. As they are smaller than antibodies they are also believed to be better able to penetrate tumour tissue *in vivo*.

The aim of the work detailed in this chapter was to use the PhD-C7C phage peptide display library to identify peptides that could bind specifically to the surface of whole live breast tumour cells. To achieve this, *in vitro* panning experiments were carried out using MCF-7 tumour cells as a target. Additionally, we investigated the use of this phage library in identifying peptides that could not only directly bind tumour cells *in vitro* but also bind tumour cells *in vivo*, thus potentially isolating tumour-homing peptide sequences. A combination of *in vivo/in vitro* panning was employed to this end, which involved selecting

phage-displayed peptides that bound to MDA-MB-231 cells *in vitro* but also localized to a xenograft MDA-MB-231-induced tumour *in vivo*.

These panning experiments resulted in the identification of a small set of heavily enriched novel peptide sequences, termed "whole cell recognizers", and they were further characterized using immuno-fluorescent cell staining, cellular protein ELISA's, flow cytometry and tissue pathology.

3.2 Results.

3.2.1. *In vitro* **bio-panning experiments using the PhD-C7C library to identify peptide sequences that bind the surface of live MCF-7 breast cancer cells.**

These bio-panning experiments aimed to identify phage-displayed peptides with the ability to bind to live MCF-7 breast cancer cells *in vitro*. An outline of these experiments can be seen in FIG. 3.1. In brief, the phage library was applied to MCF-7 cells and any phage that bound these live tumour cells were eluted and amplified. This pool of phage underwent a negative round of selection on the non-tumour MCF-12A cells in order to remove peptide sequences that would bind to non-tumour cells. This was subsequently followed by four more rounds of selective bio-panning on the MCF-7 cells. In the last round (round 6), phage clones were eluted firstly using a reducing agent (DTT) to identify peptides whose binding was dependent on their constrained form and this was followed by an acid elution (low pH glycine buffer) to elute any remaining peptides. Random phage clones were picked from the final round eluates and sequenced. A second independent bio-panning experiment was performed in an identical manner, except that three additional rounds were included; one negative selection on MCF-12A cells (round 7) and two rounds of positive selection on the MCF-7 cells (rounds 8 & 9) as indicated by the yellow, red and black boxes, respectively.

A total of 28 phage clones (14 from each eluate) were randomly picked and sequenced from the final round (round 6) of first experiment and these sequences are shown in Table 3.1. Noticeably one sequence, LSTSSTV, was heavily enriched during the bio-panning process. It was the predominant sequence eluted with DTT which suggested that perhaps the disulfide-constrained form was important for binding. However it was also the most common sequence
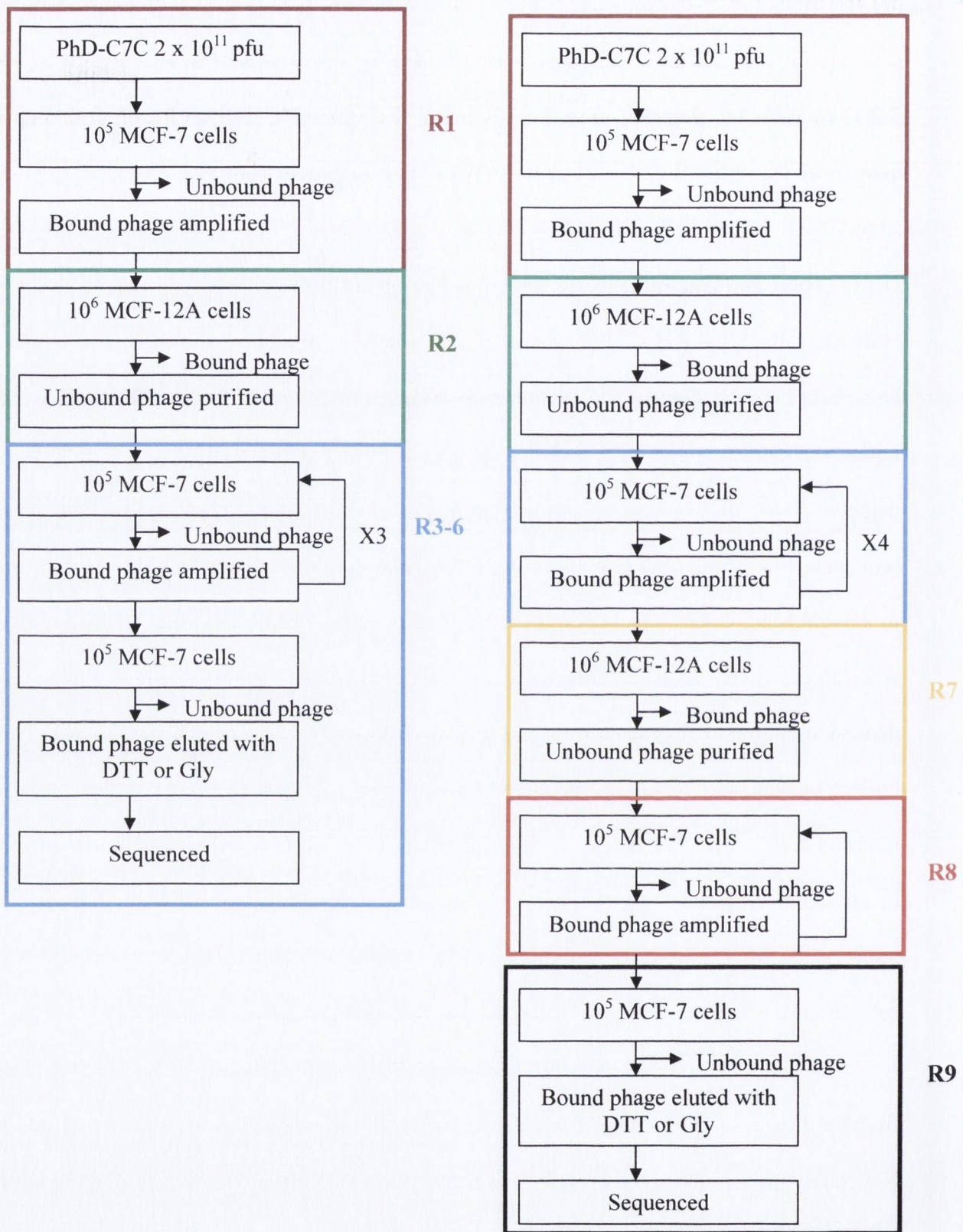
FIG. 3.1 Outline of MCF-7 *in vitro* bio-panning experiments.
R denotes panning round.

59

in the glycine buffer-eluted phage, which could be due to either cross-over between the initial DTT-elution step and subsequent glycine-buffer elution or incomplete elution with DTT. One other sequence also occurred more than once and that was ERITERF, which occurred once in each eluate. The glycine-eluted phage showed much more sequence variety than the DTT-eluted phage, suggesting that the disulfide-constrained form of the peptides was an important factor in sequence enrichment.

Table 3.1 Summary of the final round sequences identified from the first bio-panning experiment on MCF-7 cells.

Phage eluate	Sequence	Frequency
DTT	LSTSSTV	11/14
	ERITERF	1/14
	IPMLDRQ	1/14
	no insert	1/14
Glycine-buffer	LSTSSTV	4/14
	ERITERF	1/14
	SQSDTVN	1/14
	TDKLLSH	1/14
	WIHQHRN	1/14
	ATTMYAR	1/14
	TMRPYMS	1/14
	PNDRKQY	1/14
	PPHPRSK	1/14
	PSHRNPA	1/14
	DRTSRHH	1/14

Each of the sequences identified in Table 3.1 were aligned using ClustalW in order to visualize any possible motif enrichment that occurred during the panning. Each sequence was entered only once to check for common motifs across the pool of identified peptides, but as mentioned earlier LSTSSTV and ERITERF were both isolated on multiple occasions. The peptides are listed in Table 3.2 in the order in which they were aligned. The properties of the peptides are also shown. Amino acid motifs are indicated by bold type and are underlined.

Table 3.2 Alignment and properties of peptides identified from the first bio-panning experiment on MCF-7 cancer cells.

Sequence	Average hydrophilicity	Net charge
LSTSSTV	-0.5	0
SQSDTVN	0.3	-1
WIHQHRN	-0.4	1.2
PSHRNPA	0.4	1.1
PNDRKQY	1	1
PPHPRSK	0.8	2.1
IPMLDRQ	0.2	0
ATTMYAR	-0.3	1
DRTSRHH	1.1	1.2
TMRPYMS	-0.3	1
ERITERF	1	0
TDKLLSH	0.3	0.1

Peptide sequences were aligned using the ClustalW alignment tool (www.uniprot.org). Enriched amino acid motifs are underlined and in bold. Peptide properties were determined using the Peptide Property Calculator (www.innovagen.se).

Firstly, the properties of the peptides are diverse ranging from slightly hydrophobic to hydrophilic. The charge of the peptides also varies although most are positively charged. A number of amino acid motifs can be seen occurring across the peptide sequences. The first and largest occurs in the LSTSSTV and SQSDTVN peptides, which share an SXSXTV motif. Other motifs were detectable between the individually occurring sequences and these include; HRN, PXXR, MXXR and TXR. The result of this bio-panning experiment was the identification of one strongly enriched sequence, LSTSSTV, and a number of small amino acid motifs that appeared in several of the peptides identified.

In an effort to reduce the sequence variability seen in the first experiment, the second bio-panning experiment on MCF-7 cells included three more rounds of bio-panning as indicated earlier in FIG. 3.1. Forty-eight individual phage clones (24 from each elution) were randomly picked, amplified and their sequences determined. The peptide sequences are listed in Table 3.3. One sequence, MLHAQTS, was very heavily enriched and expressed by nearly 90% of all phage clones selected. Another new sequence, SKSLSPQ, was also identified albeit at a lesser frequency. Interestingly one sequence that appeared in the glycine-eluate, SQSDTVN, had also been isolated in the glycine-eluate of the first bio-panning experiment (see Table 3.1).

Table 3.3 Summary of the peptide sequences from the second MCF-7 bio-panning.

Elution	Sequence	Frequency
DTT	MLHAQTS	21/24
	SKSLSPQ	3/24
Glycine-buffer	MLHAQTS	22/24
	SQSDTVN	1/24
	SKSLSPQ	1/24

The properties and homologies of these peptide sequences are summarized in Table 3.4. MLHAQTS and SKSLSPQ share a small similarity with an LXXQ motif and SKSLSPQ also shares an SXS motif with SQSDTVN. Again the peptides display diverse properties.

Table 3.4 Properties and homologies of peptides identified in the second bio-panning experiment on MCF-7 cells.

Sequence	Average hydrophilicity	Net charge
MLHAQTS	-0.6	0.1
SKSLSPQ	0.3	1
SQSDTVN	0.3	-1

There were also some similarities between the newly identified sequences and those that were isolated in the first bio-panning experiment; MLHAQTS shares an MLXQ motif with IPMLDRQ, SKSLSPQ shares a KXLS motif with TDKLLSH, and SQSDTVN appeared in both experiments.

3.2.2 *In vivo/in vitro* **combination bio-panning experiments using the PhD-C7C phage library to identify peptides that can bind to MDA-MB-231 breast tumour cells.**

While the first bio-panning experiments were used to identify peptides that were able to bind MCF-7 tumour cells directly *in vitro*, we were also interested in isolating peptides that could not only bind tumour cells *in vitro* but also home to a tumour *in vivo*. In order to increase the likelihood of identifying peptides with tumour homing ability, a combination of *in vivo* and *in vitro* panning was performed. This was performed using another breast cancer

cell line, MDA-MB-231. This cell line is also a breast epithelial cancer cell line but, unlike MCF-7, it is relatively easy to induce a xenograft tumour in an immuno-deficient mouse. The *in vivo/in vitro* combination bio-panning protocol is outlined in FIG. 3.2. Two independent experiments were performed in an identical manner.

In brief, the PhD-C7C phage display library was injected into the tail vein of a nude mouse bearing an MDA-MB-231 induced tumour and after 30 min the mouse was sacrificed and the tumour was removed and washed. Phage localized in the tumour were recovered and amplified by incubating the tumour material in *E. coli*. The liver was also removed, washed and the phage rescued for reference purposes. The tumour-derived amplified phage were then incubated on MCF-12A cells to remove any phage that bound non-tumour cells and the unbound phage were purified. The purified phage were subsequently used in a selective round of bio-panning on the MDA-MB-231 cells *in vitro* and the bound phage were eluted and amplified. The phage were then injected into the tail vein of another nude mouse bearing an MDA-MB-231 tumour as before. This was followed by two more rounds of selection on the MDA-MB-231 cells directly *in vitro*.

Individual phage clones from the final round eluates were picked at random, amplified and sequenced. The sequence results from both *in vivo/in vitro* combination bio-panning experiments are summarized in Table 3.5. It was interesting to note the presence of only two sequences, SKSLSPQ and MLHAQTS, in the final phage eluates from both experiments. It was also interesting to note that both of these sequences had previously been identified in the *in vitro* bio-panning on MCF-7 tumour cells. This suggested that these sequences may be binding to a common cell feature present on the surface of both MCF-7 and MDA-MB-231 breast cancer cells.
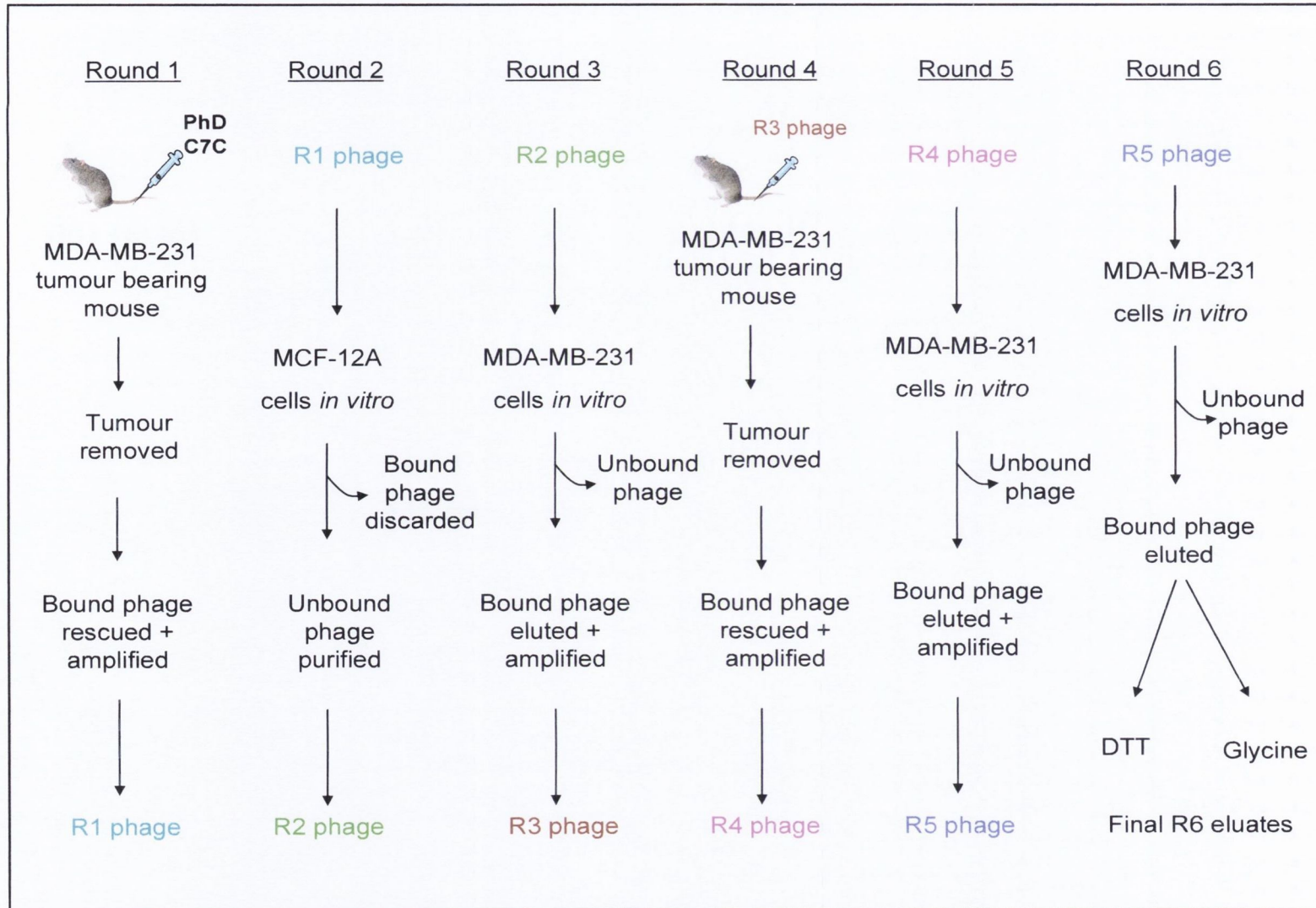
FIG. 3.2 Outline of the *in vivo/in vitro* combination bio-panning experimental protocol.

Table 3.5 Sequence results from *in vivo/in vitro* combination bio-panning experiments.

	Elution	Sequence	Frequency
First experiment	DTT	SKSLSPQ	7/12
		MLHAQTS	5/12
	Glycine buffer	SKSLSPQ	7/12
		MLHAQTS	5/12
Second experiment	DTT	SKSLSPQ	7/12
		MLHAQTS	5/12
	Glycine buffer	SKSLSPQ	5/9
		MLHAQTS	4/9

In order to verify that these two peptide sequences, SKSLSPQ and MLHAQTS, were in fact enriched through the bio-panning process during the *in vivo/in vitro* combination bio-panning experiments rather than being present at such high levels from the beginning, a sample set of phage from the earlier bio-panning rounds of the second *in vivo/in vitro* combination experiment were selected for sequencing. Five phage clones were randomly selected and sequenced from the eluates from rounds 1-4 and are these are listed in Table 3.6.

Table 3.6 Sample set of phage sequences from the second *in vivo/in vitro* combination bio-panning experiment.

Phage Clone	Round 1 Tumour	Round 1 Liver	Round 2	Round 3	Round 4 Tumour	Round 4 Liver
1	PAQFSNI	SPKTPHY	TPQALGS	MLHAQTS	SKSLSPQ	MLHAQTS
2	GNSLHSA	HHLNTRA	TTTERLT	MLHAQTS	SKSLSPQ	MLHAQTS
3	IQSNFSR	PLNNNMK	STLFHSP	MLHAQTS	MLHAQTS	SKSLSPQ
4	HHTLREM	PTASSRH	PTQSMPH	MLHAQTS	SKSLSPQ	MLHAQTS
5	KLPGAHM	QDRQQGF	TLNKTKY	MLHAQTS	SKSLSPQ	MLHAQTS

Following the first round of bio-panning, which was carried out *in vivo*, phage were still showing sequence variety. However following round 3, the phage appeared to be heavily enriched, as MLHAQTS was the only sequence detected. It was interesting to note how quickly the sequence enrichment occurred compared to the *in vitro* bio-panning on MCF-7 cells. Round 4 showed the presence of the two sequences, MLHAQTS and SKSLSPQ, which were detected in the final round eluates. This confirms that these two peptide sequences were enriched during the bio-panning process.

It was also interesting to note the presence of these two sequences in the liver fraction from round 4. This is not too surprising when you consider that the liver is a filtrating organ and substances administered intravenously can often be detected in the liver. When these experiments were underway only the tumour and liver were removed, however any future experiments should also involve the selection of other better control organs, for example the heart or lungs, to check for the presence of circulating phage.

All of the bio-panning experiments performed used an input titer of $2x10^{11}$ pfu of the PhD-C7C library, which has a complexity of over a billion peptide variants. It was therefore a fascinating finding that just two peptide sequences, MLHAQTS and SKSLSPQ, were so heavily enriched and identified in three out of four independent bio-panning experiments.

3.2.3 Selection of leading whole cell recognizer peptides for characterization.

A small number of peptide sequences were chosen for characterization and synthesis. The selection of peptides was based on the frequency of their isolation and their identification in multiple independent bio-panning experiments. These peptides were termed "whole cell recognizers" and their sequences and respective names are listed in Table 3.7. All peptides

were synthesized with a biotin tag and some peptides were also synthesized without a tag (indicated by the brackets).

Table 3.7 List of lead synthetic whole cell recognizer peptides.

Synthetic peptides:	Name:
LSTSSTV-K-Biotin	LST (and Lneg)
ACLSTSSTVCGG(-K-Biotin)	cLSTc
Biotin-K-SACSQSDTVNCGG	cSQSc
Biotin-K-SACTDKLLSHCGG	cTDKc
(Biotin-K-)SACMLHAQTSCGG	cMLHc
(Biotin-K-)SACSKSLSPQCGG	cSKSc
NLPWPANPIKVH	Scrambled

3.2.4 Characterization of synthetic whole cell recognizer peptides.

3.2.4.1 Immuno-fluorescent cell staining.

In order to test the ability of the newly synthesized whole cell recognizer peptides to bind whole tumour cells, a number of immuno-fluorescent cytology experiments were performed.

3.2.4.1.1 The flanking cysteine residues of the 7-mer peptides are important for cell binding.

Initial immuno-fluorescence experiments were performed using the LST peptide, which proved unsuccessful after numerous attempts. The peptide was re-designed (cLSTc) to include the flanking cysteine residues that are present in the peptide when it is encoded in the phage library. It was discovered using this peptide that the flanking cysteine residues of the peptide sequence are very important for cell binding and these cysteine residues were therefore included in all subsequent synthetic peptides. FIG. 3.3 shows the difference in staining observed between the LST and cLSTc peptides when incubated on MCF-7 cells (magnification 400x). The same staining pattern was observed in MDA-MB-231 and MCF-12A cells (data not shown).

It is interesting to note that in the first bio-panning experiment the phage encoding LSTSSTV were predominately eluted using the reducing agent DTT. This suggests that the reduction of the disulfide bridges formed by the flanking cysteines results in the loss of binding of the peptide to the cells and this could indicate why the LST peptide was not able to bind to the cells. The cLSTc peptide showed predominately cytoplasmic staining. Due to the fact that the LST peptide could not bind cells, it was subsequently used as a negative control in many later experiments. It is heretofore referred to as Lneg (for **L**ST **neg**ative control).

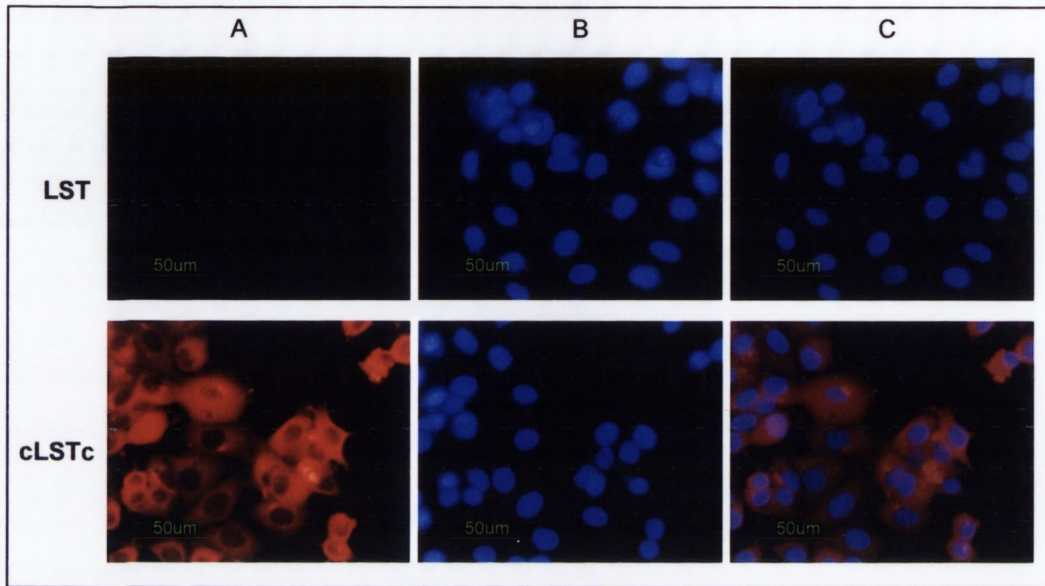FIG. 3.3 Comparison of LST and cLSTc peptide staining on MCF-7 cells.

The top row shows LST staining and the bottom row shows cLSTc staining. Panel A shows the peptide binding detected by ExtrAvidin-Cy3 (red). Panel B shows the location of the nuclei (blue). Panel C is a merge created by overlaying the photos with 50% opacity using Adobe Photoshop. Photos were taken with a Nikon Eclipse E400 microscope. Scale bars show 50μm.

3.2.4.1.2 The whole cell recognizer peptides can bind the tumour and non-tumour cell lines.

In order to test whether the newly synthesized recognizer peptides could bind whole cells, each peptide was incubated at a concentration of 100μg/ml on each of the cell lines as described in the Materials & Methods section 2.7. FIG. 3.4 shows the binding of these peptides to fixed cells from each cell line. The whole cell recognizer peptides have varying binding affinities to the cell lines. Several of the peptides (cMLHc, cSKSc and cLSTc) appeared to stain cells at a much higher level than others (cTDKc and cSQSc). It was interesting to note that the peptides with the highest cell staining intensity were those whose sequences occurred at the highest frequency during the bio-panning experiments. Due to the higher binding intensity of cMLHc, cSKSc and cLSTc, and their higher sequence frequency in the bio-panning experiments, they were chosen for further analysis.

In general all peptides displayed cytoplasmic staining, although this is less evident in the MDA-MB-231 and MCF-12A panels stained with cMLHc, cSKSc and cLSTc. However nuclear exclusion of peptide binding could be demonstrated by reducing the brightness intensity at which the images were taken (data not shown). Immuno-fluorescent cell staining was also performed using concentration gradients of the peptides which demonstrated that the peptide staining was mostly cytoplasmic (data not shown). Staining on MCF-7 cells appeared a little weaker than the other two cell lines (FIG.3.4). The peptides bound the MCF-12A cells at a similar intensity to MDA-MB-231. MCF-12A cells were used repeatedly during the bio-panning experiments in negative selection rounds to remove phage that could bind to non-tumour cells. It was therefore initially surprising to see that the peptides bound to this cell line with a similar intensity as MDA-MB-231. In order to more closely examine the staining patterns between the cells, the localization of peptide staining was studied.
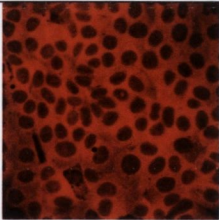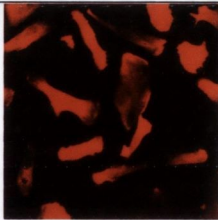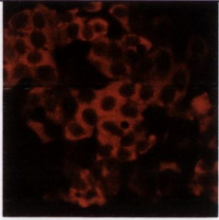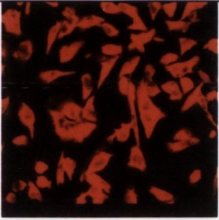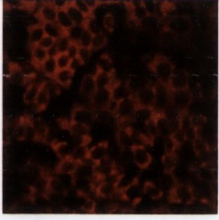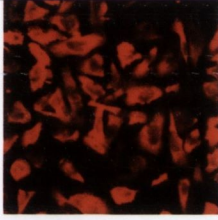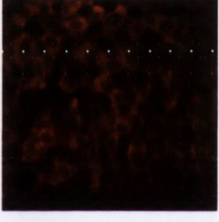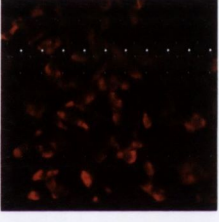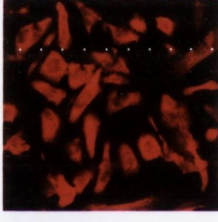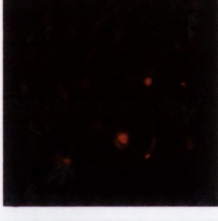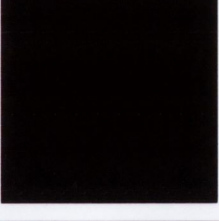
Peptide	MCF-7	MDA-MB-231	MCF-12A
cMLHc			
cSKSc			
cLSTc			
cTDKc			
cSQSc			
Background			

FIG. 3.4 Fixed cell staining with whole cell recognizer peptides.

Biotinylated peptide staining was detected by ExtrAvidin-Cy3 (red) on each cell line.

Photos were taken with an Olympus confocal microscope at a magnification of 600X.

3.2.4.1.3 Localization of peptide binding as determined by confocal microscopy.

Confocal microscopy allows you to examine cells at multiple depths, a process known as optical sectioning. Staining patterns throughout an entire cell can be visualized using this approach. Images can be captured taken at serial depths throughout a cell (known as a z stack). FIG. 3.5 shows an example of the cLSTc peptide staining in each of the cell lines. The frames consist of a z stack (1μm thick) of each cell line stained with the peptide.

Staining did appear weaker on the MCF-7 cells, with the peptide appearing to be located mainly in the cytoplasm of the cells. However, for MDA-MB-231 the staining was stronger and could be seen both in the cytoplasm but also on the cell surface. There was also a cell in frame that showed nuclear staining. MCF-12A cells also showed cytoplasmic and cell surface staining with the peptide. None of the peptides tested showed any major distinguishable staining pattern between the tumour and non-tumour cell lines (data not shown). Therefore despite negative selection on MCF-12A cells, only peptides capable of binding all three cell lines were isolated.

3.2.4.1.4 Cell staining is peptide specific.

In order to test the specificity of the peptide staining, fixed cells were incubated with biotinylated peptide either alone or in the presence of a 10-fold excess of respective unlabelled peptide or a 10-fold excess of scrambled peptide. FIG. 3.6 shows the staining results for the cSKSc peptide on MCF-7 cells (magnification 200x).

MCF-7		MDA-MB-231		MCF-12A	
Cy3	Merge	Cy3	Merge	Cy3	Merge
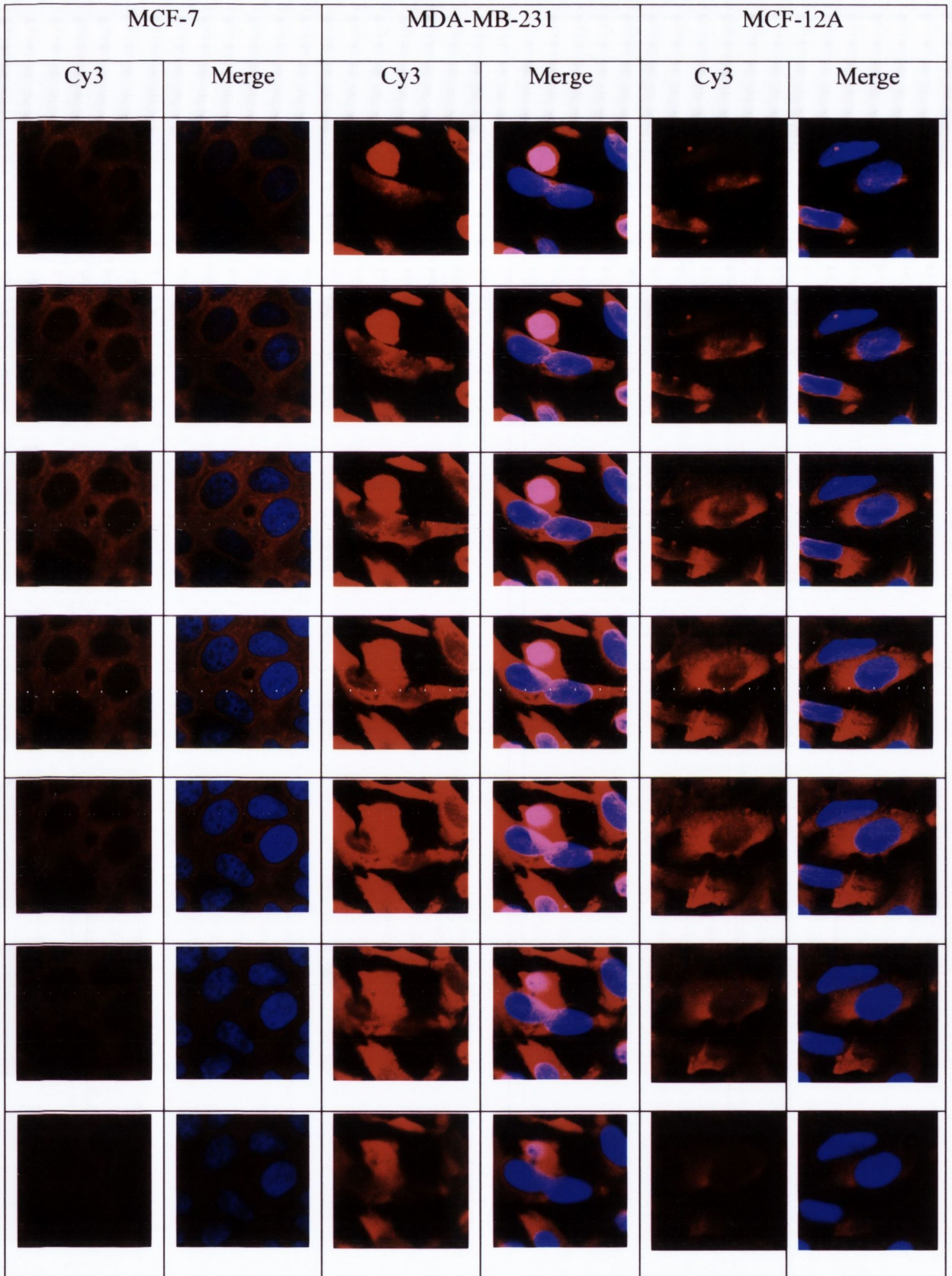
FIG. 3.5 Serial 1μm sections of cells stained with the cLSTc peptide. Panels show either cLSTc peptide alone (red) or a merged image with DAPI (blue). Magnification is 1200x.

74
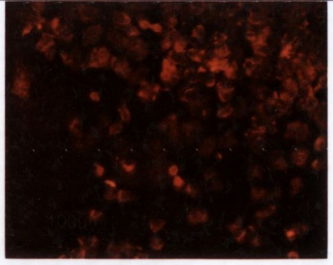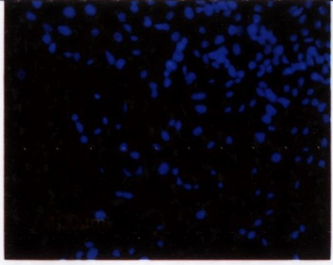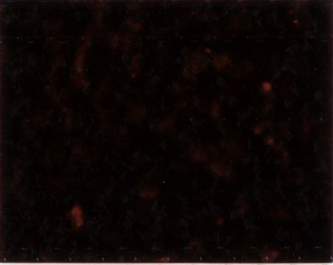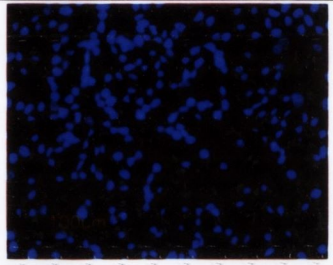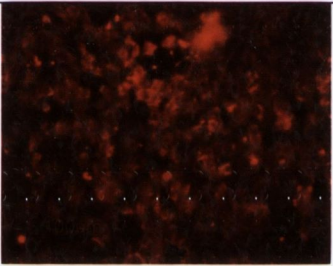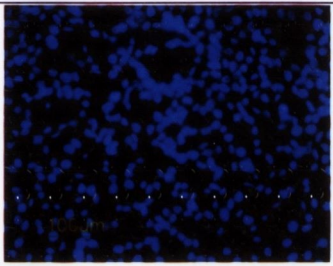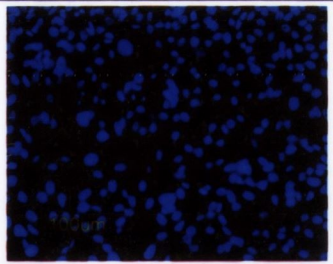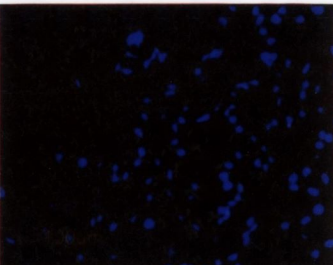
Peptide	Cy3	DAPI
cSKSc (20µg/ml)		
cSKSc + 10x free peptide		
cSKSc + 10x scrambled peptide		
cSKSc + 5mM DTT		
No peptide		

FIG. 3.6 Immuno-fluorescent staining of MCF-7 cells with the cSKSc peptide. Peptide staining was detected by ExtrAvidin-Cy3 (red). Respective DAPI images are also shown. Scale bar is 100µm. Images were taken on Nikon E100 fluorescent microscope.

FIG. 3.6 shows that unlabelled cSKSc peptide competes for binding with the biotinylated peptide which results in a substantial reduction in cell staining, whereas co-incubating with a scrambled peptide doesn't affect the binding, demonstrating that the interaction of cSKSc with MCF-7 cells is specific. It is also interesting to note that incubation with 5mM DTT significantly reduces the amount of cell staining observed. This shows that reduction of the disulfide bridge formed by the flanking cysteine residues of the peptide severely affects the peptides ability to bind cells. This again points to the importance of these residues for cell binding as seen previously by the LST peptides. This experiment was also carried out on MDA-MB-231 and MCF-12A cells and the same results were seen (data not shown). This was also the case for the cMLHc peptide (data not shown).

3.2.4.2 Enzyme-linked immuno-sorbent assays testing the binding of cMLHc and cSKSc recognizer peptides to cellular soluble protein extracts.

ELISA's were performed to test whether the cMLHc and cSKSc peptides could bind soluble cellular proteins in addition to binding whole fixed cells and to compare the levels of binding between the cellular extracts at different peptide concentrations under the same conditions (as described in Chapter 2, section 2.8). In brief, Maxisorp plates were coated with cellular soluble protein extracts from each cell line or BSA. Following blocking, biotinylated peptides were incubated in a two-fold dilution series and bound peptides were detected with extravidin-peroxidase. Wells were incubated with TMB for 5 min and the reaction was stopped with sulfuric acid, allowing the absorbance to be measured at 450nm. Lneg was used as a biotinylated negative control (one data point only: at the highest concentration of 100µg/ml). The results of one experiment can be seen in FIG. 3.7. This experiment was performed three independent times, with the same results (data not shown).
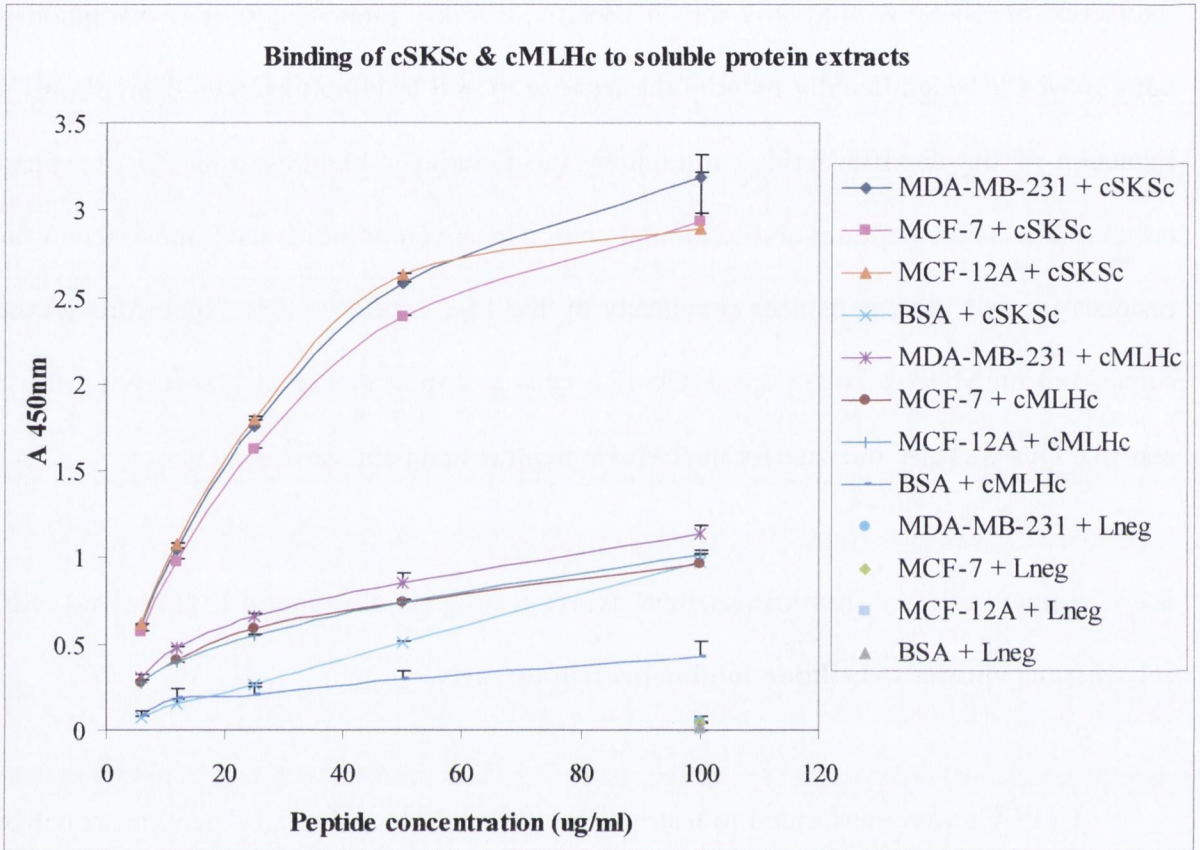
FIG. 3.7 Binding of whole cell recognizer peptides to soluble cellular protein extracts. Values

represent averages of duplicate wells. Error bars indicate the standard deviation.

Both the cSKSc and cMLHc peptide bound to the cellular proteins in a concentration-dependent manner. The cSKSc peptide bound to each cellular extract more strongly than cMLHc (approximately 2-3 fold more). The cMLHc peptide showed a slight preference for the tumour-derived proteins over the MCF-12A proteins. At the highest concentration, the peptides bound to the cellular proteins approximately 6-fold more than the BSA control. The Lneg control peptide didn't show any binding. This verifies that these two peptides can not only bind to whole fixed cells but also to cell-derived proteins and they do so in a concentration-dependent manner. It is interesting to note that the immuno-fluorescent cell staining suggested that these peptides bind to cells at similar intensities, however the ELISA results indicate a difference in the binding between the two peptides.

3.2.4.3 Flow cytometry to examine live cell recognizer peptide binding.

Flow cytometry was utilized to investigate whether the whole cell recognizer peptides could bind to live cells and to examine if any tumour specificity could be detected. Trypsinized cells were incubated with 50μg/ml of biotinylated peptides for 30min, after which the cells were washed, fixed and bound peptides were detected by streptavidin-FITC. Lneg was used as a biotinylated negative control. Duplicate samples were performed in every experiment and the experiment was repeated three times. FIG. 3.8 shows one data set from each of the three independent experiments. Graphs represent the green fluorescence detected by the FL1 channel.

Cells Exp.	MDA-MB-231	MCF-12A	MCF-7
1			
2			
3			

cMLHc —— cSKSc —— Lneg —— No peptide ——
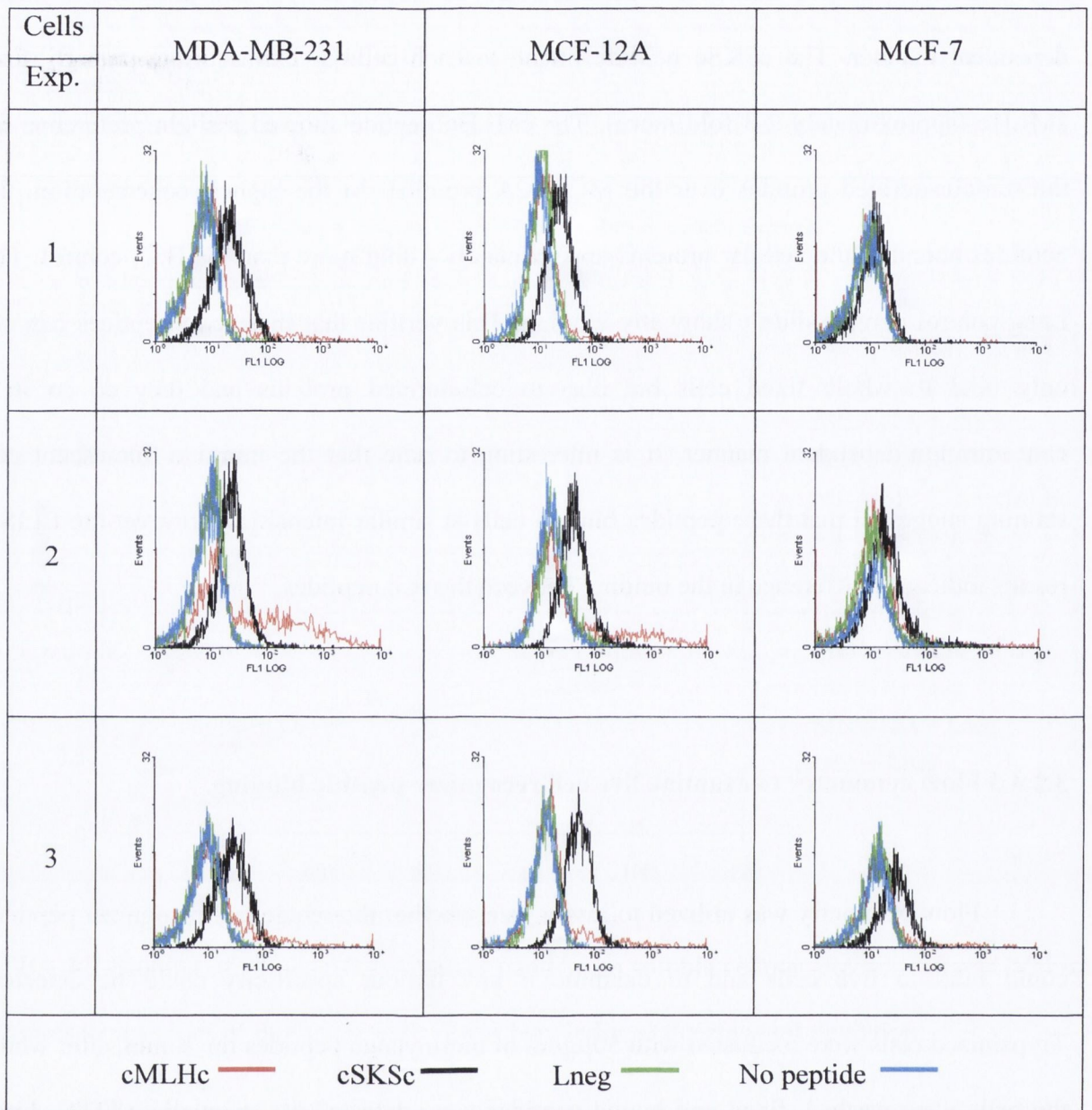
FIG. 3.8 Flow cytometry showing whole cell recognizer peptides binding to live cells. Each cell line was incubated with the two recognizer peptides cSKSc (black line) and cMLHc (red line), in addition to the negative control peptide Lneg (green line). Cells alone were also run as a background control (no peptide, blue line). Graphs represent overlays of the four samples per cell line. X-axis shows FL1 Log and the Y-axis shows the number of events. Exp. represents the experiment number.

The cSKSc peptide bound to live cells more strongly and more homogeneously than the cMLHc peptide. In the first experiment MDA-MB-231 cells showed slightly more staining than MCF-12A cells but across the three experiments there didn't appear to be any major difference between the tumour MDA-MB-231 cells and the non-tumour MCF-12A cells. However there was a noticeable difference in staining for the MCF-7 cells, which appeared to show less staining with the cSKSc peptide than the other cell lines. This is consistent with the fixed cell immuno-fluorescent staining experiments. The cMLHc peptide demonstrated a different binding pattern to that of the cSKSc peptide. The peaks were much broader and smaller than cSKSc, suggesting that the peptide bound to cells within a given population at varying degrees and that the amount of binding was lower than the cSKSc peptide. The binding also appeared stronger on the MDA-MB-231 cells, when compared to the other two cell lines. These findings are consistent with the ELISA data. The Lneg peptide showed no binding to any of the cell lines.

3.2.5 Homology of whole cell recognizer peptides to known proteins.

In order to investigate whether the whole cell recognizer peptide sequences had any homology to known proteins, a homology search was carried out using BLASTp version 2.2.24 (Altschul et al., 1997) and the human Swiss Prot database. The five most significant hits are listed in Table 3.8. The LSTSSTV sequence had the most hits with a total of 324 and the top five hits include proteins involved in actin-mobitily, gene regulation, cell cycle regulation and hemidesmosome integrity. There was also a strong sequence similarity (high score) to a number of mucins, including over 50 alignments with MUC-16 (better known as ovarian carcinoma antigen CA-125), as well as trophinin (MAGE-D3), however these are not listed on the table as they were less significant (higher E value).

Table 3.8 Homology of whole cell recognizer peptides to known proteins.

Recognizer peptide	Homologous protein	Accession No.	Shared sequence
LSTSSTV (324 hits)	Myosin-binding protein H	Q13203.4	LSTS-TV
	Pogo transposable element ZNF domain	Q7Z3K3.2	LSTS-TV
	Protein FAM186A	A6NE01.3	LSTSST
	Zinc finger homeobox protein3	Q15911.2	LS-SSTV
	Integrin beta-4	P16144.4	LSTSST
SKSLSPQ (157 hits)	Protein ALO17	Q9HCF4.2	-KSLSPQ
	Interleukin-28B	Q8IZI9.2	-KSLSPQ
	Interferon epsilon	Q86WN2.1	-KSLSPQ
	Nucleolar transcription factor 1	P17480.1	-KSLSPQ
	Interleukin-29	Q8IU54.1	-KSLSPQ
MLHAQTS (107 hits)	Phosphatidylglycerophosphate synthase 1	Q32NB8.1	MLHAQT
	tRNA-dihydrouridine synthase 1-like	Q6P1R4.1	MLHAQ
	C-type lectin domain family 18 member A	A5D8T8.3	MLH-+TS
	C-type lectin domain family 18 member C	Q8NCF0.2	MLH-+TS
	C-type lectin domain family 18 member B	Q6UXF7.1	MLH-+TS

SKSLSPQ had a total of 157 hits with the top five hits including a lymphoma proto-oncogene, a number of interleukins and a transcription factor. MLHAQTS had the fewest homology hits with 107, however it had the most significant hit (E value 6.5) of all the peptides tested and showed alignment with phosphatidylglycerophosphate synthase 1, an enzyme involved in the biosynthesis of phospholipids. It also had homology with a number of sugar binding proteins, however these homologies were less significant.

81

3.2.6 Examination of the ability of the whole cell recognizer peptides to bind patient tissue samples.

3.2.6.1 Immuno-fluorescent staining of breast tumour tissues.

The whole cell recognizer peptides, cSKSc and cMLHc, both showed strong binding to each of the three cell lines using fixed cell immuno-fluorescent staining. Concentration-dependent binding to soluble cellular proteins was also demonstrated, although cSKSc showed a higher level of binding to this protein fraction than cMLHc. This was also the case with the live cell staining, as demonstrated by flow cytometry. However the cMLHc showed slightly more binding to MDA-MB-231 tumour proteins in the ELISA and to the live tumour cells with flow cytometry. The cMLHc peptide was therefore used to investigate whether this peptide could distinguish between normal and tumour cells *in situ*. This was achieved by examining the ability of the cMLHc peptide to bind to patient breast tumour tissues.

FFPE-breast tumour tissue samples were supplied by our collaborators in Prof. Elaine Kay's lab, at the Department of Pathology, RCSI Education & Research Centre, Beaumont Hospital. In brief, sections were de-waxed, underwent heat-induced antigen retrieval, blocked and incubated with the cMLHc peptide (1µg/ml), which was detected using extravidin-Cy3, as described in Chapter 2, section 2.11.1. Nuclei were imaged by inclusion of DAPI in the mounting media. Slides were examined using a Nikon E100 fluorescent microscope and photographed immediately. These images are displayed in FIG. 3.9 (magnification 200x).
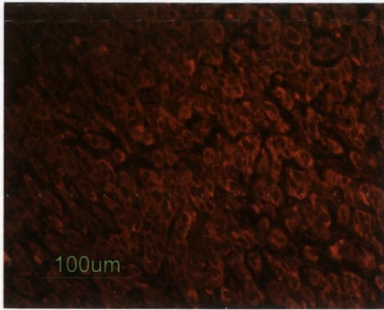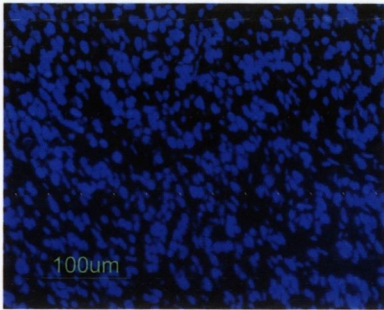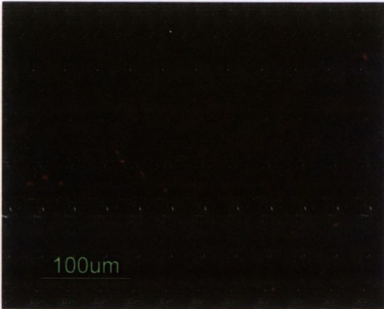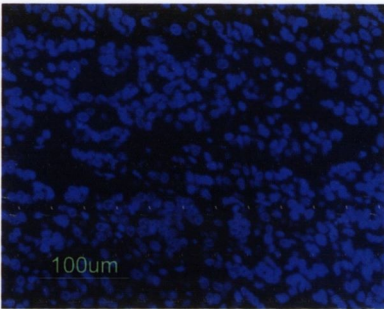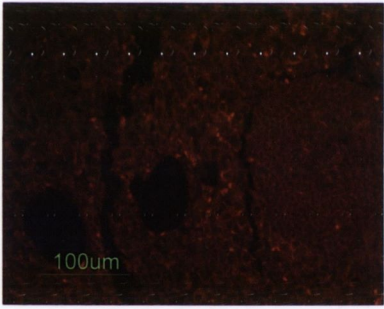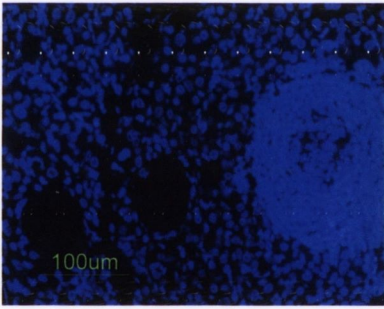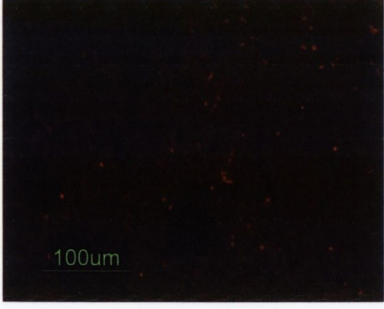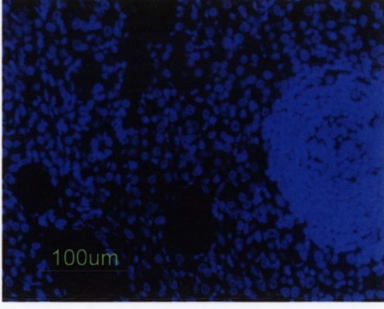
Tissue	Sample	Cy3	DAPI
Breast tumour tissue 1	cMLHc (1µg/ml)		
	Background		
Breast tumour tissue 2	cMLHc (1µg/ml)		
	Background		

FIG. 3.9 Immuno-fluorescent tissue staining with the cMLHc peptide. Peptide staining detected by Cy3 (red), respective tissue background fluorescence and corresponding DAPI images indicating the position of the nuclei (blue) are shown. Photos taken with a Nikon E100 fluorescent microscope.

The cMLHc peptide showed binding to both of the breast tumour tissues tested. The binding appeared to be localized mainly in the cytoplasm of the cells. However it was difficult to visualize a specific site of peptide binding. Rather most, if not all, of the cells within the tissue appeared to be stained with the peptide.

3.2.6.2 Examination of whole cell recognizer peptide organ-specificity using TMA's.

The cMLHc peptide previously showed binding to both MDA-MB-231 and MCF-7 breast tumour cell lines, as well as the MCF-12A non-tumour breast cell line. It also showed rather evenly distributed cytoplasmic binding to cells within two breast tumour tissue sections. We therefore wanted to investigate whether the binding of this peptide was organ- or tissue-specific. To examine the staining patterns to multiple organs and tissues, TMA technology was used.

TMA's containing 48 tissue cores derived from 8 different organs were purchased from Creative Biolabs Inc. Approximately half of the tissue cores were derived from tumour tissue and the other half derived from respective normal tissue from other patients. The identification of peptides with specific organ staining could provide an indication of potential clinical uses. TMA's were processed in an similar manner as the previous tissue sections and were stained with the cMLHc, cSKSc and cLSTc peptides. Peptide binding was again detected using extravidin-Cy3 and counterstained with DAPI. An additional slide without a peptide was processed in an identical manner to examine tissue auto-fluorescence and any background fluorescence from the staining procedure. One set of tumour and non-tumour tissue samples stained with the cMLHc peptide are shown in FIG. 3.10 and FIG. 3.11, respectively.
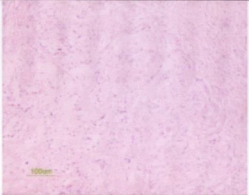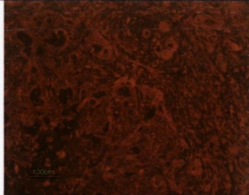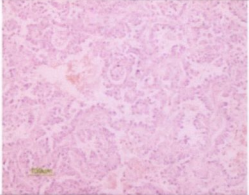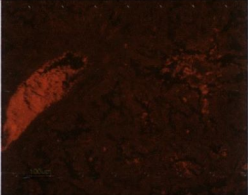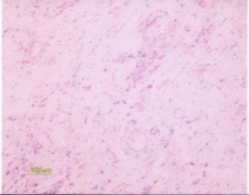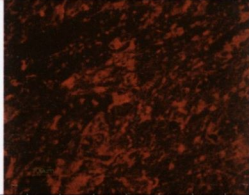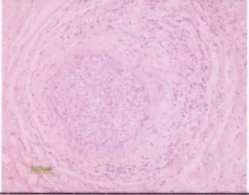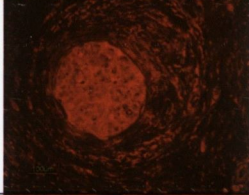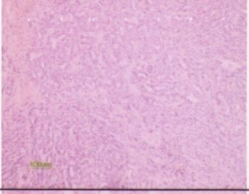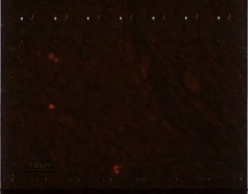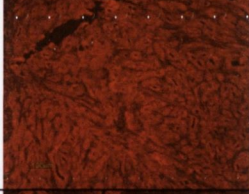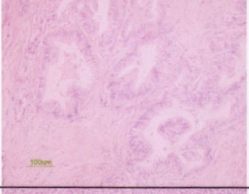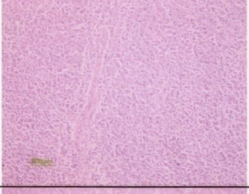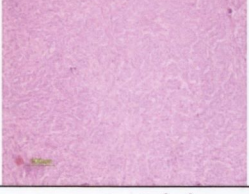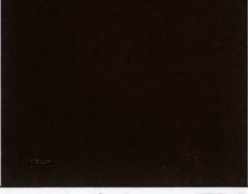
Tumour tissue	H&E	Background	cMLHc
Liver			
Lung			
Cerebrum			
Breast			
Prostate			
Intestine			
Kidney			
Epiploon			

FIG. 3.10 Immuno-fluorescent staining of tumour tissues (TMA) with cMLHc. H&E is hematoxylin & eosin. Peptide binding detected by extravidin-Cy3 (red). Magnification 200X.
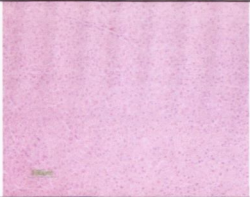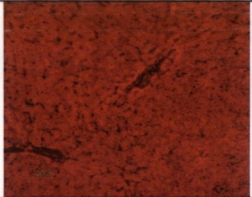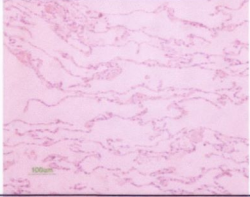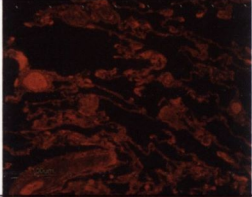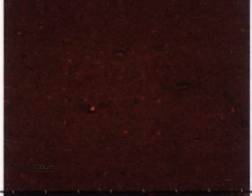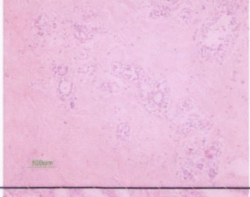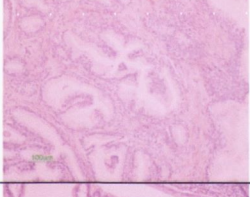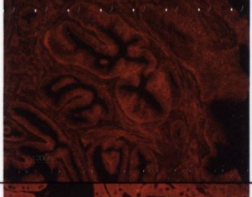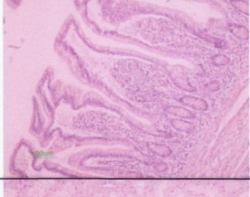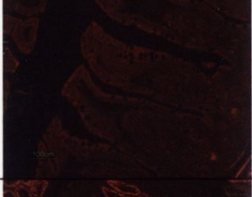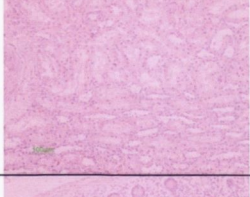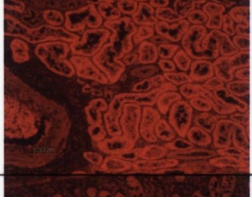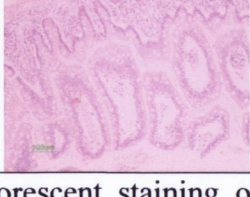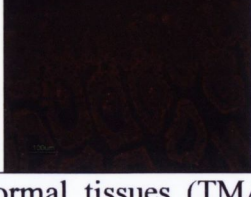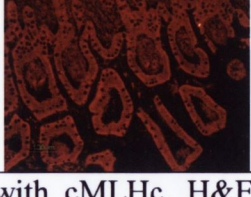
Normal tissue	H & E	Background	MLH
Liver			
Lung			
Cerebrum			
Breast			
Prostate			
Intestine			
Kidney			
Epiploon			

FIG.3.11 Immuno-fluorescent staining of normal tissues (TMA) with cMLHc. H&E is hematoxylin & eosin. Peptide binding detected by extravidin-Cy3 (red). Magnification is 200X.

The cMLHc peptide bound to all the tumour tissues tested. It also appeared to bind to most of the normal tissues also, however binding to normal lung, cerebrum and breast tissue appeared to be lower. The cLSTc peptide showed a very similar pattern and intensity of staining as the cMLHc peptide, however the cSKSc peptide stained all of the sections more intensely, including all of the normal tissues tested (data not shown).

It was difficult to visualize any sites of specific staining within the tissues and the presence of tissue auto-fluorescence made it extremely difficult to quantify levels of specific staining. DAB staining is more routinely performed in diagnostic pathology labs to evaluate tissue bio-markers. Although fluorescent staining can be more sensitive, chemical staining with substrates such as DAB have several advantages which include; tissue auto-fluorescence is overcome, the staining doesn't fade or quench and the slides can be stored permanently for future analysis.

DAB staining with the cMLHc peptide was performed by our collaborator Robert Cummins, senior medical scientist in the lab of Prof. Elaine Kay at the Department of Pathology, RCSI Education & Research Centre, Beaumont Hospital as described in Chapter 2, Section 2.11.3. The cMLHc peptide (500ng/ml) showed binding to all tissues tested (76 cores from 20 tissues) and a sample set, including normal tonsil, ovarian tumour and breast tumour tissues, is shown in FIG. 3.12. The peptide is therefore not specific to breast tissue, as previously hypothesized. In addition, the peptide appeared to bind most cell types present in the tissues, including lymphocytes, and was also present in the stroma. It therefore didn't appear to demonstrate any cell, tissue or organ specificity, which was consistent with the results seen in the previous fluorescent tissue staining experiments.

Normal tonsil tissue	
Ovarian tumour tissue (metastatic breast cancer)	
Breast tumour tissue	
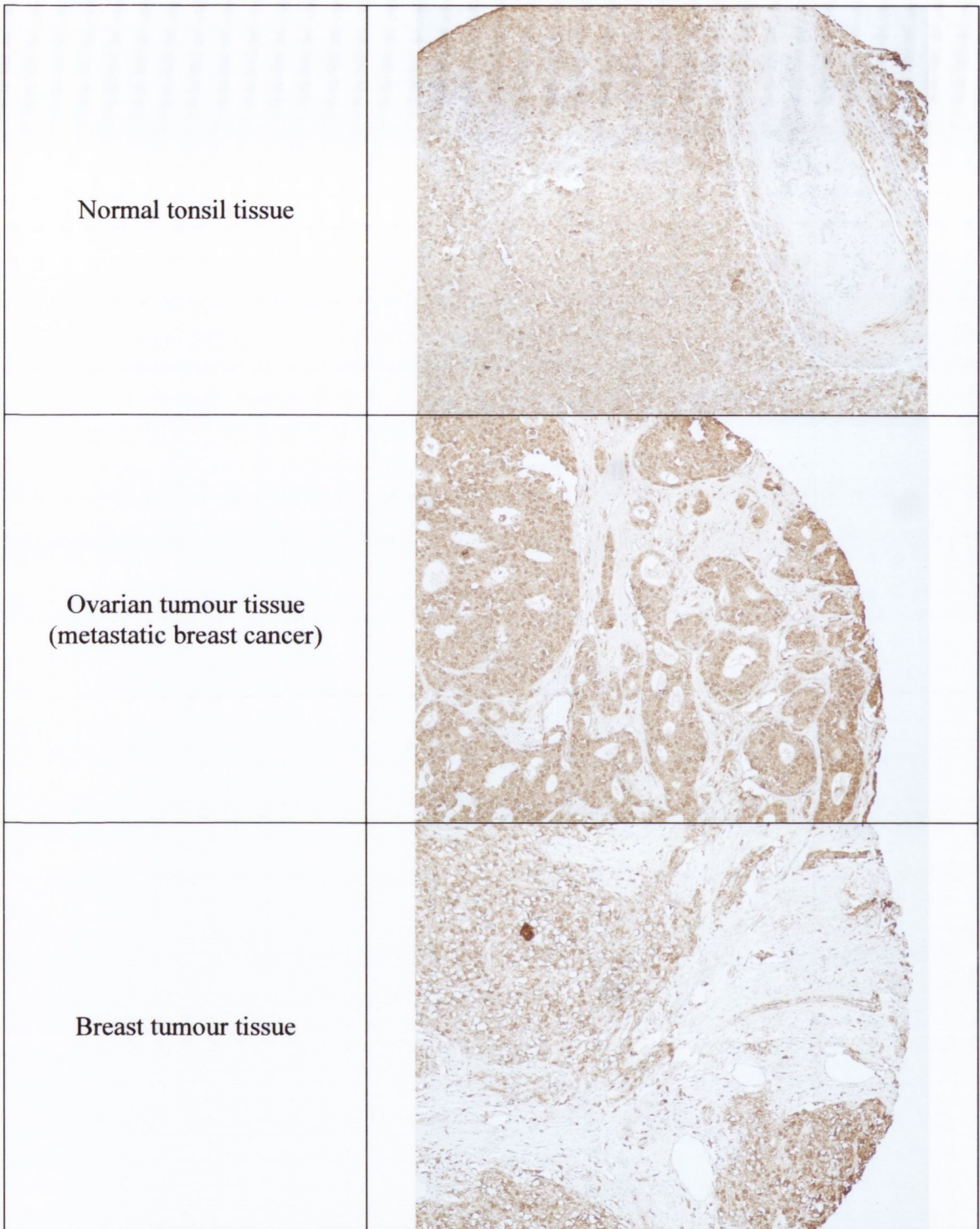
FIG. 3.12 DAB staining of patient tissue cores with the cMLHc peptide.

Magnification 100x.

3.3 Discussion.

The aim of this chapter was to identify peptides that could bind to whole breast tumour cells. This was achieved firstly in two bio-panning experiments on MCF-7 cells using the PhD-C7C phage library. The first experiment identified one heavily enriched sequence, LSTSSTV, in addition to eleven other novel peptide sequences. Sequence alignment led to the identification of a number of putative cell-binding motifs; SXSXTV, HRN, PXXR, MXXR and TXR. The second experiment yielded two newly identified heavily enriched peptide sequences; MLHAQTS and SKSLSPQ, in addition to one sequence that had also been isolated in the first experiment: SQSDTVN. When aligned with the first round sequences another small set of motifs were identified; MLXQ, SXS, KXLS and LXXQ.

By lengthening the second bio-panning experiment by three rounds more sequence enrichment was evident. Twelve different peptide sequences were identified in the first bio-panning compared to three sequences in the second. Therefore *in vitro* bio-panning on live cells yielded better sequence enrichment after nine rounds when compared to six. These experiments resulted in the identification of a total of fourteen novel peptides sequences, and a number of putative motifs, that bound to live MCF-7 tumour cells *in vitro*.

A second bio-panning approach was employed to identify peptides that bind to MDA-MB-231 tumour cells. This involved selecting peptides that could home to an MDA-MB-231-induced tumour *in vivo*, but also directly bind MDA-MB-231 tumour cells *in vitro*. Two peptide sequences; MLHAQTS and SKSLSPQ, dominated in both experiments. It was interesting to note that both of these peptides were identified in the second MCF-7 bio-panning experiment and this suggests that these sequences may be binding to a common cell feature present on the surface of both MCF-7 and MDA-MB-231 breast cancer cells. Both peptides were shown to become enriched after just three rounds in the MDA-MB-231 bio-

panning experiment. Therefore *in vivo* bio-panning requires fewer rounds of selection than *in vitro* bio-panning in order to enrich peptides, however the establishment of xenograft tumours can be time-consuming and expensive. Interestingly *in vivo* bio-panning has shown to result in enrichment of peptides or peptide motifs in a small number of rounds (Krag et al., 2006). This is believed to be due to the fact that phage binding to other organs are instantly depleted from the selected phage pool (Laakkonen and Vuorinen, 2010).

Tri-peptide motifs have been shown to be sufficient to confer selectivity to a particular target. Pasqualini and Ruoslahti performed the first ever documented *in vivo* bio-panning experiment in 1996 and since then have gone on to identify peptides that home to a wide variety of organs and tumours in mice, in addition to human tumours in xenograft models (reviewed (Laakkonen and Vuorinen, 2010)). They identified the peptide motif RGD which is now known to bind members of the integrin family and home to tumour vasculature *in vivo*. They also identified a second specific motif, NGR, which binds to aminopeptidase N which is upregulated during angiogenesis. It is now believed that tumours upregulate factors involved in angiogenesis, which can provide targets whose expression are low or absent in normal tissues (Laakkonen and Vuorinen, 2010). In fact both RGD and NGR have been used to target a number of different drugs to tumours in animals with great success and both have now entered clinical trials (Laakkonen and Vuorinen, 2010; Shadidi and Sioud, 2003).

The ability to translate homing peptides originally identified in animal models to human treatment is currently being investigated by the afore-mentioned clinical trials. However two bio-panning studies have been performed in humans. The first was performed in 2002 and involved injecting a brain-dead cancer patient with a phage library (CX$_7$C), similar to the one used in this work, and isolating organ homing phage by needle biopsy (Arap et al., 2002). They identified tripeptide motifs that homed to different organs, one of which was LSP which homed to fat. This motif is shared with the SKS<u>LSP</u>Q sequence identified in this study.

90

Interestingly one of their peptides (RRAGGS, motif AGG) localized in the prostate and had sequence homology to IL-11. They subsequently demonstrated that the peptide was a true mimic of IL-11 with specificity for the prostate and are now evaluating its clinical relevance (Arap et al., 2002).

The second experiment conducted in humans was a Phase I clinical trial with eight patients with stage IV cancer (Krag et al., 2006). One patient with breast cancer was administered with a random peptide phage library ($X_4CX_{10}CX_4$) and after 30min a tumour nodule was surgically removed. Phage purified from this tumour were amplified and re-administered to the patient, followed by surgical removal of another tumour nodule. An enrichment of tumour-specific peptide sequences was observed. The most heavily enriched peptide occurred in 56 out of the 90 clones analyzed and had the sequence GSPQCPGGFNCPRCDCGAGY. It is interesting to note that this peptide has three amino acids in common with our newly identified SKSLSPQ peptide. Another peptide isolated from the same tumour, RHTVCRVSLSSVQGSCSHEY, also shared some sequence homology to both SKSLSPQ and LSTSSTV.

These studies show that peptide sequence enrichment can occur very quickly and that peptide motifs as short as three amino acids in length can demonstrate target specificity. It is also interesting to note the sequence similarity between some of the peptides isolated from the studies carried out in cancer patients to the peptides isolated in this study. The LSTSSTV peptide has homology to a documented ligand specific to tumour cells in breast cancer tissue (SSTA) and with a ligand to cell surface receptor CD-21 (RMWPSSTVNLSAGRR) (Aina et al., 2007).

The lead whole cell recognizer peptides were firstly tested for their ability to bind each of the cell lines using fixed cell immuno-fluorescent staining. The three whole cell recognizer peptides, cMLHc, cSKSc and cLSTc showed much stronger cell staining than cTDKc and

91

cSQSc. It was particularly interesting to note the difference in staining intensity between cSKSc and cSQSc as they shared an SXS motif. In addition the cSKSc peptide shared a KXLS motif with cTDKc, however as the cSKSc peptide staining appeared stronger than cTDKc, this motif must not be the main determinant for cell binding.

The three whole cell recognizer peptides (cMLHc, cSKSc and cLSTc) bound to both MCF-7 and MDA-MB-231 tumour cells but also bound to the non-tumour MCF-12A cells. The MCF-12A cells were used to deplete phage binding to normal cells during the bio-panning experiments but yet each of the peptides could bind to these cells. However this doesn't appear to be a unique occurrence, as similar experiments carried out by other groups have shown that even more subtractive selection steps may not generate a cell-specific peptide. One group used three rounds of subtractive selection on either HeLa (cervical cancer) or 293 (embryonic kidney) cells, prior to each of the four rounds of selection on MDA-MB-231 cells and failed to find a peptide specific for MDA-MB-231 (Rasmussen et al., 2002). It is possible that there may not be many differences between the surfaces of the three cell lines used in this study. Indeed, peptides isolated for binding one tumour cell type also bound the other, in addition to the non-tumour cells. Future whole cell bio-panning experiments should aim to use isogenic tumour and non-tumour cells and this approach may perhaps be a better model for isolating more specific tumour cell surface targets.

Confocal microscopy showed that the peptides bound fixed cells from each cell line and localized in the cytoplasm and cell surface of these cells. The specificity of the peptide-binding was demonstrated by the fact that co-incubation with an excess of unlabeled peptide but not a scrambled peptide caused a major reduction in cell staining. It was also shown that the binding of the peptides is largely dependent on their cyclic nature, as absence of the flanking cysteine residues (as demonstrated by the Lneg and cLSTc peptides) or reduction of the disulfide bridge formed between the cysteines (using DTT) abolished cell staining.

Both the cSKSc and cMLHc peptides were shown to bind to soluble cellular protein extracts at a higher level than a control protein. Characterization of the cLSTc was not possible due to limited amounts of available peptide, as the chemical synthesis of the peptide proved difficult. The cSKSc peptide bound to the cellular protein extracts at a higher level than cMLHc, and this would suggest that they either bound to different cellular targets or they bound to the same target but with different affinities. The cMLHc peptide appeared to bind to MDA-MB-231-derived proteins at a slightly higher level than proteins derived from the other two cell lines. Both peptides bound their cellular targets in a concentration-dependent manner.

Flow cytometry was used to evaluate the ability of these two peptides to bind to live cells. Interestingly the cSKSc peptide bound to the cells at a higher level and more homogenously than the cMLHc peptide. This higher level of binding was consistent with the ELISA data. The difference observed for the cMLHc peptide between the fixed and live cell staining would suggest that the cellular receptor for this peptide was not present or was altered in the live cell experiment. As trypsin digestion was employed to prevent cell aggregation during flow cytometry, it is possible that the target bound by cMLHc is present in the extracellular matrix of the cells and that this target was partially digested or removed by incubation with trypsin. This would be consistent with the ELISA finding that cMLHc binds soluble protein extracts at a lower level than cSKSc, as extracellular matrix proteins, cell surface proteins and lipids can often be quite insoluble. This also suggests that these two peptides bind to different cellular targets.

The homology searches provide a possible indication of the proteins mimicked by the whole cell recognizer peptides, which may provide clues to their cellular binding partners. For example, if LSTSSTV truly mimicked integrin beta 4, it may therefore be binding to integrin alpha 6, with which it forms a receptor for laminin. In the case of SKSLSPQ, which has homology to a number of interleukins, it may bind to an interleukin receptor. Whereas

MLHAQTS may bind a phospholipid as it had homology with an enzyme involved in phospholipid biosynthesis, or it may bind a sugar as it also had homology to lectin domain proteins. This would be consistent with the indication that cMLHc may bind a target present in the extracellular matrix or on the cell surface. The true identity of the cellular receptors remains to be determined, but homology searches do provide food for thought.

Extracellular matrix proteins have functions in cell adhesion, migration, proliferation and gene regulation and remodeling of the extracellular matrix is believed to be an important factor in tumour angiogenesis and metastasis. Akula et al (Akalu et al., 2007) identified a cryptic extracellular matrix epitope in laminin that regulates tumour cell behaviour and generated a peptide called STQ (STQNASLLSLTV), which binds this epitope and inhibited angiogenesis, tumour growth and metastasis in an animal model. They used truncated versions of the peptide to determine its functional domains but couldn't localize its function to any one domain. The truncated peptide with the most activity was LSLTV. It is interesting to note the sequence similarity of the STQ peptide and its truncated peptide to our LSTSSTV peptide. It is especially interesting to note that LSTSSTV has homology to integrin beta-4, which together with integrin alpha-6, is known to form a receptor for laminin.

As the whole cell recognizer peptides bound to the MDA-MB-231 tumour cells, MCF-7 tumour cells and non-tumour MCF-12A cells, all three of which are derived from breast epithelial cells, in addition to localizing to an MDA-MB-231 xenograft breast tumour *in vivo*, we hypothesized that perhaps the peptides were breast-specific. To assess the specificity of the whole cell recognizer peptides in tissues, their distribution in breast tissue sections and TMA's was examined. The cMLHc peptide was shown to bind to breast tumour tissue sections using immuno-fluorescence. The peptide could be seen in the cytoplasm of the cells but didn't appear to bind to a specific area within the tissue sections rather it seemed to bind most cells evenly. TMA's were subsequently incubated with the whole cell recognizer

94

peptides to determine whether they had any organ specificity. Using immuno-fluorescent tissue staining there didn't appear to be any obvious organ or tumour specificity but tissue auto-fluorescence made it difficult to critically evaluate or quantify the staining. DAB staining of a TMA with the cMLHc peptide confirmed that the peptide didn't have any notable organ or cell specificity. The ability of the whole cell recognizer peptides to bind multiple cell and organ tissue types suggests that the peptides bind to a target common to many human cells.

The result of the work detailed in this chapter was the identification of a set of novel peptides, using phage display, selected for their ability to bind whole breast tumour cells and to my knowledge these particular peptides have never been isolated or published before, nor have they been isolated in studies examining target-unrelated peptides identified from phage libraries (Menendez and Scott, 2005). They share some sequence similarity and motifs to peptides identified with specificity to particular human organs and tumours, however the significance of these motifs remains to be determined. They also show homology to known proteins, including a variety of extracellular matrix proteins, enzymes and cell signaling molecules and the identification of the cellular binding partners of the peptides could provide useful information about the surface proteins expressed on these cells.

The overall aim of this project was the generation of peptides that can specifically bind to tumour cells and the generation of tumour antigen mimotopes with the potential to induce immune activity. As the peptides identified here didn't show any notable tumour or organ specificity, in addition to the fact that we had no knowledge of the immunogenicity of their putative cellular binding targets, they were not taken any further into development. We rather focused our work on a group of proteins known to chaperone immunogenic tumour antigens. This group of proteins belongs to the HSP70 family and the identification of peptides that bind to these protein complexes is described in the next chapter.

Chapter 4:

Generation and characterization of HSP70-PC recognizer peptides.

4.1 Introduction

HSP70 is a known chaperone protein, with multiple functions in normal cells including protein folding, protein transport and stress responses. More importantly in the context of cancer, it has been shown to be associated with a pool of antigenic and immunogenic peptides when purified from tumour cells. HSP70 and its associated peptide complex (HSP70-PC) have been shown to be capable of stimulating anti-tumour immune responses and this is thought to be largely due to the presentation by HSP70 of its associated peptides to the cell surface for presentation by the MHC Class I pathway (Przepiorka and Srivastava, 1998). HSP70-PC's have also been shown to be capable of activating an immune response by directly presenting peptides to antigen presenting cells (Srivastava, 2002). However the identity of the peptides present in the HSP70-PC's remains unidentified or unpublished. Since cancers are heterogeneous in nature, it has postulated that tumour antigens can be patient-specific and that such antigens will form part of the repertoire of peptides associated with HSP70. Based on this hypothesis a number of clinical trials in which autologous HSP70-PC's are being used to stimulate immune responses are currently being conducted (Srivastava et al., 2009).

Our interest in HSP70-PC's comes from their association with this reservoir of unidentified tumour antigens. Although some tumour antigens can be patient-specific, for example a unique single-nucleotide polymorphism (SNP) causing an amino acid change, other tumour antigens could be shared, for example aberrantly- or over-expressed proteins or aberrantly modified proteins. We chose to use HSP70-PC's purified from two breast tumour cell lines, MDA-MB-231 and MCF-7, as a source of breast tumour antigens. The aim of this chapter was to identify peptides using the phage-peptide display library PhD-C7C that could specifically bind to tumour antigens associated with HSP70 and thus generate peptides termed

"HSP70-PC recognizers". Such peptides have the potential to act as homing molecules for tumour cells. In addition, they have potential for use in the generation of tumour mimotopes using mirror image phage display. The specificity of a select few HSP70-PC recognizers was analyzed by protein binding assays and immuno-histochemical staining on patient tumour tissues.

4.2 Results

4.2.1 Purification of HSP70-PC's from breast cell lines.

The aim of this study was to identify peptides that can specifically bind tumour antigens, as such peptides can potentially be used as cancer biomarkers or as homing molecules for the delivery of therapeutic agents directly to cancer cells. As HSP70-PC's derived from tumours are known to contain pools of immunogenic tumour antigens, we chose to use HSP70-PC's purified from breast cancer cell lines as a source of breast tumour antigens. HSP70-PC's were purified from the cell lines using ADP-affinity chromatography as described in Chapter 2, section 2.12. The use of ADP ensures that peptides associated with HSP70 are retained, whereas the use of ATP is known to dissociate the peptides (Srivastava, 1997). Affinity-purified HSP70-PC's from the two breast cancer cell lines, MDA-MB-231 and MCF-7 and the non-tumour MCF-12A breast cell line were separated by SDS-PAGE and the presence of HSP70 within the extracts was verified by Western blot, as shown in FIG. 4.1.

Bands of approximately 70kDa are seen in the control human recombinant HSP70 (hrHSP70) sample and in each of the cellular HSP70-PC extracts. These bands were confirmed as HSP70 using a monoclonal anti-HSP70 antibody. The affinity-purified HSP70-PC extracts also showed the presence of three unknown proteins. Since these proteins were not recognized by the anti-HSP70 antibody, it is unlikely that they are degradation products of HSP70. Therefore these proteins were either associated with the HSP70-PC's or proteins that were co-purified by their affinity to the ADP-agarose column used during the purification. Initial attempts to further separate the HSP70-PC's from the other proteins by fast purification liquid chromatography (FPLC) were unsuccessful and due to the low amounts of native HSP70-PC's available further FPLC experimentation was not feasible.
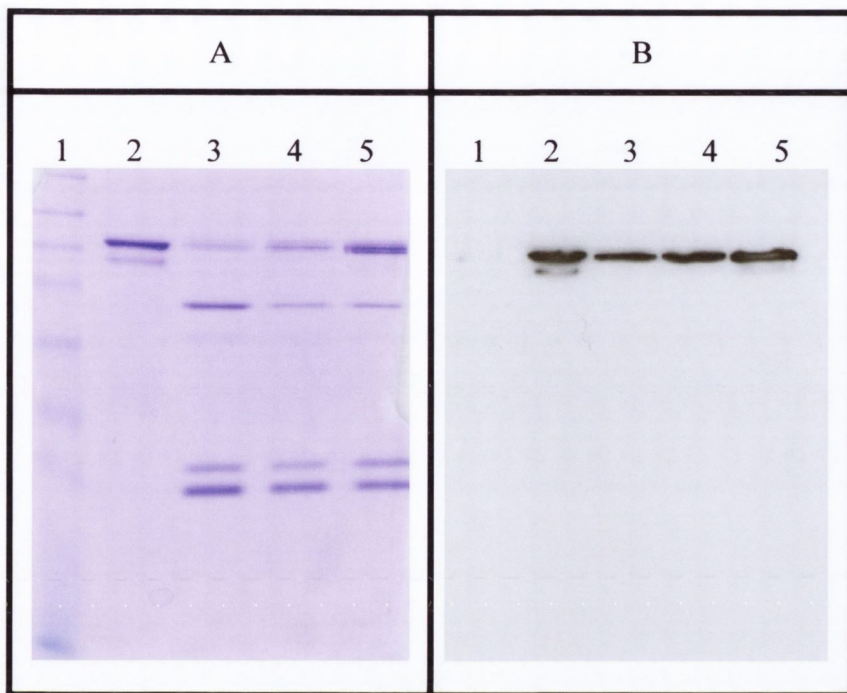
FIG. 4.1 SDS-PAGE and corresponding Western blot of purified cellular HSP70-PC's.

Panel A: 12% SDS-PAGE gel stained with Coomassie Brilliant Blue. Panel B: corresponding

Western blot probed with anti-HSP70 antibody. Lane 1: molecular weight markers; 175, 83,

62, 47.5, 32.5, 25, 16.5kDa (top to bottom). Lane 2: hrHSP70 (1µg). Lanes 3, 4 and 5; affinity

purified HSP70-PC's from MCF-7, MDA-MB-231 and MCF-12A cell lines, respectively.

4.2.2. Identification of HSP70-PC co-purifying proteins by MALDI-TOF peptide mass fingerprinting.

To identify the unknown proteins present in the affinity-purified HSP70-PC extracts, proteins were separated by SDS-PAGE and stained with Coomassie. The strongest protein bands were excised, as indicated in FIG. 4.2, and digested with trypsin *in situ* (as described in Chapter 2, section 2.14). The top box contains three tightly packed bands; a fainter upper band (1) and two lower darker bands (2 and 3), all of which are expected to be members of the HSP70 protein family. Bands 4, 5 and 6 represent the unknown proteins. Tryptic peptides were analyzed using MALDI-TOF peptide mass fingerprinting by Gwen Manning at the Mass Spectrometry Resource, Conway Institute, UCD. Proteins were identified by a Mascot search using the human Swiss-Prot database and the top three identifications are shown in Table 4.1. A protein score of 90 or above was considered significant and confidence interval (C.I.) of 100% was considered a positive identification.

Each of the three closely packed bands (1-3) in the 70kDa range were confirmed as HSP70 protein family members. The three unknown proteins (4, 5 & 6) were positively identified as actin and nucleoside diphosphate kinases A and B, respectively. These results were confirmed in a second independent analysis (data not shown). The three newly identified non-HSP proteins are known to interact with ADP. It is therefore likely that they were present in the HSP70-PC extracts due to their ability to bind ADP during affinity chromatography rather than being important components of the HSP70-PC's. It is worth noting that these proteins were not able to be separated from HSP70 by either centrifugal molecular weight cut-off columns or by gel filtration. This suggested that although the proteins appear smaller in size on an SDS-PAGE gel, they appear to be present in a higher molecular weight complex in the extracts which makes them difficult to separate from the HSP70-PC's.
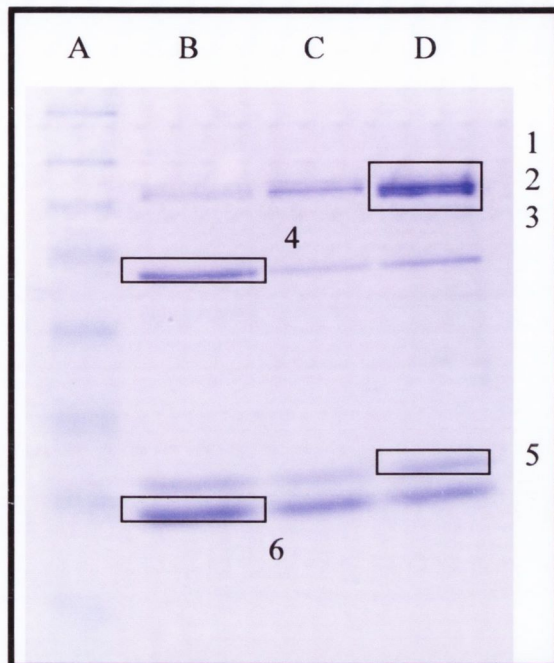
FIG. 4.2 Separation and selection of proteins present in affinity-purified HSP70-PC extracts for MALDI-TOF peptide mass fingerprinting. HSP70-PC's were affinity-purified using ADP-agarose and were separated on a 12% SDS-PAGE gel. Following Coomassie Blue staining, the strongest bands (1-5) indicated by the boxes were excised for digestion with trypsin. Lane A: molecular weight markers; 175, 83, 62, 47.5, 32.5, 25, 16.5kDa (top to bottom). Lanes B, C and D contain affinity-purified HSP70-PC's from MCF-7, MDA-MB-231 and MCF-12A cell lines, respectively.

Table 4.1 Summary of MALDI-TOF peptide mass fingerprinting protein identification results.

Band	Identified protein	Swiss-Prot Acc. No.	Protein MW	Protein Score	C. I. (%)
1	Stress-70 protein, mitochondrial	GRP75	73634.8	510	100
	78kDa glucose-regulated protein	GRP78	72288.4	345	100
	Heat shock cognate 71kDa protein	HSP7C	70854.2	248	100
2	Heat shock 70kDa protein 1	HSP71	70009	1040	100
	Heat shock 70kDa protein 1L	HS71L	70331.3	575	100
	Heat shock 70kDa protein 6	HSP76	70984.2	515	100
3	Heat shock cognate 71kDa protein	HSP7C	70854.2	1010	100
	Heat shock-related 70kDa protein 2	HSP72	69977.9	379	100
	Heat shock 70kDa protein 1	HSP71	70009	239	100
4	Actin, cytoplasmic 1	ACTB	41709.7	704	100
	Actin, cytoplasmic 2	ACTG	41765.8	703	100
	Actin, alpha cardiac muscle 1	ACTC	41991.9	324	100
5	Nucleoside diphosphate kinase A	NDKA	17137.7	737	100
	Nucleoside diphosphate kinase B	NDKB	17286.9	274	100
	Putative nucleoside diphosphate kinase	NDK8	15519	132	100
6	Nucleoside diphosphate kinase B	NDKB	17286.9	606	100
	Putative nucleoside diphosphate kinase	NDK8	15519	433	100
	Nucleoside diphosphate kinase A	NDKA	17137.7	277	100

4.2.3 HSP70-PC bio-panning.

Two strategies of bio-panning were performed to identify peptides that bind to the HSP70-PC's. In the first bio-panning experiment, the total ADP-agarose affinity-purified HSP70-PC extracts were used as a target (as described in Chapter 2, section 2.15). In brief, the total HSP70-PC extracts from a given cell line were coated onto a Maxisorp plate and following blocking, were incubated with the PhD-C7C phage library. Bound phage were eluted and amplified and underwent a total of six rounds of bio-panning. All rounds were performed identically with the exception of round 3, in which the phage were incubated on hrHSP70 in order to remove phage binding only to the HSP70 moiety. Three separate experiments were performed using affinity-purified HSP70-PC extracts derived from the MCF-7 and MDA-MB-231 tumour cell lines and the MCF-12A non-tumour cell line for comparison. Table 4.2 shows a summary of the sequences identified from these bio-panning experiments.

Table 4.2 Peptide sequences and frequencies of isolation from the HSP70-PC bio-panning from breast tumour and non-tumour cell lines.

MCF-7		MDA-MB-231		MCF-12A	
Sequence	Frequency	Sequence	Frequency	Sequence	Frequency
PHLQGKV	6/10	PSPFKQF	9/10	HSISPQK	6/10
RAVSHPT	2/10	TSMMPYK	1/10	HPWPYVQ	2/10
ISNHHLL	1/10			FPFWPNK	1/10
VQNAKHI	1/10			TQYSEPQ	1/10

The six rounds of bio-panning (5 selective, 1 subtractive) showed an enrichment of phage sequences. One potentially strong unique recognizer sequence; PHLQGKV, PSPFKQF and HSISPQK was identified in MCF-7, MDA-MB-231 and MCF-12A, respectively. The peptide sequences identified in each cell line were different and no common peptide motifs could be identified.

Since the affinity-purified HSP70-PC extracts derived from each cell line also contained a number of co-purifying non-HSP proteins, another strategy of bio-panning was required to ensure that selection of phage was based on binding to the peptides associated with HSP70 and not to the common co-purifying proteins present in the extracts. Since the co-purifying proteins were not easily separated from the target proteins, a second strategy was developed employing the use of a monoclonal anti-HSP70 antibody to capture the HSP70-PC's, thereby allowing their separation from the other proteins.

In order to ensure that this approach would allow for the separation of the co-purifying proteins from the HSP70-PC's, a proof of principle experiment was performed. HSP70-PC's purified from MDA-MB-231 cells were incubated firstly with the anti-HSP70 antibody and this complex was then incubated with Protein A/G-linked agarose, as described in Chapter 2, section 2.16.1. Unbound proteins were washed away. Both the Protein A/G-agarose-bound fraction and unbound fractions were then boiled in protein sample buffer and analyzed by SDS-PAGE. As previously shown, the affinity-purified HSP70-PC extracts from MDA-MB-231 contained HSP70 and three co-purifying proteins (FIG. 4.3, lane 2 bands). This fraction contained approximately 0.5µg of HSP70-PC's as determined by comparison with known controls (data not shown). The Protein A/G agarose bound fraction contains a 70kDa band representing HSP70 (FIG. 4.3, lane 3 black box). In addition there are two other protein bands approximately 50 and 25kDa in size which represent the reduced heavy and light chains of the IgG anti-HSP70 antibody, respectively. Half of the total sample was loaded on the gel, which

105

correlates with approximately 1μg of HSP70-PC's. The unbound proteins (1/10 of sample) show the presence of faint bands representing the co-purifying non-HSP proteins (lane 4, white boxes). The other major bands represent proteins such as serum albumin present in the ascites fluid of the antibody stock (compare lanes 4 and 5). This experiment demonstrated monoclonal antibody affinity chromatography allows for the successful separation of the HSP70-PC's from the co-purifying proteins.

A second bio-panning experiment was performed using affinity-purified HSP70-PC's as described in detail in Chapter 2, section 2.16.2 and as outlined in FIG. 4.4. Briefly, two rounds of selection were carried out on HSP70-PC's absorbed onto plastic microtiter (MT) plates and eight rounds of selection were performed on the Protein A/G-agarose-antibody captured HSP70-PC's. Subtractive selection of the phage on the Protein A/G-agarose and antibody was performed in most rounds to ensure removal of non-target related phage. Additionally, in the initial rounds subtractive bio-panning with hrHSP70 was carried out to remove phage binding solely to the HSP70 moiety of the HSP70-PC's. Any remaining phage were eluted with a low pH glycine buffer and amplified in *E. coli*. In later rounds specific elution of phage bound to the peptides associated with HSP70 was carried out by incubation with ATP. The presence of ATP is known to dissociate the peptides from HSP70 and would thereby allow for the isolation of any peptide-specific phage. Ten rounds of bio-panning were performed in total and phage were sequenced after rounds 4, 5, 6 and 10 in order to evaluate sequence enrichment. HSP70-PC's from each cell line were separately bio-panned.
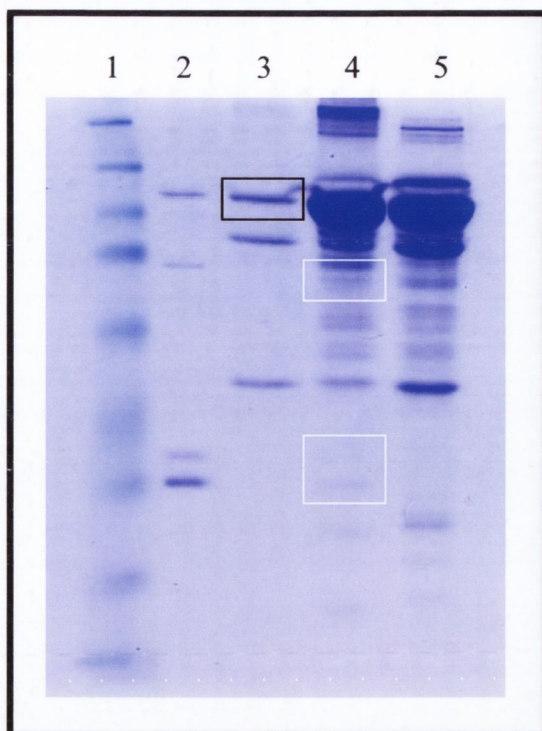
FIG. 4.3 Fractions from the Protein A/G agarose-antibody-HSP70-PC capture experiment.
Lane 1: Protein size ladder; 175, 83, 62, 47.5, 32.5, 25, 16.5, 6.5 kDa from top down. Lane 2:
MDA-MB-231 affinity-purified HSP70-PC extract (approx. 0.5µg pure HSP70-PC). Lane 3:
Protein A/G-agarose-bound proteins (1/2 of total sample, expected approx. 1µg HSP70-PC's).
Lane 4: Unbound proteins (1/10 of total sample). Lane 5: Anti-HSP70 antibody stock 1µl
(approx. 28µg protein). The black box highlights the presence of HSP70 in the column-bound
fraction. The white boxes indicate the locations of the three unrelated proteins present in the
unbound fraction.
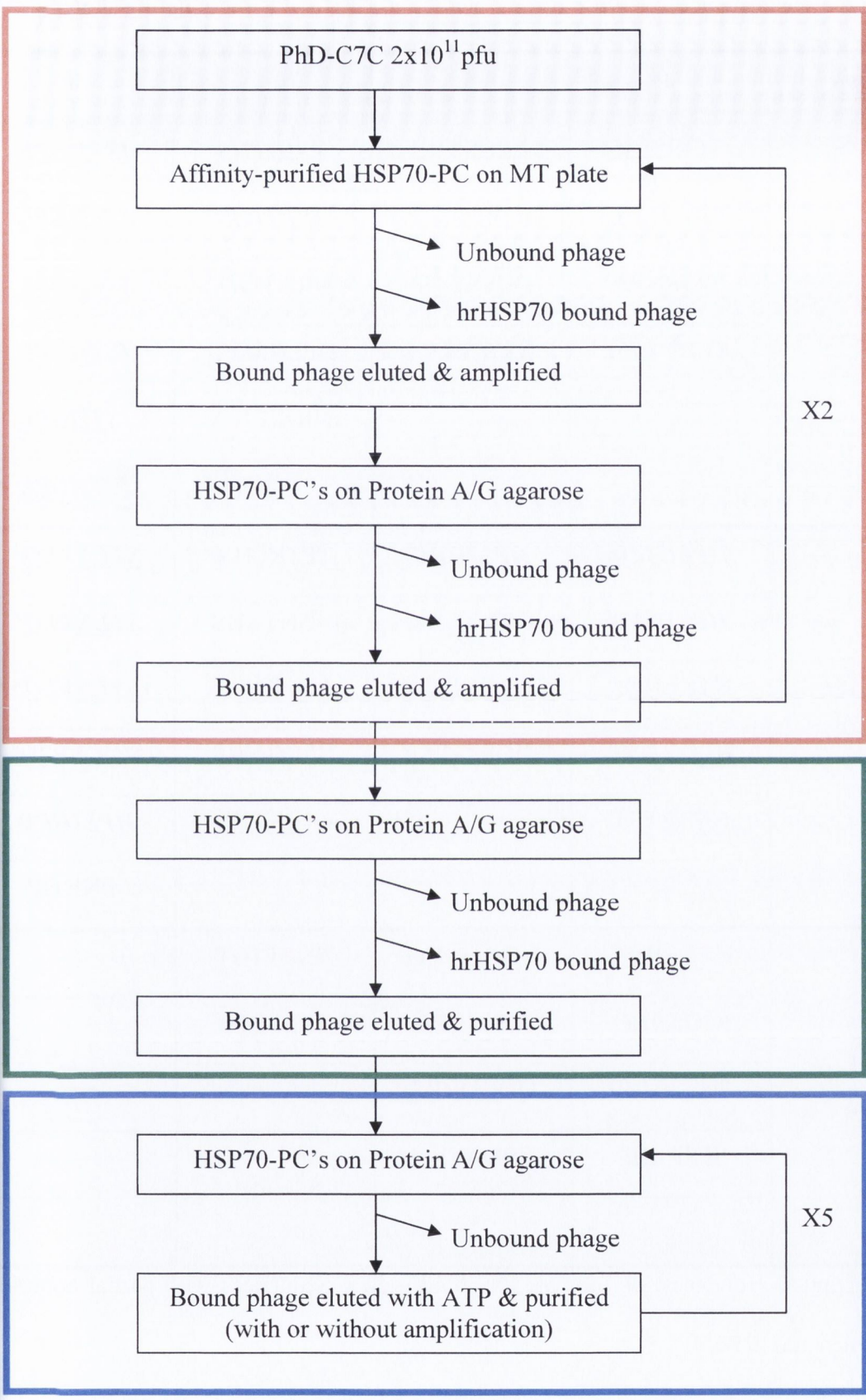
FIG. 4.4 Outline of the second HSP70-PC bio-panning experiment.

Table 4.3 Peptide sequences identified from the second HSP70-PC bio-panning strategy.

Round	4	5	6	10
MDA-MB-231 HSP70-PC's	STNISPM	LEGSKRS	*TSIGTHS*	*ISTHGPL*
	THL**PL**RL	TQRPDKS*	*TSIGTHS*	*ISTHGPL*
	PRTSNPH	QDSKQNR	NRATLST	*ISTHGPL*
	KVHNRFA	*KVHNRFA*	DPLNMYT	*ISTHGPL*
			NIGKPHQ	*ISTHGPL*
				ISTHGPL
MCF-7 HSP70-PC's	*HPLIHPD*	*HPLIHPD*	TPTRLHY	*STLNVLQ**
	HPLIHPD	DRVKSNK	NGNYSHS	*STLNVLQ**
	NTKLHQS	HSGYLKS	N**SPLN**PS	*STLNVLQ**
	HPQYKYL	DGPSRPM	NMVESRF	TQKWPPH*
	NYTLTST		GH**ISR**H**L	*HPLIHPD*
				APNETRS
MCF-12A HSP70-PC's	NTLARLA	VQGGVHQ	KNPTTGT	
	NIGKPHQ	*HPLIHPD*	TKSFQFL	
	TDSWHHS	QDGDRRS		
	SPSRLHS	GSLWFKA		

Recurring peptide sequences are indicated by bold italics. Sequences with partial homology are underlined and in bold.

As shown in Table 4.3, this second HSP70-PC bio-panning strategy led to definite peptide enrichment after ten rounds. Different recognizer peptides were isolated for each tumour cell line. A single peptide sequence, ISTHGPL, dominated the final phage pool sequenced from MDA-MB-231. Certain motifs could be seen to be developing throughout the experiment which led to the final sequence and these include THXPL and IXTH. Four peptides were identified in the final round from MCF-7. One of these sequences, STLNVLQ, was present in 50% of clones sequenced and an SXLN motif can be seen occurring in an earlier round. Both TQKWPPH and APNETRS appear solely in the final round from MCF-7 but HPLIHPD was also identified in round 5 from MCF-12A and also in the earlier rounds 4 and 5 with MCF-7. This sequence must therefore be binding to a common protein or peptide associated with HSP70 in both of these cell lines and is therefore not tumour-specific. No peptide sequences could be isolated from the final round of MCF-12A. In order to investigate this occurrence, a small number of phage clones were randomly picked from rounds 2, 4, 5, 6 and 10 and the presence of a peptide insert was analyzed by PCR (data not shown). The frequency of phage with inserts is summarized in Table 4.4. The number of phage with peptide inserts was inversely proportional to the number of bio-panning rounds.

Another interesting observation was that some of the newly identified sequences (denoted with *) in Table 4.3 bore homology to peptide sequences identified previously in our lab (Arnaiz et al., 2006) from a bio-panning experiment with HSP70-PC's from MDA-MB-231 cells. This homology is shown in Table 4.5. This previous bio-panning experiment was carried out using a different strategy and a different phage-peptide display library (PhD-12, NEB) but with a common goal of isolating peptide recognizers of MDA-MB-231 derived HSP70-PC's. Common motifs identified include; LNV, WPPH and TQRP-K.

Table 4.4 Frequency of phage with peptide inserts during the second HSP70-PC bio-panning.

Round	HSP70-PC's bio-panned	Number of phage with inserts	Average with inserts (%)
2	MCF-12A	5/5	93
	MDA-MB-231	5/5	
	MCF-7	4/5	
4	MCF-12A	4/5	86
	MDA-MB-231	4/5	
	MCF-7	5/5	
5	MCF-12A	6/10	63
	MDA-MB-231	4/10	
	MCF-7	9/10	
6	MCF-12A	2/10	60
	MDA-MB-231	8/10	
	MCF-7	8/10	
10	MCF-12A	0/20	20
	MDA-MB-231	6/20	
	MCF-7	6/20	

Table 4.5 Comparison of previously and newly identified HSP70-PC recognizers.

Origin	Sequence homology	Cell line-derived HSP70-PC's
Previously identified 12-mer	AIPNK**LNVWPPH**	MDA-MB-231
Panning round 10	ST**LNV**LQ	MCF-7
Panning round 10	TQK**WPPH**	MCF-7
Previously identified 12-mer	SQEL**TQRP**Y**K**WH	MDA-MB-231
Panning round 5	**TQRP**D**K**S	MDA-MB-231

4.2.4 Characterization of the HSP70-PC recognizer peptides.

A small number of HSP70-PC recognizer peptides were selected for synthesis and preliminary characterization and are listed in Table 4.6. The peptides were selected based on their enrichment and predominating presence in the final round of bio-panning. Also two of the previously identified 12-mer peptides were included due their sequence homology to some of the newly identified sequences. Each peptide contained a small spacer sequence (CGGG) at the C-terminal to allow for linkage of these peptides to various tags and molecules. A control peptide was also synthesized, denoted "Scram", which contained a scrambled variety of amino acids present in all the other peptides. The peptides were generally hydrophobic in nature and were neutral or positively charged.

Table 4.6 Selected HSP70-PC recognizer peptides and properties.

Peptide name	Peptide sequence	Mean hydrophilicity	Net charge
cSTLc	CSTLNVLQCGGG	-0.6	-0.1
cTQKc	CTQKWPPHCGGG	-0.3	1
cISTc	CISTHGPLCGGG	-0.5	0
cTQRc	CTQRPDKSCGG	0.6	0.9
AIP	AIPNKLNVWPPHCGGG	-0.4	1
SQE	SQELTQRPYKWHCGGG	0	1
Scram	NLPWPANPIKVH	-0.5	1.1

4.2.4.1 Homology to known proteins.

To determine if any of these peptides represent sequence motifs present in known cellular proteins and thus potential interacting partners of HSP70-PC's, homology searches were carried out using BLASTP (Altschul et al., 1997). The parameters used are described in Chapter 2, section 2.10. This type of analysis can indicate the most significant homologies (Table 4.7), however due to the size of the peptides and the complexity of the database, the E values were very high (data not shown). The most significant hit (E value 6.9) was with the AIP recognizer which showed homology with receptor tyrosine-protein kinase erbB-3. This was especially interesting as the homologous sequence, P-KLNV-15aa-WPPH, contained both of the motifs, LNV and WPPH, identified as common HSP70-PC recognizer peptide motifs listed in Table 4.5. In fact the same protein was the most significant hit for TQK. This protein belongs to the epidermal growth factor receptor (EGFR) family, the same family that includes HER-2.

4.2.4.2 HSP70-PC recognizer peptide protein binding assays.

To verify that the newly identified recognizer peptides interact with their HSP70-PC target proteins, a binding assay was carried out. Initial experiments using individual phage clones to examine their interaction with the HSP70-PC's in a plate-based method similar to that described by the manufacturers proved unsuccessful. We believe that this approach was not sensitive enough due to the limited amount of native HSP70-PC's which could be purified, in addition to the low molar amounts of peptide displayed by the phage clones. To overcome this, a solution-based protein binding assay section was devised using synthetic peptides rather than phage-displayed peptides, in order to increase the sensitivity of the assay.

113

Table 4.7 Homology of HSP70-PC recognizer peptides to known proteins.

Recognizer peptide	Homologous protein	Swiss-Prot Acc. No.	Homology
STL (128 hits)	Cell surface glycoprotein MUC18	P43121	STLNVL
	Cytoskeleton-associated protein 5	Q14008	TLN+LQ
	DNA repair and recombination protein RAD54B	Q9Y620	TLN+LQ
	Exocyst complex component 2	Q96KP1	ST---LNVLQ
TQK (109 hits)	Receptor tyrosine-protein kinase erbB-3	P21860	Q-WPPH
	CDC4-like protein	P50851	WPPH, TQ-W
	Protein FAM110B	Q8TC76	WPPH
	WD repeat-containing protein 7	Q9Y4E6	WPPH
IST (104 hits)	Thyroglobulin	P01266	ISTHG-L
	C3 and PZP-like alpha-2-macroglobulin domain-containing protein 8	Q8IZJ3	+STH-PL
	Protein furry homolog	Q5TBA9	THGPL
	HEAT-repeat containing protein 6	Q6AI08	+STH-PL
AIP (136 hits)	Receptor tyrosine-protein kinase erbB-3	P21860	P-KLNV-15aa-WPPH
	Ankyrin repeat and death-domain-containing protein 1B	A6NHY2	IPNKLN+
	Fibronectin type III domain-containing protein 1	Q4ZHG4	P—LNVWP
	Receptor tyrosine-protein kinase erbB-4	Q15303	AI-P-KLNV-15aa-WPP
SQE (134 hits)	Aggrecan core protein	P16112	SQEL-QRP
	Asialoglycoprotein receptor 1	P07306	QRPY-W
	Utrophin	P46939	S+ELTQR
	Histone-lysine N-methyltransferase NSD3	Q9BZ95	LTQ-PY-KW

Firstly the HSP70-PC recognizer peptides were bound to magnetic beads. To confirm that small peptides could be linked to magnetic beads, a control experiment was performed using two N-terminally biotinylated peptides (called bSQS and bTDK) and one non-biotinylated peptide (called NTL). The peptides were linked to magnetic beads via their carboxy-terminal using N-(3-dimethylaminopropyl)-N'-ethylcarbodiimide hydrochloride, as described in Chapter 2, section 2.17. Peptide-linked beads or beads alone were incubated in triplicate with extravidin-peroxidase allowing detection of the biotinylated peptides (detailed in Chapter 2, section 2.18). The successful detection of the biotinylated peptides on the magnetic beads is shown in FIG. 4.5. The amount of enzyme activity detected was very similar for both bTQK and bSQS indicating that both were present in similar amounts on the magnetic beads. No activity was detected with the non-biotinylated control peptide or the beads alone indicating that enzyme activity was dependent on the binding of extravidin-peroxidase to the biotin tagged peptides. This experiment confirmed that small peptides could be successfully linked to the magnetic beads.

The HSP70-PC recognizer peptides listed in Table 4.6 were linked to the amino-coated magnetic beads via their C-terminal glycine residue using the approach described above. The bead-linked peptide recognizers were incubated with their respective cell-derived HSP70-PC's and bound HSP70-PC's were detected using an anti-HSP70 antibody, as described in Chapter 2, section 2.19. Results were plotted as fold binding over unlinked beads from three separate experiments. The results of the binding of MCF-7 derived HSP70-PC's to its derived recognizer peptides; cSTLc and cTQKc, in addition to AIP and the scrambled peptide (Scram) are shown in FIG. 4.6.

Peptide-bead linkage control experiment
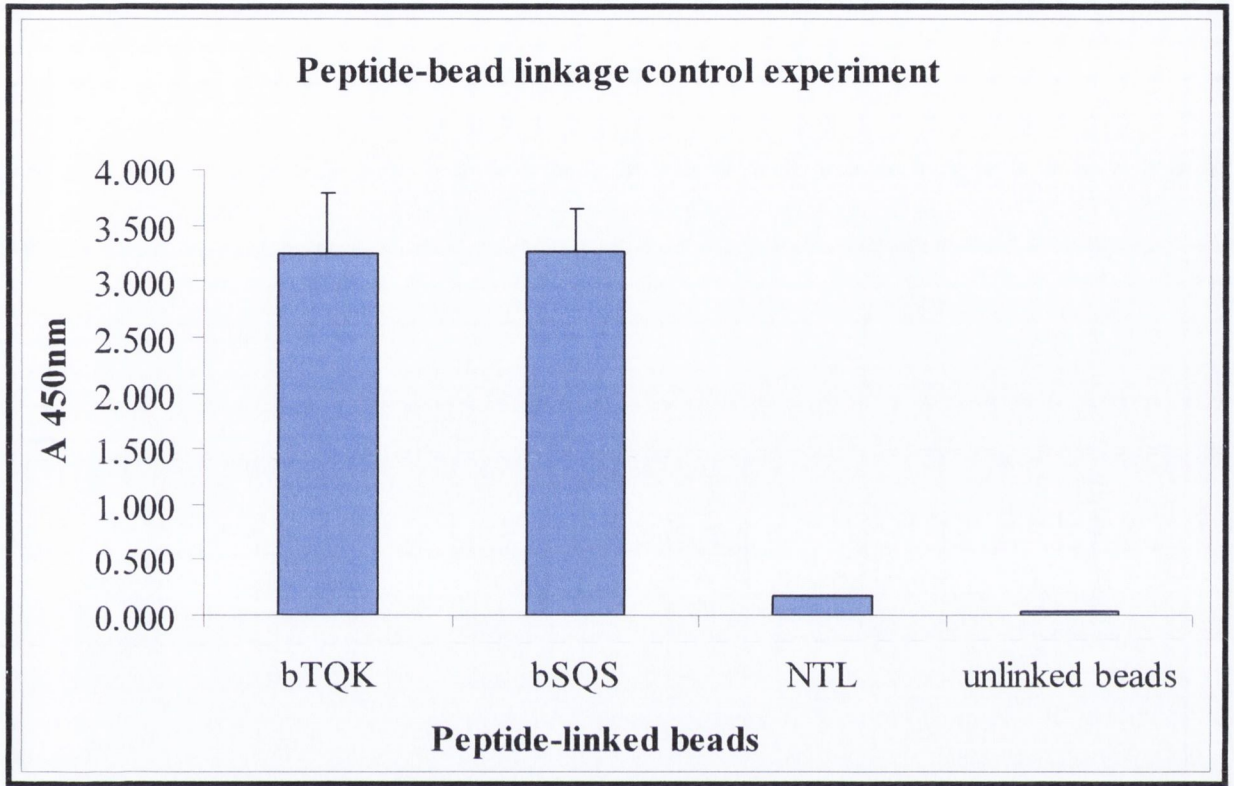
FIG. 4.5 Detection of biotinylated peptides linked to magnetic beads.

Biotin-tagged peptides detected by extravidin-peroxidase and TMB. Reaction was stopped
with sulfuric acid and absorbance was read at 450nm. Columns represent triplicate samples
with the error bars indicating the standard deviation.
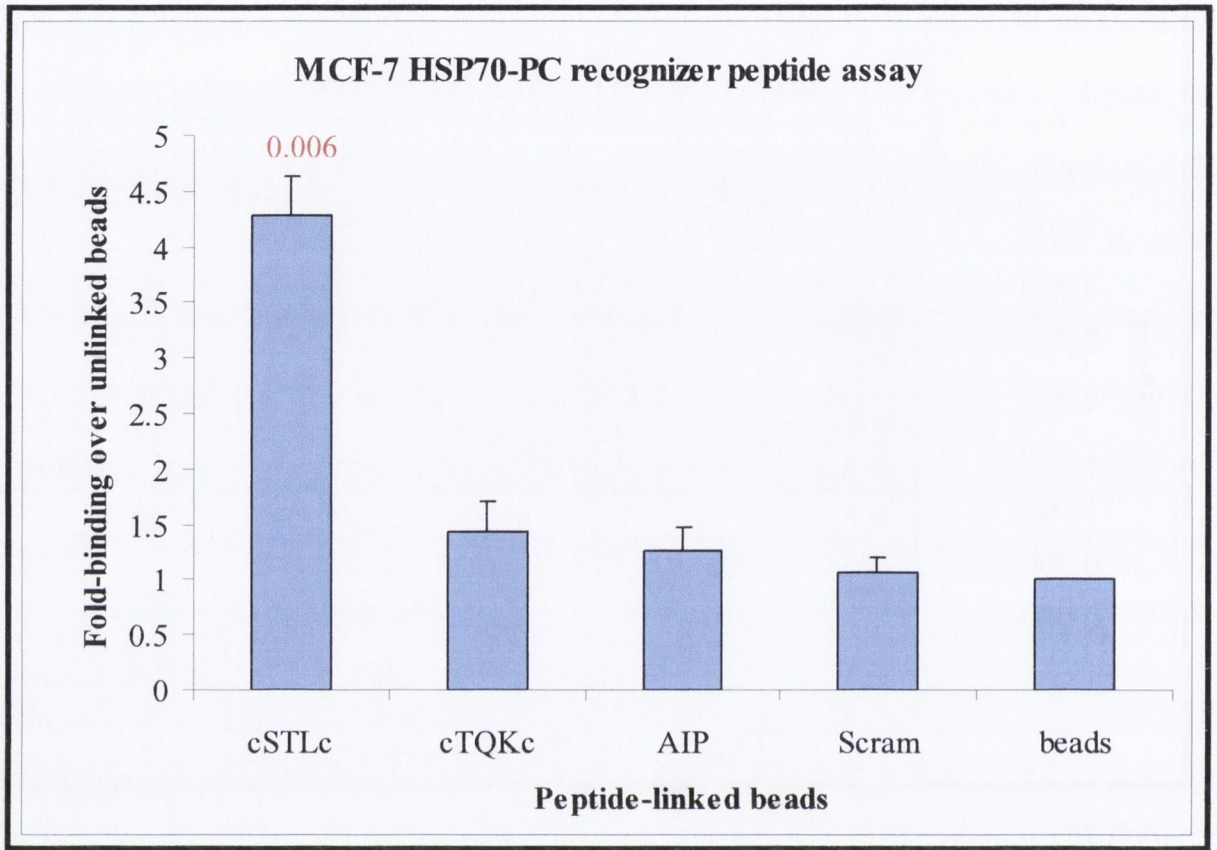
FIG. 4.6 Levels of MCF-7 HSP70-PC binding to its derived recognizer peptides.

Binding is shown as fold over control unlinked beads ("beads"). Data is representative of three independent experiments. Error bars indicate standard error. Significant P values (less than 0.05) are indicated (red).

The cSTLc peptide appeared to be the strongest MCF-7 derived HSP70-PC recognizer peptide. It showed over a four-fold increase in binding over the unlinked beads, which was statistically significant, unlike the Scram control peptide which showed no difference. Interestingly the cSTLc peptide was the most heavily enriched sequence in the MCF-7 HSP70-PC panning (see Table 4.3), indicating a correlation between the enrichment of specific sequences in bio-panning experiments and a protein-peptide interaction. The data thus validates the cSTLc peptide as a true HSP70-PC recognizer.

Unlike cSTLc, the cTQKc peptide didn't show a statistically significant level of binding. This sequence only occurred once in the final bio-panning eluate but it contained a four amino acid homology to the previously identified AIP peptide. The AIP peptide also failed to show a significant amount of binding in this assay. However both peptides showed a higher amount of binding than the negative control Scram peptide and the unlinked beads. The difference between cSTLc and AIP suggests that the common LNV motif is not solely responsible for the interaction with the HSP70-PC's. Rather the cSTLc peptide must contain a new motif, either linear or discontinuous, that is responsible for its interaction with the HSP70-PC's. For example, one of the peptides in round 6 (see Table 4.3) showed partial homology to the cSTLc peptide, which could indicate a possible SXLN motif.

The same experimental approach was carried out for assessing the authenticity of the MDA-MB-231 derived HSP70-PC recognizer peptide sequences. These included previously identified SQE, newly identified cISTc and cTQRc and the negative control Scram peptide. The results are shown in FIG. 4.7
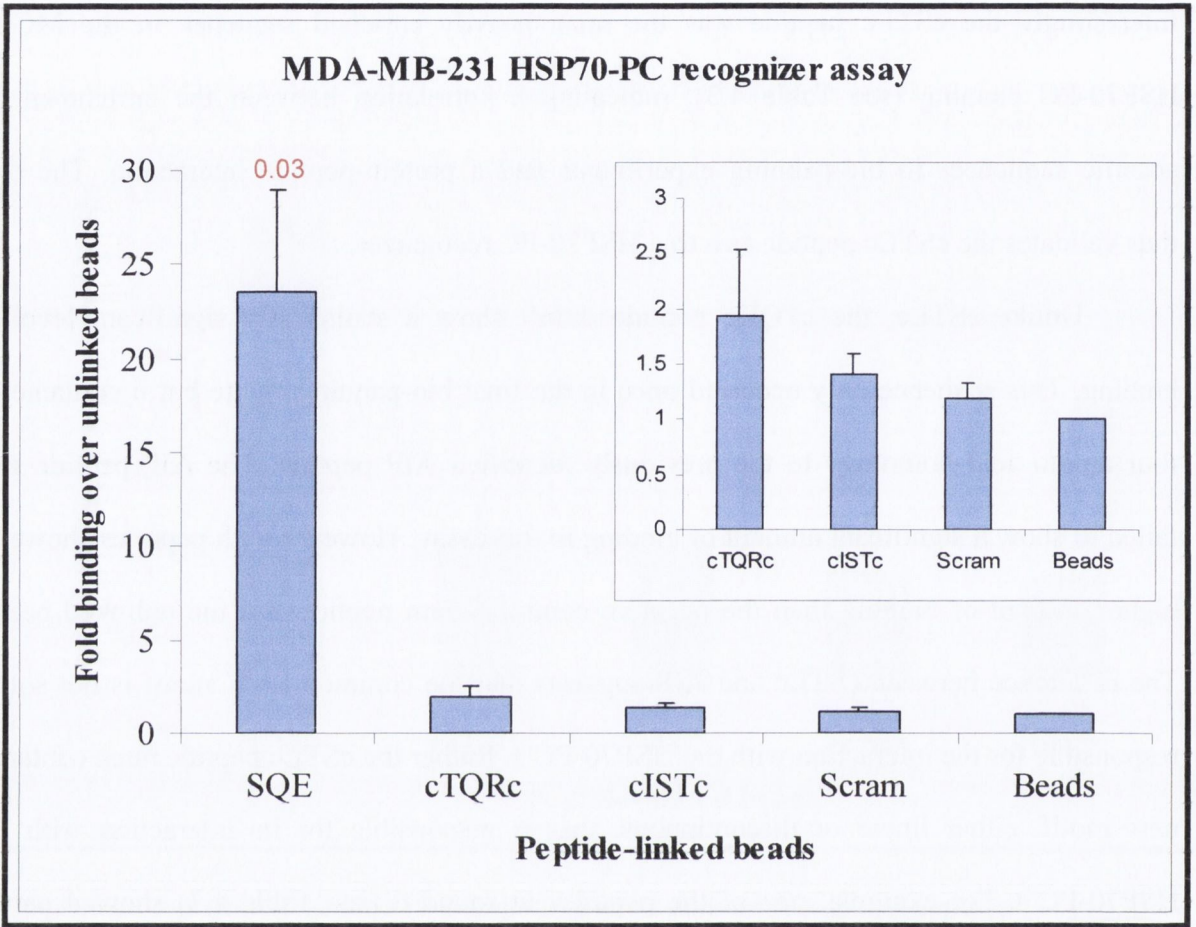
FIG 4.7 Levels of MDA-MB-231 derived HSP70-PC's binding to its recognizer peptides.
Values are representative of three separate experiments. Binding is indicated as fold over
unlinked beads. Error bars indicate standard error. Significant P values are indicated (red).
Insert contains identical graph without SQE.

The results show an extremely high level of interaction between the SQE peptide with the MDA-MB-231 derived HSP70-PC's. This previously identified 12-mer had a five amino acid homology with the cTQRc peptide, which was not a heavily enriched sequence and was only detected once in round 5 of the bio-panning (see Table 4.3) but was included in this assay due its homology with SQE. The results show that the five amino acids shared by the peptides are not the only determining factor for interaction with the HSP70-PC's. The cTQRc peptide did show a higher level (nearly 2-fold over unlinked beads) of binding compared to the two negative controls, however it didn't produce a statistically significant difference compared to the unlinked beads in this case. The cISTc peptide also showed a higher level of binding compared to the negative controls, although it was a little lower than cTQRc. However this interaction was also not statistically significant in this case.

4.2.4.3 Cell staining with HSP70-PC recognizer peptides.

Three recognizer peptides; SQE, AIP and cISTc were chosen for further characterization and mimic peptide development (the latter described in the next chapter). This decision was based on the sequence data from the bio-panning experiments, in addition to the homology of the previously identified 12mer peptides with a number of the newly identified cysteine-flanked 7mers. SQE had a five amino homology to cTQRc and also bound strongly to HSP70-PC's in the bead assay. AIP was selected as it contained two motifs, LNV and WPPH, common to two newly identified cSTLc and cTQKc, respectively. The cISTc peptide was chosen as it was the sole peptide sequence identified in the final round of MDA-MB-231 derived HSP70-PC bio-panning. Unfortunately the cSTLc peptide was not characterized any further, but remains an interesting candidate for future studies.

To investigate whether these HSP70-PC recognizer peptides could bind to whole tumour cells, immuno-fluorescent cell staining was performed. Only two of the selected HSP70-PC recognizer peptides (SQE and cISTc) could be successfully synthesized by our suppliers (GL Biochem Ltd.) with a biotin tag for use in cell staining (Table 4.8). A small spacer (SA) was included in bIST between the biotin tag and first cysteine residue. These peptides were tested for their ability to bind the MDA-MB-231 tumour cells, as well as the MCF-12A non-tumour cells using immuno-fluorescence. Biotinylated peptides (20µg/ml) were incubated on blocked fixed cells and binding was detected using ExtrAvidin-Cy3 (as described in Chapter 2, section 2.7). FIG. 4.8 shows this cell staining in the presence of a positive control peptide (whole cell binding peptide, cMLHc) and a negative control peptide (Lneg) previously described in Chapter 3 (magnification 200x).

Table 4.8 Biotinylated HSP70-PC recognizer peptides.

Peptide sequence	Peptide name
Biotin-K-SQELTQRPYKWHCGG	bSQE
Biotin-K-SACISTHGPLCGG	bIST

121
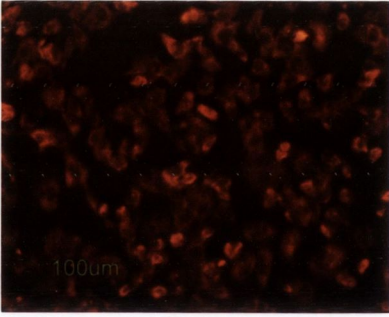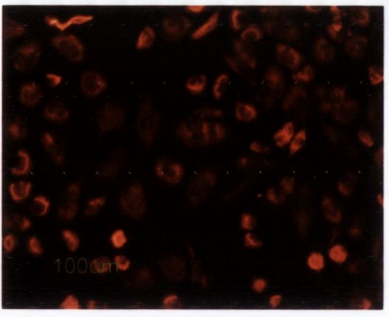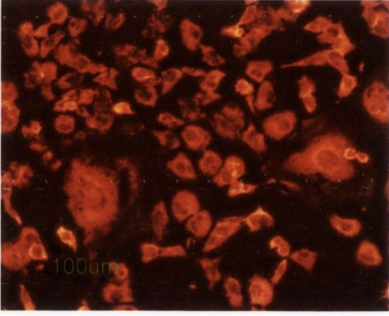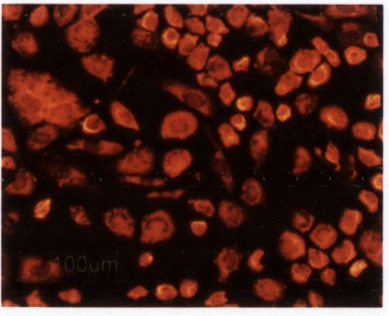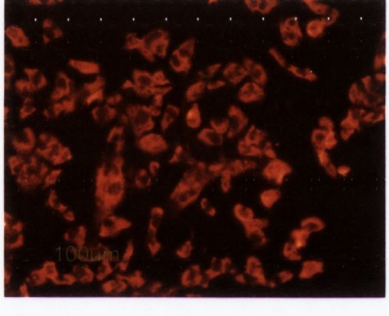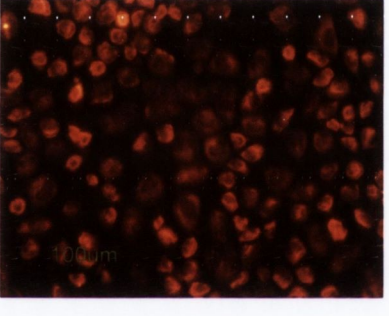
Peptide	MDA-MB-231	MCF-12A
bIST		
bSQE		
cMLHc		
Lneg		

FIG 4.8 Fixed cell staining with the HSP70-PC recognizer peptides.

Cell-bound biotinylated peptides were detected with ExtrAvidin-Cy3 (red). Photos were taken with Nikon E100 fluorescent microscope.

122

Both peptides bound to the MDA-MB-231 tumour cells as well as to the MCF-12A non-tumour cells, but the bSQE peptide bound to cells much more intensely than bIST. However the binding didn't appear to be localized to one part of the cell, rather staining could be seen both in the cytoplasm but also seemed to extend to the farthest reaches of the extra-cellular matrix. The bIST peptide appeared to stain cells more specifically and is clearly located in the cytoplasm of the cells. In some cells, the peptide staining appears to be slightly more intense around the nuclear membrane.

4.2.4.4 Identification of HSP70-PC recognizer peptide cellular binding partners.

In order to try and identify the cellular targets of HSP70-PC recognizer peptide binding, a protein pull-down experiment was performed. MDA-MB-231 cellular soluble protein extracts (2mg) were incubated with the HSP70-PC recognizer peptides (AIP, SQE and cISTc) which were linked to magnetic beads (as described in Chapter 2, section 2.20) or with unlinked beads alone ("Beads"). Unbound proteins were removed by washing. A fraction (1/20) of the unbound proteins and the total final wash samples were separated by SDS-PAGE (FIG. 4.9A). The unbound protein samples (lanes 1-4) show a large excess of MDA-MB-231 proteins, while the last wash samples (lanes 6-10) are relatively free of proteins.

The total bound protein fractions from each peptide are shown in FIG. 4.9B. HSP70-PC's (10µg) from MDA-MB-231 were also run on the gel for comparative purposes (lane 2). AIP and SQE bound five major proteins (lanes 3 and 4, respectively: bands 5, 6, 7, 8 and 10), however these bands appeared at a similar intensity in the Beads only sample. The cISTc peptide, on the other hand, bound five other proteins indicated by the bands numbered 1, 2, 3, 4 and 9, in addition to the five common proteins. Two of these bands (7 and 8) appeared to be stronger than in the other samples.
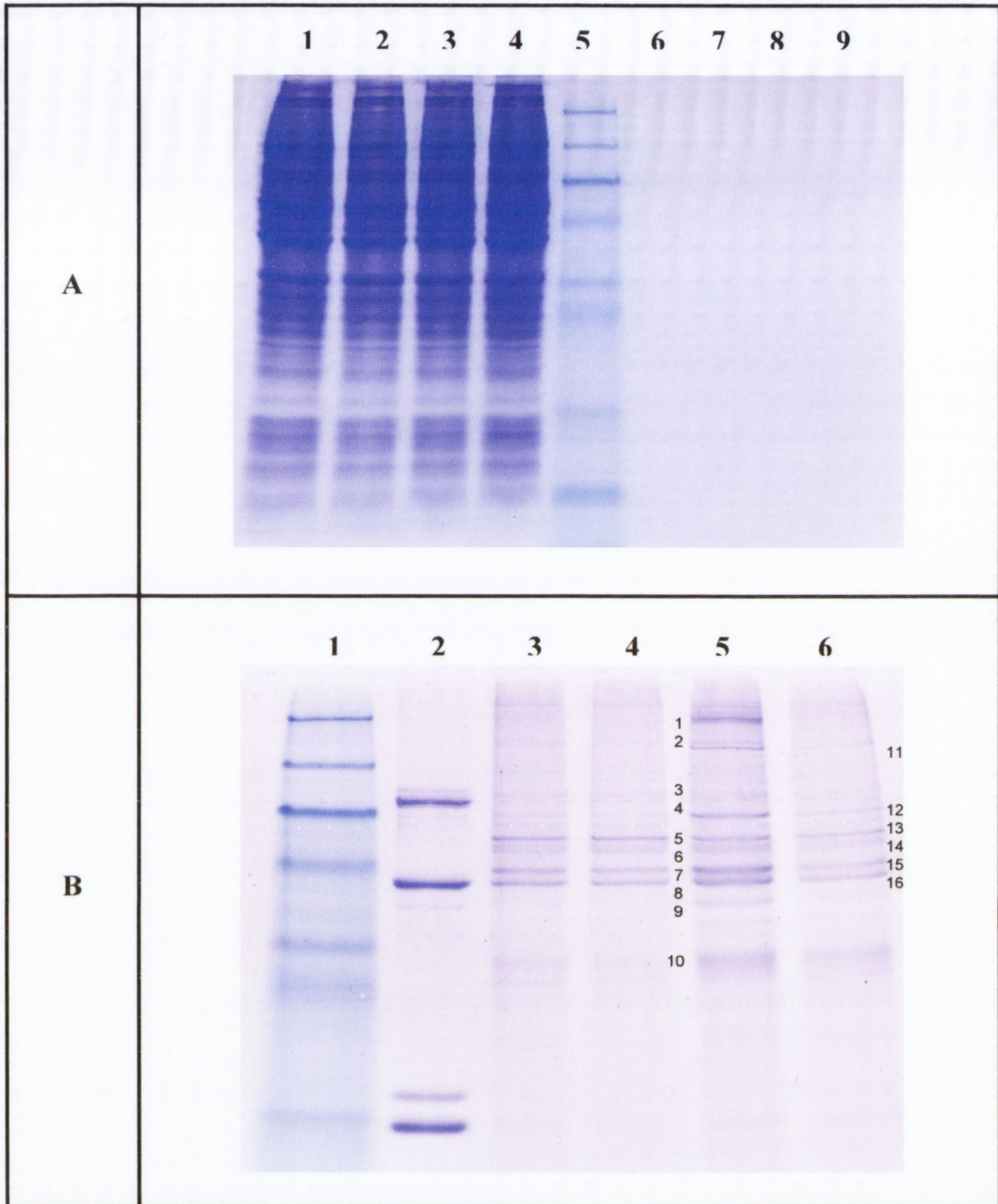
FIG. 4.9 Coomassie-stained SDS-PAGE gels from the pull-down experiment.

Panel A; Lanes 1-4; unbound proteins from AIP, SQE, cISTc and Beads, respectively. Lane 5: molecular weight markers; 175, 83, 62, 47.5, 32.5, 25, 16.5 and 6.5kDa. Lanes 6-10; total final wash samples from AIP, SQE, cISTc and Beads, respectively. Panel B; Lane 1: molecular weight markers; 175, 83, 62, 47.5, 32.5, 25 and 16.5kDa. Lane 2: affinity-purified HSP70-PC's. Lanes 3-6; bound protein fractions from AIP, SQE, cISTc and Beads, respectively.

Bands 1-10 from the cISTc fraction, along with the corresponding bands (11-16) present in the Beads only fraction were excised from the gel, digested with trypsin and prepared for MALDI-TOF peptide mass fingerprinting as described in Chapter 2, section 2.14. The protein identification results were derived using a Mascot search of the human SwissProt database and the top hits are shown in Table 4.9. A protein score of 90 was considered significant with a confidence interval (C.I.) of 100% considered a positive identification. Band 10 was confirmed as Alpha-S1-casein (MW 24513.4) which represents the blocking buffer used in this experiment (data not shown).

The cISTc peptide pulled down a member of the HSP70 family of proteins, GRP78 (band 3), validating its association with the HSP70-PC's. A number of various subunits of eukaryotic translation initiation factor 3 were also pulled down (bands 1, 2 and 4). Vimetin, tubulin and actin appeared to be present non-specifically as they also appeared in the control sample (bands 5, 6 and 8 for cISTc and bands 13, 14, 16 for control beads, respectively). Interestingly cISTc band 7, which was stronger than band 15 of similar size in the control lane, showed a positive identification for a putative elongation factor 1-alpha-like 3 protein while the latter corresponded with keratin. However the identification of keratin in band 15 is not likely to be a true identification as the C.I. was 0% and the size of the protein does not correspond with the estimated protein size from the gel. This was also the case with the results obtained for band 11. Band 12 was also identified as keratin, a common contaminant in mass spectrometry, and although the score was low the estimated protein size from the gel could correspond with keratin. As the protein scores and C.I.'s were low for bands 11, 12 and 15, this indicates that those results were not significant. Unfortunately mass spectrum data was not obtained for band 9 and so that protein remains unidentified. These results provide an indication of the possible cellular binding partners of the cISTc recognizer peptide.

Table 4.9 Identification of HSP70-PC recognizer peptide binding proteins.

Band	Est. size (kDa)	Identified protein	Swiss-Prot name	Protein MW	Protein score	C.I. (%)
1	140	Eukaryotic translation initiation factor 3 subunit A	EIF3A	166468.3	230	100
2	100	Eukaryotic translation initiation factor 3 subunit B	EIF3B	92433.8	82	99.99
3	70	78kDa glucose-regulated protein	GRP78	72288.4	93	100
4	60	Eukaryotic translation initiation factor 3 subunit E-interacting protein	IF3EI or EIF3L	66684.4	248	100
5	52	Vimentin	VIME	53619.1	502	100
6	50	Tubulin alpha-1B chain *	TBA1B	50119.6	248	100
7	47	Putative elongation factor 1-alpha-like 3	EF1A3	50153.1	100	100
8	45	Actin, cytoplasmic 1 *	ACTB	41709.7	300	100
9	40	*No spectrum obtained*				
11	100	Indoleamine 2,3-dioxygenase	I23O	45297.2	29	0
12	60	Keratin, type II cytoskeletal 1	K2C1	65978	48	68.9
13	52	Vimetin	VIME	53619.1	276	100
14	50	Tubulin beta chain *	TBB5	49639	163	100
15	47	Keratin, type II cytoskeletal 1	K2C1	65978	36	0
16	45	Actin, cytoplasmic 1 *	ACTB	41709.7	341	100

* denotes more significant hits but all in the same family of proteins. Est. size refers to the estimated size as determined by the gel position in FIG. 4.9B.

126

4.2.4.5 Staining of patient tumour tissues with the cISTc peptide.

The cISTc peptide sequence was heavily enriched during the MDA-MB-231 derived HSP70-PC bio-panning experiment. While only low levels of interaction with HSP70-PC's were identified in the bead binding assay, the peptide showed localized cellular staining in both MDA-MB-231 and MCF-12A breast cells. It was also the only peptide that pulled down putative cellular binding targets. The ability of this peptide to bind to tumour cells within patient tumour tissues was therefore investigated and compared to the localization of HSP70 as determined using an anti-HSP70 monoclonal antibody. Tissue staining was performed by Robert Cummins, in the lab of Prof. Elaine Kay at the Department of Pathology, Beaumont Hospital as described in Chapter 2, Section 2.11.3. FFPE-TMA's underwent antigen retrieval prior to incubation with the cISTc peptide and the distribution of both the cISTc peptide (200µg/ml) and anti-HSP70 antibody (1/500 dilution) were visualized with DAB on serial TMA's which were counterstained with hematoxylin.

The staining patterns of the anti-HSP70 antibody and the cISTc peptide in a breast tumour tissue core are shown in FIG. 4.10. Both the antibody and peptide appeared to localize in the same areas of the tumour tissue, with staining largely absent from the stroma. Staining with the anti-HSP70 antibody and cISTc peptide was also examined in another breast tumour tissue core (FIG. 4.11) derived from an oestrogen and progesterone receptor positive (ER+ and PR+, respectively) tumour. Again both the HSP70 and cISTc peptide appear to localize to the same regions within the tumour tissue, although the staining for HSP70 is stronger than the cISTc peptide. Binding of the anti-HSP70 antibody and cISTc peptide to an ovarian tumour tissue developed from metastatic breast cancer is shown in FIG. 4.12. Interestingly in this case the HSP70 staining appears stronger than in the previous breast tumours, whereas the cISTc peptide staining is much weaker, if at all present.
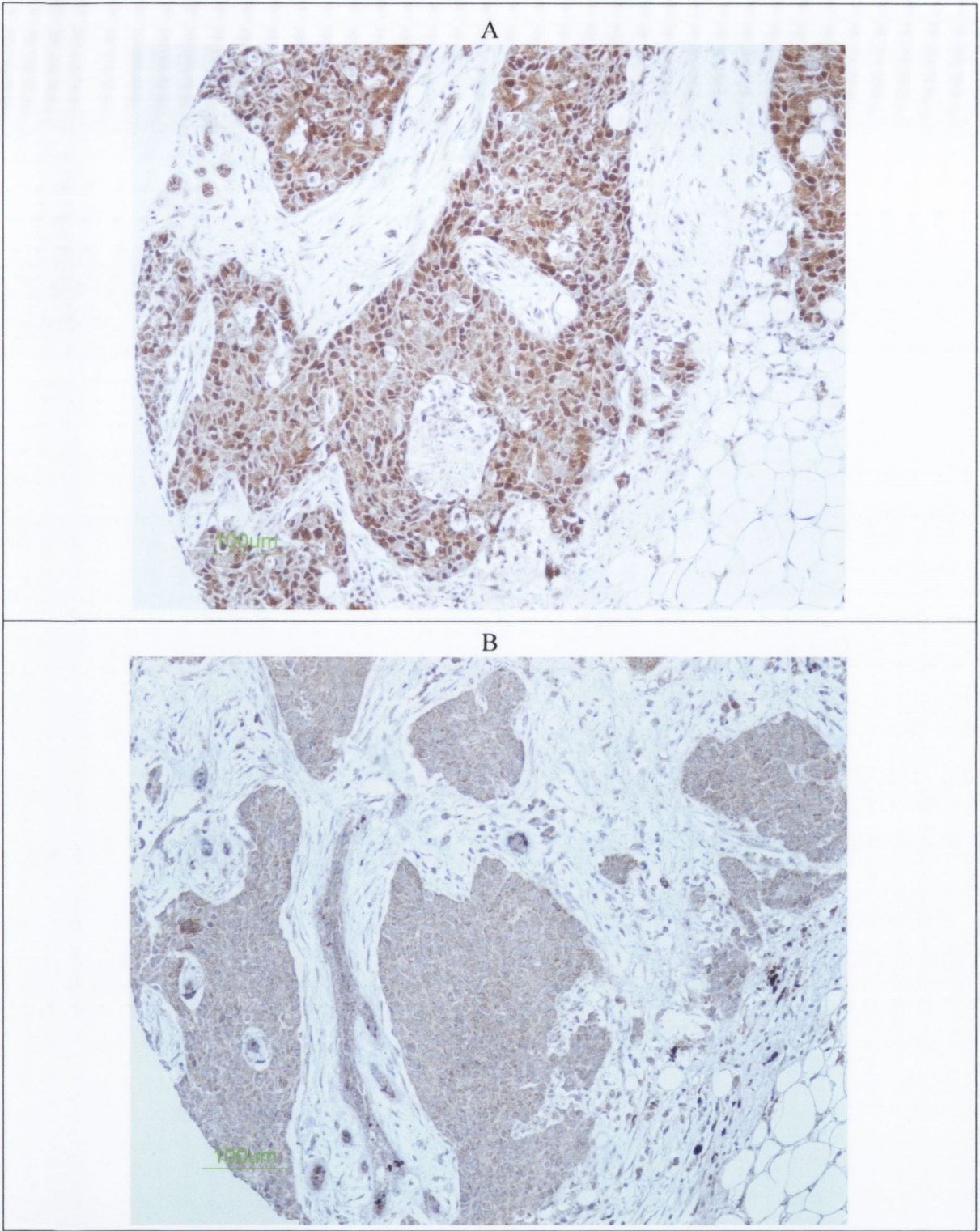
FIG. 4.10 DAB staining of breast tumour tissue core incubated with anti-HSP70 antibody (Panel A) or cISTc peptide (Panel B). Magnification 100x.
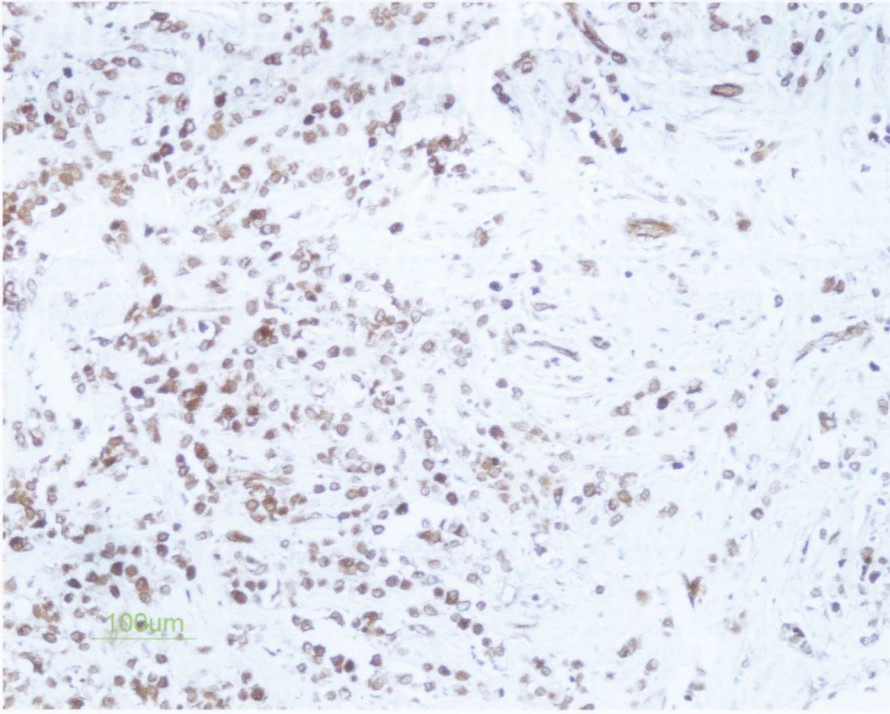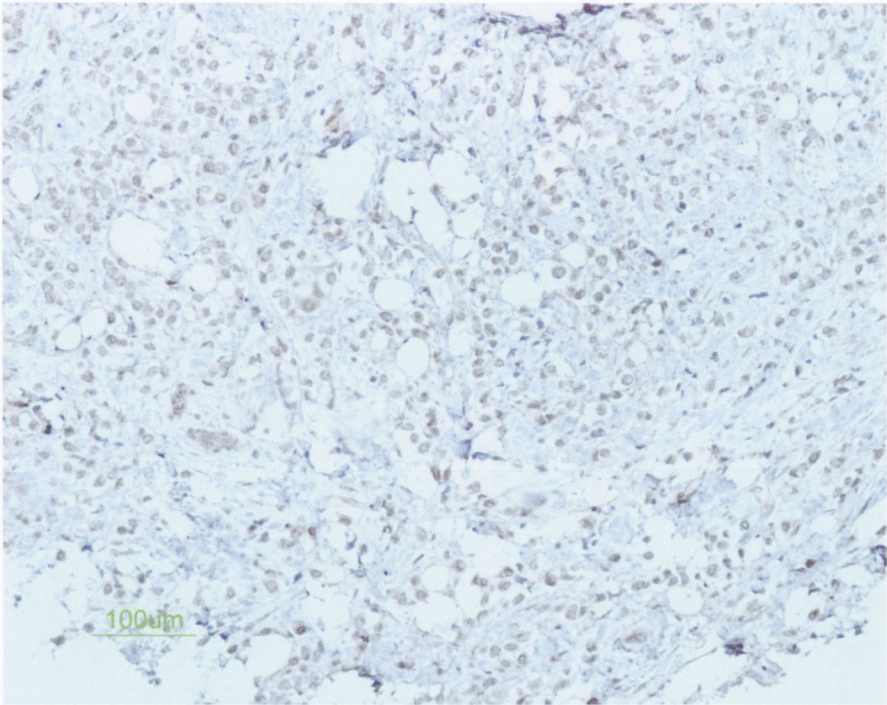
FIG. 4.11 DAB stained breast tumour (ER+, PR+) tissue incubated with anti-HSP70 antibody (Panel A) or cISTc peptide (Panel B). Magnification 100x.
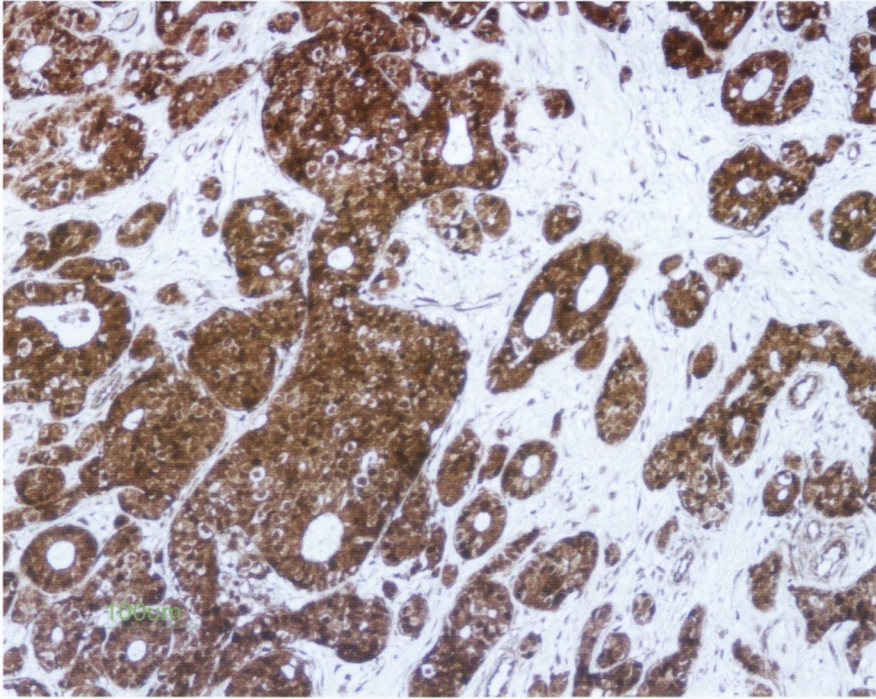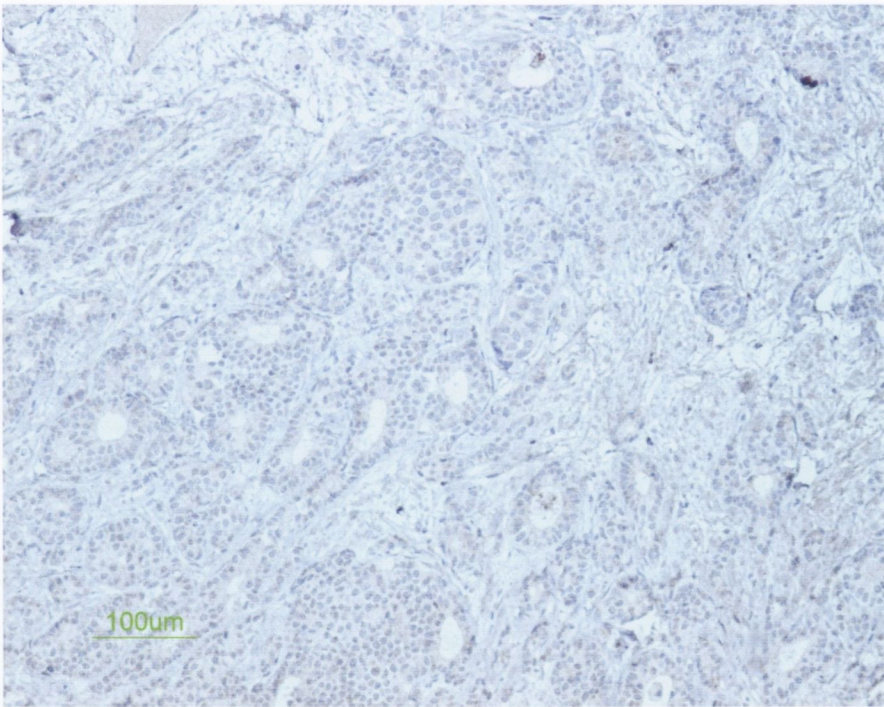
FIG. 4.12 DAB staining of ovarian tumour tissue (metastatic breast cancer) incubated with

anti-HSP70 antibody (Panel A) or cISTc peptide (Panel B). Magnification 100x.

Different staining patterns were also evident in a number of other tumour tissue cores (FIG. 4.13). Staining was evident for both HSP70 and to a lesser extent with cISTc in a groin tumour tissue, however HSP70 appeared to be heavily localized surrounding a number of cells within the tissues, as seen by the intense black rings. This pattern was not seen for cISTc. Another example of differences between the distribution of HSP70 and cISTc can be seen in the rectal tumour tissue, where HSP70 is detected but cISTc peptide staining is less obvious. It was also interesting to note that not all breast tumour tissues showed positive staining for HSP70 or cISTc, as demonstrated by the absence of staining in another breast tumour tissue shown in the last panel in FIG. 4.13.

These results show that HSP70 can be detected in a number of different tumour tissues. In the breast tumour tissues that stained positively for HSP70, a similar staining pattern could be seen for the cISTc peptide. However in the case of an ovarian tumour and rectal tumour tissue, HSP70 staining could clearly be seen, whereas staining with the cISTc peptide was very weak, if at all present. This suggests that the cISTc peptide may preferentially bind breast tumour tissue and may in fact be binding to a tumour antigen associated with HSP70 which is present uniquely or more abundantly in breast tumour tissue. This would also suggest that the repertoire of peptides associated with HSP70 may be different in breast and ovarian tumours.
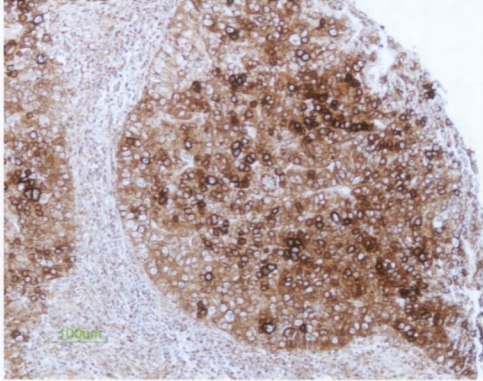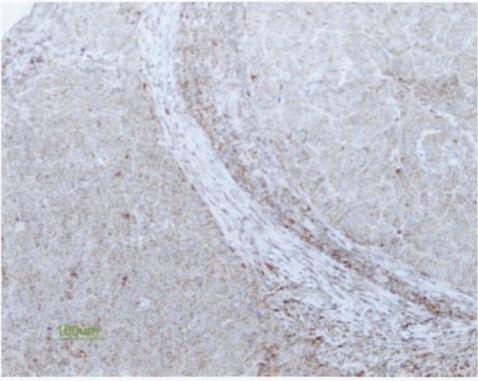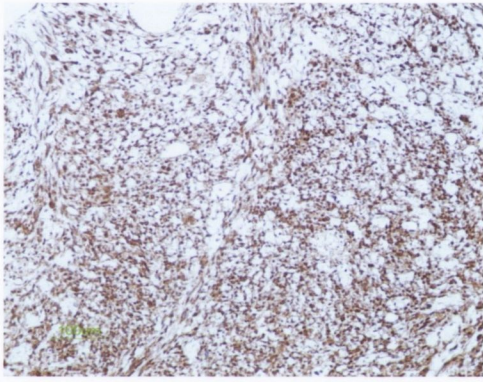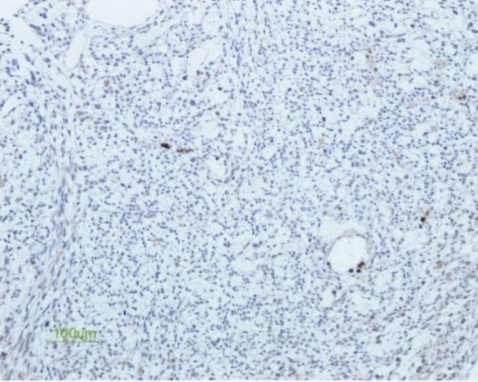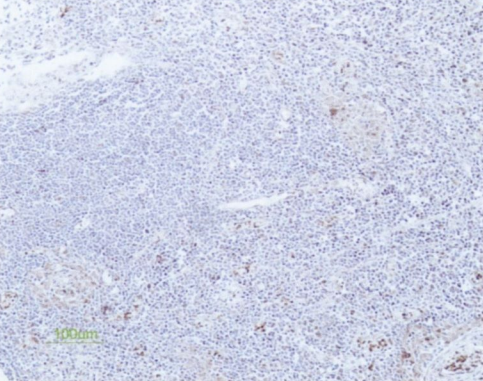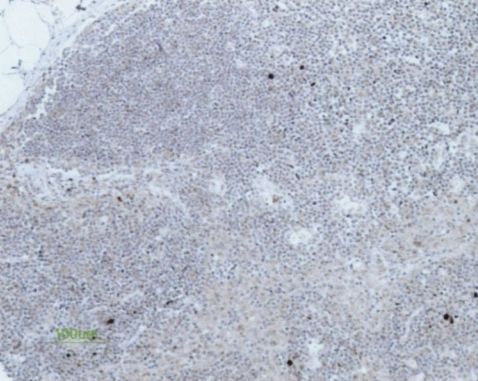
Tumour tissue	A	B
Groin lymph node (unknown metastasis)		
Rectal tumour		
Breast tumour		

FIG. 4.13 DAB staining of multiple tumour tissues incubated with anti-HSP70 antibody

(panel A) and the cISTc peptide (panel B). Magnification 100x.

4.3 Discussion.

The aim of this chapter was identify synthetic peptides that could bind to breast tumour antigens present in HSP70-PC's. This involved firstly the purification of HSP70-PC's from two tumour cell lines; MDA-MB-231 and MCF-7. This was achieved using ADP-affinity chromatography and the presence of HSP70 in the extracts was confirmed by Western blot. An initial bio-panning experiment was performed using these extracts in a standard plate-based method and after six rounds of bio-panning, peptide sequence enrichment was evident. However due to the presence of three, subsequently identified, unrelated co-purifying proteins in the extracts, another method of bio-panning was pursued in order to ensure specificity to the HSP70-PC target proteins of interest. The three co-purifying unrelated proteins were identified as actin and nucleoside diphosphate kinases A and B by MALDI-TOF peptide mass fingerprinting.

The second and main HSP70-PC bio-panning experiment employed the use of immuno-precipitation to capture the HSP70-PC's and allow their separation from the co-purifying proteins present in the affinity-purified extracts. This allowed for the successful separation of the HSP70-PC's from the other proteins. Subtractive selection was performed throughout the panning, ensuring that any phage binding to the HSP70 moiety, the monoclonal antibody, the Protein A/G agarose, BSA or plastic were removed. Specific elution of the peptides associated with HSP70 using ATP was performed in the later rounds, to again enhance and ensure phage specificity to our target tumour antigens.

By continuing the bio-panning experiment to ten rounds and monitoring sequence enrichment in successive rounds, it was possible to narrow the number of candidate peptides to a smaller, more manageable quantity. Different recognizer peptides were isolated for the two tumour cell line-derived HSP70-PC's. MDA-MB-231 derived HSP70-PC's interacted

with a unique peptide sequence: ISTHGPL. Certain motifs could be seen to be developing throughout the experiment which led to the final sequence. These motifs are THXPL and IXTH.

MCF-7 derived HSP70-PC bio-panning showed a bit more variety in the final round yielding three new sequences. However it too showed an enrichment of one particular sequence, STLNVLQ, with an observed SXLN motif occurring in an earlier round. Non-tumour MCF-12A HSP70-PC's didn't yield any final round sequences, which led to the observation that as the panning rounds increased, so too did the rate of insert loss in the phage. The exact cause of this is not known but it is possible that the presence of a foreign cysteine-constrained peptide on the phage surface slows phage virion assembly and thus causes an evolutionary disadvantage. Therefore phage without an insert could out-compete peptide-expressing phage after a series of amplifications.

Another interesting finding was that the newly identified tumour-derived HSP70-PC recognizer peptides shared partial sequence homology to two previously identified HSP70-PC recognizers (Arnaiz et al., 2006). The SQELTQRPYKWH peptide shared a five amino acid homology (TQRPXK) with TQRPDKS, while AIPNKLNVWPPH shared partial homology to both STLNVLQ (shared LNV motif) and TQKWPPH (shared WPPH motif). Both SQE and AIP were identified from a previous PhD-12 library in a bio-panning experiment on MDA-MB-231 derived HSP70-PC's (Arnaiz et al., 2006). The fact that there was such a noticeable sequence homology between peptides identified in two totally independent screenings using different phage libraries, each with a starting pool of approximately 10^9 peptide variants, was a very interesting finding. Due to the observed homology, both AIP and SQE were selected for use in mimic peptide development, as described in the next chapter. The cISTc peptide was also selected as it was the sole peptide identified in the MDA-MB-231 HSP70-PC bio-panning performed here.

134

Using synthetic recognizer peptides linked to magnetic beads a working recognizer specificity assay was developed. Of the MCF-7 HSP70-PC recognizer peptides, cSTLc showed the strongest interaction with the HSP70-PC's. It was interesting that this peptide was the most frequently enriched sequence identified in the bio-panning. cTQKc and AIP did show binding levels higher than the control but from the data available in this case, the binding wasn't statistically significant. It is possible that those peptides, which share a four amino acid homology, bind to less abundant peptide associated with HSP70 and that due to the small amounts of native HSP70-PC's available, it wasn't possible to detect a significant interaction here. Another point to note is that due to the difference in binding levels between cSTLc and AIP, it doesn't appear that their common three amino acid motif (LNV) is the determining factor in target binding. The cSTLc peptide is therefore a novel sequence binder. Unfortunately cSTLc was not further characterized in this study but remains an interesting and novel HSP70-PC recognizer peptide with possible use in future work.

In the case of the MDA-MB-231 HSP70-PC recognizer peptides, SQE showed the highest level of binding. The cTQRc peptide shares a five amino acid homology to SQE but showed a markedly different level of binding, which indicates that these five amino acids are not solely responsible for SQE binding. Both cTQRc and cISTc showed a lower level of binding that wasn't statistically significant in this case, although both peptides showed a higher level than the two negative controls. It's possible that, like AIP and cTQKc, they bind with a lower affinity or to a peptide that is low in abundance in the HSP70-PC's. The cISTc peptide was heavily enriched in the bio-panning, however that did not correlate with the highest level of binding to the HSP70-PC's in this instance. Although the results of these assays are not all statistically significant, they did provide an indication that the peptides bind to the HSP70-PC's at a level higher than the two negative controls. Higher quantities of available HSP70-PC's or the use of surface plasmon resonance would be possible ways of

increasing the sensitivity of the measurement of interaction between the recognizer peptides and the HSP70-PC's.

Two of the three peptides (SQE and cISTc) chosen for use in mimic peptide development (as detailed in Chapter 5) were synthesized with a biotin tag for use in cellular staining experiments. AIP could not be successfully made by our supplier (GL Biochem Ltd.). Both SQE and cISTc were tested for their ability to bind whole fixed cells using immuno-fluorescence. Both peptides appeared to bind to the MDA-MB-231 tumour cells and the MCF-12A non-tumour cells, although they appeared to have slightly different staining patterns. SQE appeared to bind to the cells more strongly causing a brighter fluorescent signal and the staining was present in the cytoplasm of the cells but also across the entire extra-cellular matrix. On the other hand cISTc showed a slightly cleaner staining pattern, with the staining localized mainly in the cytoplasm and sometimes appeared to be stronger around the nuclear membrane.

In an attempt to identify the cellular binding partners of the key recognizer peptides, a protein pull down experiment was performed using MDA-MB-231 tumour cell-derived protein extract and the three MDA-MB-231-derived HSP70-PC recognizers; AIP, SQE and cISTc. Interestingly, the cISTc peptide pulled down a number of unique protein bands. These proteins were analyzed by MALDI-TOF peptide mass fingerprinting and successful identification was made for five of the six cISTc-specific protein bands.

The first main identification to note is that of GRP78, a member of the HSP70 family of proteins. This reinforces the specificity of cISTc as a true HSP70-PC recognizer, in addition to being the most heavily enriched peptide sequence identified in the HSP70-PC bio-panning. Interestingly, in a study by Jakobsen et al (Jakobsen et al., 2007), GRP78 was identified as the cellular target of a human scFv antibody that bound to live breast cancer cells derived from a patient tumour. GRP78 has been shown to be over-expressed in many cancers resulting in

136

increased cell surface expression and has been put forward as a potential new biomarker for many cancers including breast cancer (Lee, 2007). As GRP78 over-expression is associated with higher pathological grade, recurrence, poor prognosis and drug resistance in breast cancers, it represents a possible new target for immunotherapy. In another study a peptide called Pep42 (CTVALPGGYVRVC) capable binding GRP78, was coupled to Taxol and shown to selectively kill cancer cells *in vitro* (Kim et al., 2006). Interestingly Pep42 has three amino acids in an inverse orientation that are common to cISTc.

The second interesting observation from the cISTc pull-down experiment was the identification of three subunits (A, B and L) of the eukaryotic translation initiation factor 3 (eIF3). Individual over-expression of subunits A, B, C, H and I of eIF3 has been shown to result in the malignant transformation of the immortal NIH3T3 fibroblast cell line (Zhang et al., 2007). Over-expression of eIF3 subunits have been detected in many cancers, including breast cancer and it is thought to contribute to tumorigenesis by either causing hyperactive global protein translation and/or by affecting the rate of translation of a subset of mRNA's which encode proteins involved in cell cycle regulation (Silvera et al., 2010).

Another interesting identification was that of the putative elongation factor 1-alpha-like 3 protein. This has 92% homology to the elongation factor 1-alpha 2 protein which was recently put forward as a putative ovarian oncogene (Sharma et al., 2007). The protein identification revealed some interesting results, however further work would be required to confirm the cellular binding partner of cISTc. It is possible that it could bind one of these proteins which results in the whole complex being pulled down. For example, GRP78 is normally present in the endoplasmic reticulum where it could associate with translational machinery. It is also possible that cISTc may bind to a common motif in each of the proteins that was presented as a peptide by the HSP70-PC's. Future work could employ the use of cDNA expression libraries or antibody binding competition experiments to verify the cellular

137

receptors for the HSP70-PC recognizer peptides, followed by amino acid substitutions to determine the exact sites of binding.

The distribution of cISTc within patient tumour tissues provided some interesting results. The cISTc peptide localized in the same areas as HSP70 in two breast tumour tissues. However cISTc peptide staining was significantly lower in the ovarian and rectal tumour tissue when compared to HSP70. The cISTc peptide may therefore have potential as a breast tumour homing peptide. Future work could examine the distribution of cISTc in a larger number of clinical specimens and examine *in vivo* tumour homing in breast tumour xenograft models.

The aim of this project was the generation of breast tumour mimotopes using mirror image phage display. Towards this end, three of the tumour derived HSP70-PC recognizer peptides (AIP, SQE and cISTc) were chosen for use in mimic peptide synthesis as described in the next chapter.

Chapter 5:

Generation and characterization of putative tumour antigen mimic peptides.

5.1 Introduction

Cancer immunotherapy aims to generate an anti-tumour immune response in cancer patients. The identification of tumour antigens is essential for generating targeted anti-cancer therapies. Monoclonal antibodies, antibody fragments or tumour-homing peptides can be designed to deliver a cytotoxic agent to a tumour cell. Another approach is to stimulate human immune cells to target and destroy a tumour. Adoptive immunotherapy involves the *ex vivo* manipulation of immune cells and subsequent re-administration with the aim of evoking an anti-tumour immune response. This has previously been performed with T cells, where autologous tumour-specific T cells are purified, expanded *in vitro* and re-administered to the patient and this has shown clinical responses in patients with melanoma and lymphoma (Brenner and Heslop, 2010). Drawbacks of this approach include the potentially low number of tumour-reactive T cells purified, the potential absence of tumour-specific T cells caused by tumour immune evasion and the fact that T cells can be destroyed *in vivo* due to the immunosuppressive environment (Brenner and Heslop, 2010).

Another approach in adoptive immunotherapy is the use of autologous dendritic cells (DC's) for immunotherapy. DC's are important antigen-presenting cells and are considered to be one of the first initiators of immune responses. They are present in small amounts in the blood and are present in most tissues where they constantly sample the antigenic content of their environment by a variety of methods including phagocytosis, pinocytosis and receptor-mediated endocytosis (O'Neill and Bhardwaj, 2005). They can subsequently process and present antigens on both MHC class I and II molecules. When exposed to local inflammatory mediators (danger signals), such as TNF-α or LPS, DC's become activated or "matured", migrate to lymph nodes and activate T cell responses, however in the absence of maturation signals they are believed to maintain immune tolerance (O'Neill and Bhardwaj, 2005). DC's

therefore require two main factors to induce a tumour-specific immune response; a tumour antigen and a danger signal.

Mimotopes are epitope-mimicking structures conventionally isolated by bio-panning the epitope-binding sites of monoclonal antibodies specific for known tumour antigens. The majority of antibodies are believed to recognize discontinuous (conformational) epitopes and it has been shown that small peptides act as successful mimotopes (Riemer and Jensen-Jarolim, 2007). Mimotopes can be used as a monotherapy to elicit anti-tumour immune responses but rapid turnover and the inability to induce long-lasting immune responses are limiting factors. However mimotopes can be combined with other therapies to induce a stronger and more lasting response, for example presentation of a mimotope by matured DC's can induce more specific, stronger and longer lasting immunity.

The aim of this chapter was to generate breast tumour mimotopes using the newly identified HSP70-PC recognizer peptides with the technique of mirror-image phage display. Our hypothesis is that since the HSP70-PC recognizer peptides physically interact with HSP70-associated antigens, then any peptide that can physically interact with a HSP70-PC recognizer peptide may mimic the original antigen. In addition, the use of an unknown tumour antigen reservoir (HSP70-PC's) allows for an unbiased selection and generation of potential mimotopes of previously unidentified tumour antigens. The ability of the mimotopes to stimulate human immune responses was examined by incubation of *ex vivo* matured monocyte-derived DC's primed with the individual mimotopes, with autologous peripheral blood mononuclear cells (PBMC's) *in vitro*.

5.2 Results

5.2.1 Bio-panning of the HSP70-PC recognizer peptides with the PhD-C7C library to identify putative breast tumour mimotopes.

Three HSP70-PC recognizer peptides; AIP, SQE and cISTc were chosen for use in the generation of putative tumour antigen mimotopes. As described in the previous chapter, these peptides were chosen based on their enrichment during the HSP70-PC bio-panning experiment (cISTc) or due to their homology with a range of newly identified HSP70-PC recognizer peptides (AIP and SQE). The PhD-C7C phage library has been used throughout this project and is again used here to identify cyclic 7-mer peptides specific for the three HSP70-PC recognizer peptides. The PhD-C7C bio-panning experiment was performed as described in Chapter 2, section 2.21.1 and an outline of the experiment is shown in FIG. 5.1.

In brief, HSP70-PC recognizer peptides were linked to magnetic beads and incubated with the phage library. Unbound phage were removed by washes. Peptide-bound phage were eluted with cognate peptide and amplified. This process was repeated three times after which, a competitive elution was performed using peptides with homology to the target peptides in order to identify any potential motifs that were essential for the binding interactions (FIG. 5.1, R4). The phage eluted from round 4 were subjected to four more rounds of bio-panning (FIG. 5.1, R5-8) in which bound phage were eluted with cognate peptide. Individual phage clones were isolated and sequenced after rounds 4 and 8. The peptide sequences identified from bio-panning using SQE, AIP and cISTc with the PhD-C7C library are shown in Tables 5.1, 5.2 and 5.3, respectively.

```
┌─────────────────────────────────────────────────────────────────────┐
│                    ┌─────────────────────────┐                        │
│                    │   PhD-C7C 10¹¹ pfu       │                        │
│                    └─────────────────────────┘                        │
│                                │                                       │
│                                ▼                                       │
│                    ┌─────────────────────────┐                        │
│                    │ AIP, SQE or cISTc        │◄───────┐       R 1-3   │
│                    │ linked magnetic beads    │        │               │
│                    └─────────────────────────┘        │               │
│                                │                       │               │
│                                └──► Unbound phage   X3 │               │
│                    ┌─────────────────────────┐        │               │
│                    │ Elute with cognate       │────────┘               │
│                    │ peptide & amplify        │                        │
│                    └─────────────────────────┘                        │
└─────────────────────────────────────────────────────────────────────┘
```

FIG. 5.1 Outline of mimic bio-panning using the PhD-C7C phage library.
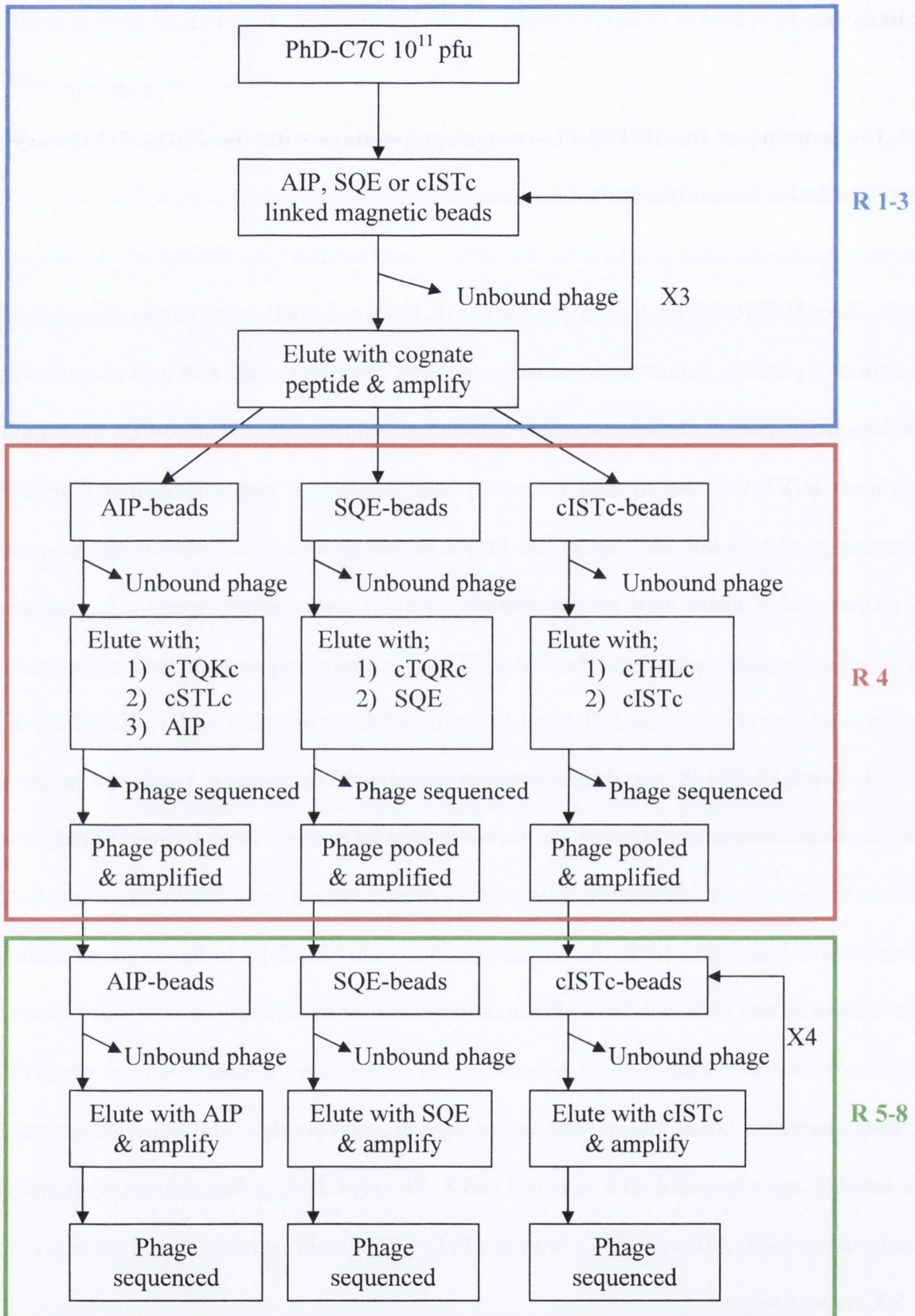
FIG. 5.1 Outline of mimic bio-panning using the PhD-C7C phage library.

Table 5.1 Mimic peptide sequences and properties identified by bio-panning the SQE peptide with the PhD-C7C phage library.

Recognizer panned: SQELTQRPYKWHCGGG			
Elution with;	*Peptide sequences*	*Mean Hydrophilicity*	*Net charge*
Round 4			
CTQRPDKSCGGG	PIERGLS	0.4	0
	TT**KS**AGH	0.2	1.1
	QDPYGKN	0.6	0
	NP**SP**I**KS**	0.3	1
	SSLKSMT	0.1	1
SQELTQRPYKWHCGGG	**LSSPVTY**	-0.8	0
	LSSPVTY	-0.8	0
	G**IKS**HAS	0.1	1.1
	KAGMHRM	0.3	2.1
	SSLKSMT	0.1	1
	TDSRIAQ	0.5	0
	NFNNIAH	-0.7	0.1
Round 8			
SQELTQRPYKWHCGGG	**LSSPVTY** (6/6)	-0.8	0

Recurring peptides and peptide motifs are underlined and in bold. The homology between the SQE target peptide and cTQRc peptide is underlined. Brackets indicate frequency of occurrence.

The final round of bio-panning using SQE as a target yielded one heavily enriched sequence, LSSPVTY, which was present in 100% of clones sequenced. Interestingly this peptide sequence was identified in approximately 30% of phage clones sequences after elution with SQE in round 4. Other sequence enrichment was observed after round 4, where the SSLKSMT peptide was eluted with both cTQRc and SQE. cTQRc and SQE recognizer peptides share a five amino acid homology (TQRPXK) and due to the fact that the SSLKSMT sequence was eluted with both peptides, this shared motif may be important for binding. A number of small motifs were common among several sequences, such as IKS, KS and SXXK. In general the peptides identified were mostly hydrophilic and either neutral or positively charged. The exception was LSSPVTY and one other sequence which were hydrophobic and neutral.

Partial enrichment of phage sequences could also be seen after four rounds of bio-panning on AIP with the PhD-C7C library as indicated in Table 5.2. In this case one peptide, LQTPYRA, was observed in the phage pool eluted with both the cSTLc and AIP peptides. AIP shares a three amino acid homology (LNV) with cSTLc and it's therefore possible that this tri-peptide motif is responsible for binding to LQTPYRA. In addition another peptide eluted at this stage with AIP showed homology to this sequence with a shared TXYR motif. The SNASIKA peptide eluted by cSTLc in round 4 shares a SXAXXK motif with the SEALTKS peptide eluted in same round with AIP. This again suggests the possible importance of the LNV motif in peptide binding. The SNASIKA peptide was also one of the only two sequences identified in the final round of bio-panning. Only 20% of phage clones eluted with AIP after round 8 contained peptide sequences and frequency of peptide loss from the phage was very high in this experiment.

145

Table 5.2 Mimic peptide sequences and properties identified by bio-panning the AIP peptide with the PhD-C7C phage library.

Recognizer panned: AIPNKLNVWPPHCGGG			
Elution with;	Peptide sequences	Mean Hydrophilicity	Net charge
Round 4			
CTQK<u>WPPH</u>C	HNALRAM	-0.2	1.1
	QQHRMAS	0.2	1.1
	STTTPTY	-0.5	0
	EKTYGPR	0.9	1
	PAIPNLA	-0.6	0
CST<u>LNV</u>LQC	**<u>LQTPYRA</u>**	-0.3	1
	HGQAMKS	0.2	1.1
	<u>SNASIKA</u>	0.1	1
	SSDSTSK	1	0
	SVSHHTY	-0.7	0.2
AIPNK<u>LNV</u>W<u>PPH</u>CGGG	NDDHMPA	0.6	-1.9
	<u>SE</u>A<u>L</u>T<u>K</u>S	0.6	0
	IAGNIPH	-0.6	0.1
	KNPHLMR*	0.4	2.1
	TP<u>TK</u>Y<u>R</u>H	0.3	2.1
	<u>LQTPYRA</u>	-0.3	1
Round 8			
AIPNKLNVWPPHCGGG	NSAGVAY (1/2)	-0.6	0
	<u>SNASIKA</u> (1/2)	0.1	1

Recurring peptides and peptide motifs are underlined and in bold. The homology between the recognizer peptides is underlined. * indicates sequence occurred in another independent experiment. Brackets indicate frequency of sequence occurrence.

The sequence results from the cISTc bio-panning are shown in Table 5.3. Unlike that observed for SQE and AIP bio-panning, no specific enrichment of peptide sequences was observed following four rounds of cISTc bio-panning. This could be due to either the cyclic nature of the peptide or its slightly smaller size. However by round 8, sequence enrichment was evident. One peptide, TNTLSNN, was heavily enriched in the final round and was present in 80% of the clones sequenced. This peptide shared a small two amino acid motif (SN) with the DVRSNLM peptide which was eluted with cISTc in round 4. As this was the only noticeable similarity to sequences identified in round 4, the enrichment of this sequence must have occurred in the later rounds.

One other sequence, LAPNQAA, was identified in the final round but was present in only 20% of the phage sequenced. This sequence shared a PXQA motif with the WPPQARA peptide eluted with cTHLc in round 4. The cTHLc peptide shares a four amino acid motif (THXPL) with cISTc and was identified during the HSP70-PC bio-panning experiment that led to the identification of cISTc (see Chapter 4: Table 4.3). As the PXQA motif was present in both the LAPNQAA sequence eluted in the final round with cISTc, as well as the WPPQARA peptide sequence eluted with cTHLc in round 4, it suggests a possible interaction between the PXQA and THXPL motifs. Both final round peptides, TNTLSNN and LAPNQAA are neutral and hydrophobic.

The KNPHLMR peptide sequence occurred in both the AIP and cISTc bio-panning experiments. It occurred in round 4 of both experiments and was eluted with both AIP and cISTc (as indicated by the * in Tables 5.2 and 5.3).

Table 5.3 Mimic peptide sequences and properties identified by bio-panning the cISTc peptide with the PhD-C7C phage library.

Recognizer panned: CISTHGPLCGGG			
Elution with;	Peptide sequences	Mean hydrophilicity	Net charge
Round 4			
CTHLPLRLCGGG	NHNRGPT	0.4	1.1
	DKAQSAQ	0.8	0
	KEIHQGL	0.3	0.1
	WPPQARA	-0.2	1
CISTHGPLCGGG	VSNEILH	-0.3	-0.9
	NPKIEHY	0.2	0.1
	SPGTGAT	-0.1	0
	PSDLPQL	0	-1
	SPNPFNR	0.2	1
	KSSVHFM	-0.3	1.1
	HRPHSPF	0	1.2
	DVRSNLM	0.3	0
	KNPHLMR*	0.4	2.1
Round 8			
CISTHGPLCGGG	TNTLSNN (4/5)	-0.2	0
	LAPNQAA (1/5)	-0.4	0

Recurring peptides and peptide motifs are underlined and in bold. The homology between the recognizer peptides is underlined. * indicates sequence occurred in another independent experiment. Brackets indicate frequency of sequence occurrence.

One observation during the bio-panning experiments using the PhD-C7C phage library was that there was a general increase in the frequency of insert loss from the phage in the final round of bio-panning. Table 5.4 shows the frequency of insert loss during the three PhD-C7C bio-panning experiments. This phenomenon of insert loss with the PhD-C7C library was also observed during the HSP70-PC recognizer bio-panning detailed in the previous chapter (refer to Chapter 4, Table 4.4). There appears to be a correlation between an increasing frequency of insert loss and number of bio-panning rounds, with the exception of the SQE bio-panning. All of the phage clones isolated in round 8 of the SQE bio-panning contained the same sequence (LSSPVTY) which could suggest that the loss of peptide inserts may be sequence specific.

Table 5.4 Frequency of insert loss from phage during the PhD-C7C bio-panning experiments.

Recognizer peptide bio-panned	Bio-panning round	Average insert loss (%)
cISTc	4	5
	8	50
AIP	4	30
	8	80
SQE	4	32
	8	0

5.2.2 Bio-panning of the HSP70-PC recognizer peptides with the PhD-12 phage library to identify putative mimotopes.

To investigate whether the frequency of insert loss seen with PhD-C7C occurred with other phage-peptide display libraries and to potentially identify additional mimic peptides, an alterative phage library, PhD-12, was used in new set of bio-panning experiments. The PhD-12 phage library is also an M13 phage library constructed in a similar manner as PhD-C7C, except that it expresses linear 12-mer peptides on the phage surface. PhD-12 was used to identify linear 12-mer peptides that bind to the three HSP70-PC recognizers: AIP, SQE and cISTc. The experimental outline is shown in FIG. 5.2 and detailed in Chapter 2, section 2.21.2. In brief, HSP70-PC recognizer peptides were linked to magnetic beads, incubated with the phage library and bound phage were eluted with cognate peptide and amplified. Four rounds of bio-panning were performed and ten phage from the final round were isolated and amplified. Five phage were randomly selected for sequencing and the results are listed in Table 5.5.
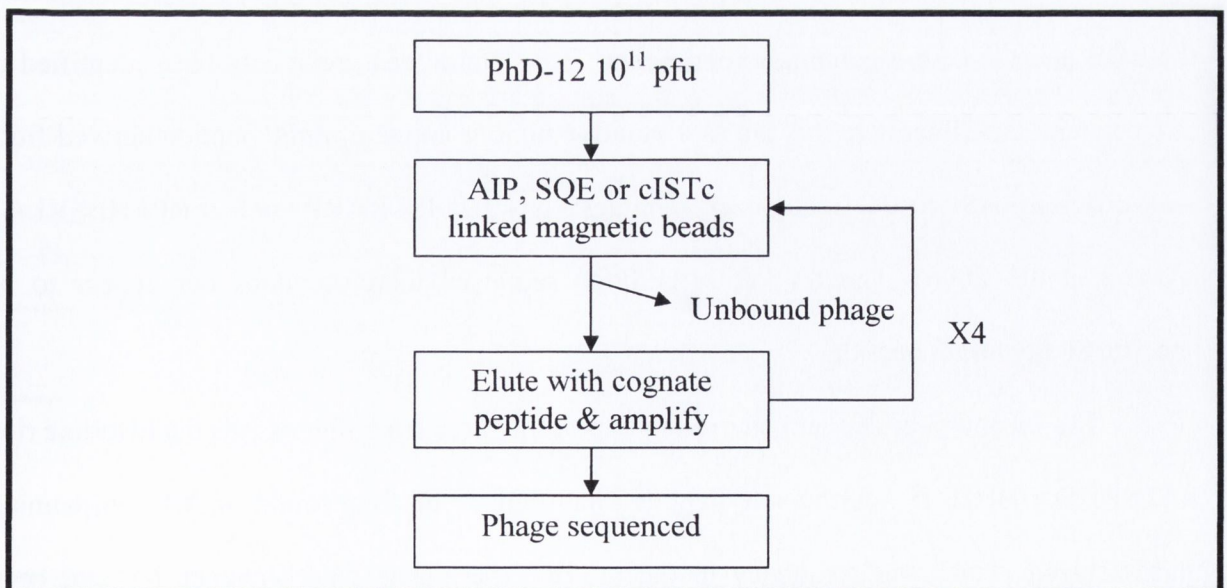
FIG. 5.2 Outline of mimic bio-panning using the PhD-12 phage library.

Table 5.5 Mimic peptide sequences and properties identified by bio-panning of the SQE, AIP and cISTc HSP70-PC recognizer peptides with the PhD-12 phage library.

Recognizer bio-panned	Mimic peptide sequence	Frequency	Mean hydrophilicity	Net charge
SQELTQRPYKWHCGGG	SVSVGMKPSPRP	4/5	0.2	2
	GLKIWSLPPHHG	1/5	-0.5	1.2
AIPNKLNVWPPHCGGG	KSLSRHDHIHHH	5/5	0.3	1.5
CISTHGPLCGGG	SVSVGMKPSPRP	3/5	0.2	2
	KSLSRHDHIHHH	1/5	0.3	1.5
	SCCHYSSQLTPS	1/5	-0.5	0

Strong enrichment of phage sequences was evident after four rounds of bio-panning in each experiment. Two peptides were seen to occur in independent experiments. The first is SVSVGMKPSPRP, which was the most heavily enriched peptide sequence identified in both the SQE and cISTc bio-panning experiments. This peptide has previously been identified in independent experiments in this lab as a putative tumour antigen mimic peptide derived from two different HSP70-PC recognizer peptides; NNYDDISLRARP and IERPLHESVLAT (Arnaiz et al., 2006). The SVSVGMKPSPRP sequence therefore does not appear to be specific to any target peptide.

The second peptide that occurred in two of the three experiments was the histidine rich KSLSRHDHIHHH. It was the sole peptide identified in the final round of AIP bio-panning and occurred at a lower frequency in the cISTc experiment. This sequence has not been

previously identified and could suggest a commonality in the target bound by these two peptides. One additional sequence identified, SCCHYSSQLTPS, was unique to the cISTc bio-panning and could reflect a target specific to the cISTc peptide.

An additional observation from the bio-panning experiments with the PhD-12 phage library was that, of the thirty individual phage clones that were selected and amplified from the final round of bio-panning, 100% contained an insert as confirmed by PCR (data not shown). Therefore the frequency of insert loss seen in all previous bio-panning experiments appears to be a phenomenon associated with the constrained PhD-C7C phage library.

5.2.3 Mimic peptides chosen for further characterization and synthesis.

Three of the newly identified mimic peptide sequences were chosen for further characterization and synthesis and these are listed in Table 5.6. The selection of the peptides was based on their presence in the final round of bio-panning and frequency of occurrence. Only 7-mer peptides were pursued as the 12-mer peptides demonstrated a lack of target specificity. A small spacer (GG) was added to the C-terminal of the peptides to allow for tagging of the peptides without interference to the C-terminal cysteine residue.

Table 5.6 List of synthetic mimic peptides.

Derived from recognizer:	Mimic peptide sequence	Mimic name
SQE	CLSSPVTYCGG	LSS
cISTc	CTNTLSNNCGG	TNT
	CLAPNQAACGG	LAP

5.2.4 Homology to known proteins.

Homology searches to known proteins were carried out in order to examine the possible origin of the newly identified mimic peptides, using BLASTP and the human SwissProt database. The top five most significant hits are listed in Table 5.7. Both TNT and LSS had many regions of homology to members of the mucin family of proteins but these hits were not rated as significant as others. Nevertheless, TNT shared homology with MUC-17 involving six regions containing the (T)NTLS motif, whereas LSS shared 22 regions of homology with MUC-16 (CA-125). Mucins contain variable numbers of tandem repeat domains in their N-terminal which are sites of O-glycosylation. Aberrant glycosylation in tumours is believed to expose peptide epitopes suitable for tumour targeting, so the homology of the mimic peptides to these repeats could be significant.

5.2.5 Interaction of synthetic mimic peptides with HSP70-PC recognizer peptides.

In order to confirm that the newly synthesized mimic peptides could bind their respective HSP70-PC recognizer peptide, a binding assay was performed as described in Chapter 2, section 2.22. Briefly, mimic peptides or a control peptide (alpha factor) were linked to magnetic beads and subsequently incubated with their respective HSP70-PC recognizer peptides (the latter being biotinylated). The bound peptides were detected by extravidin-peroxidase and TMB. The reaction was stopped with sulphuric acid and the absorbance was read at 450nm.

Table 5.7 Homology of mimic peptides to known proteins.

Mimic peptide	Homologous protein	Accession No.	Shared sequence
LSSPVTY (167 hits)	Testisin (serine protease 21)	Q9Y6M0.1	LS-PVTY
	EGF-like module receptor 2	Q9UHX3.2	LSSPVT+
	Ig kappa chain region C	P01834.1	LSSPVT
	Transmembrane protease serine 11E	Q9UL52.2	LSSPV-Y
	Bcl-2-like protein 13	Q9BXK5.1	LS-PVTY
TNTLSNN (132 hits)	A-kinase anchor protein 11	Q9UKA4.1	TNTLSN
	Nucleoporin Nup214	P35658.2	NTL-NN
	Abl interactor 2	Q9NYB9.1	NTL-NN
	Leucine-rich repeat containing protein 50	Q8NEP3.5	T+TLSN
	PH and SEC7 domain-containing protein 1	A5PKW4.2	T+TLSN
LAPNQAA (123 hits)	Rest corepressor 2	Q8IZ40.2	LAPNQ
	Transforming acidic coiled-coil-containing protein 2	O95359.3	LAPNQ
	Protein 4.1	P11171.4	LAPNQ
	Breast cancer-associated antigen BRCAA1	Q4LE39.2	LAPNQ
	Autophagy-related protein 13	O75143.1	LAPNQ

The binding of the SQE peptide to its respective mimic, LSS, is shown in FIG. 5.3. The results show that SQE binds to LSS but at a rather low level. The binding of SQE to LSS was statistically significant (P value of 0.03), which was not the case with the control peptide. The ability of the cISTc recognizer peptide to bind its derived mimic peptides is shown in FIG. 5.4. The cISTc peptide bound to the TNT mimic peptide over four-times more than to the unlinked beads and this binding was statistically significant with a P value of 0.003. The cISTc recognizer peptide also bound to LAP but at a lower level than TNT, whereas it showed no significant binding to the control peptide. It is interesting to note that TNT was the most heavily enriched sequence in the final round of the cISTc bio-panning, whereas LAP was present at a lower frequency (see Table 5.3) and their frequency of enrichment appears to correlate with their level of binding to cISTc.

These binding assays verified that the new synthetic mimic peptides bind specifically but with different affinities to the recognizer peptides from which they were derived. In addition, the cISTc peptide appeared to demonstrate the most specificity and had the strongest interaction with the TNT mimic peptide.
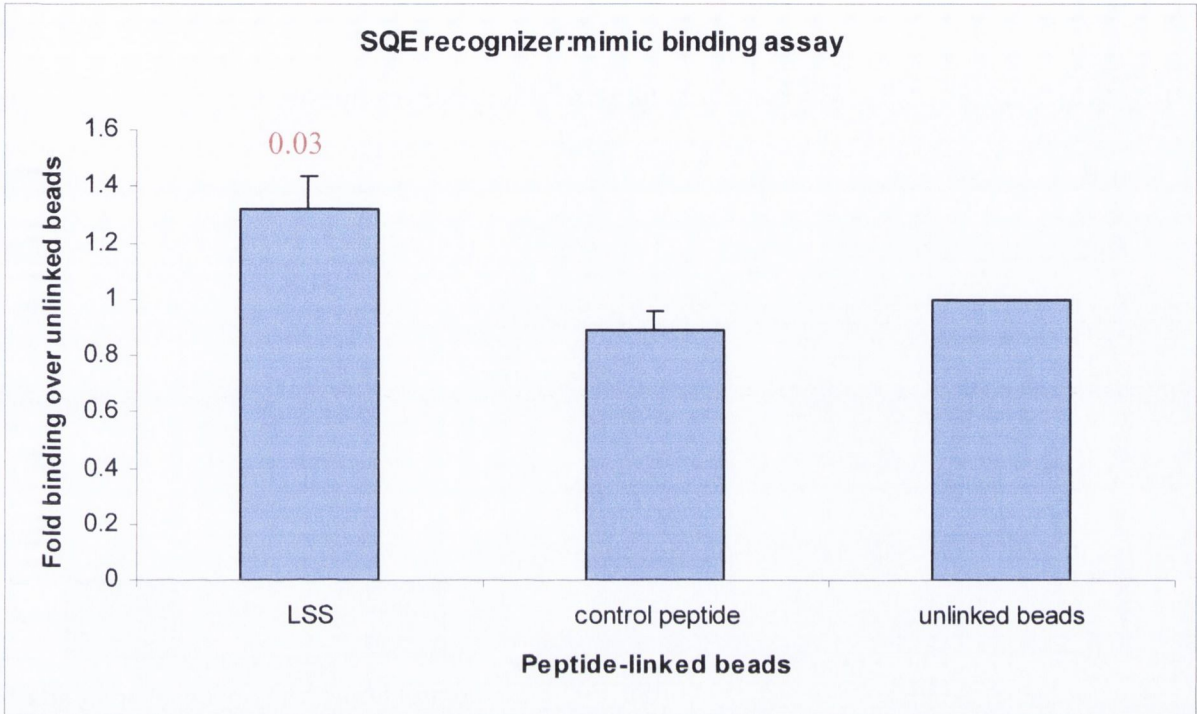
FIG. 5.3 Binding of the SQE recognizer peptide to the LSS mimic peptide. Data is representative of 5 experiments. Standard error indicated. Significant P values shown (red).
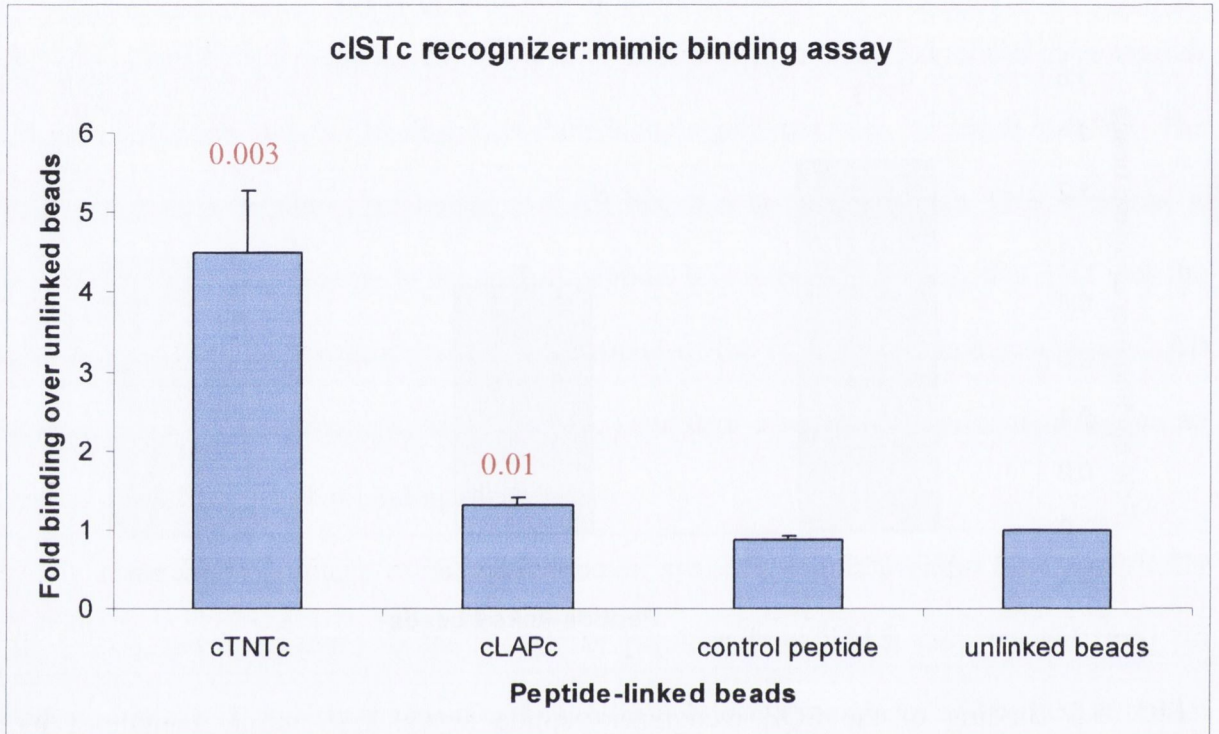
FIG. 5.4 Binding of the cISTc recognizer peptide to the TNT and LAP mimic peptides. Data is representative of 6 experiments. Standard error indicated. Significant P values shown (red).

5.2.6 Characterization of the ability of the tumour antigen mimic peptides (mimotopes) to stimulate human immune responses *in vitro*.

In order to evaluate the potential therapeutic value of the newly identified mimotopes, we examined their ability to induce human immune responses *in vitro*, in a manner similar to previously described methods (Arnaiz et al., 2006). Monocyte-derived autologous DC's loaded with the three new mimic peptides; LSS, TNT and LAP were tested for their ability to induce CD8+ T cell activity *in vitro*.

5.2.6.1 Overview of immune assay procedure.

An outline of the immune assay procedure is shown in FIG. 5.5. In brief, PBMC's were purified from buffy coat packs by Ficoll gradient centrifugation and CD14+ cells were positively selected using CD14 Microbeads, as described in Chapter 2, section 2.23.1. Half of the CD14+ cells were immediately incubated with GM-CSF and IL-4 for 6 days to induce differentiation into DC's (as described in Chapter 2, section 2.23.2). A photo of the differentiated DC's on day 6 is shown in FIG. 5.6. The second half of CD14+ cells were maintained in un-supplemented media for later use and the CD14- PBMC's were maintained in standard culture media.

The DC's were matured by incubation with LPS and TNF-α for 24hr (as described in Chapter 2, Section 2.23.3). The following day the supernatant was removed and DC maturation was monitored by measuring IL-12 production present in the supernatant. IL-12 is secreted by matured DC's and is important for T cell activation (O'Neill and Bhardwaj, 2005). The DC's were then incubated with the mimic peptides overnight. The following day the peptide-loaded DC's were co-incubated with the CD14- PBMC's at a ratio of 1:10,

158

respectively (detailed in Chapter 2, section 2.23.4). Supernatants were removed at days 3, 6 and 8 to be assayed for the presence of interferon-γ, which is produced by activated T cells.

Following 8 days of incubation, the DC/CD14- PBMC cells were incubated with a fresh batch of autologous DC's pulsed with the mimotopes. In this instance the DC's were matured with TNF-α only. LPS, a potent DC activator, was not included so that immune responses specific to the mimotopes could be measured. Supernatants were collected at 3-day intervals following the second stimulation (days 11, 14 and 17) for subsequent interferon-γ assays.

5.2.6.2 IL-12 assay to measure DC maturation.

DC maturation is an important step for their immune stimulatory function and can be measured by detecting IL-12 production by the DC's. The first batch of DC's was matured by incubation with LPS and TNF-α. The second batch was matured only with TNF-α. Following 24hr incubation, the supernatants were removed and assayed for IL-12. Levels of IL-12 were determined by comparison with known standards in a capture ELISA and the results are shown in FIG. 5.7. The first batch of DC's showed nearly 5-times more IL-12 production than the second batch. This difference is most likely due to the absence of LPS during maturation of the second batch of DC's. However both batches showed detectable levels of IL-12 production and this indicates that the DC's underwent maturation and were therefore able to take up and present the mimic peptides.

159
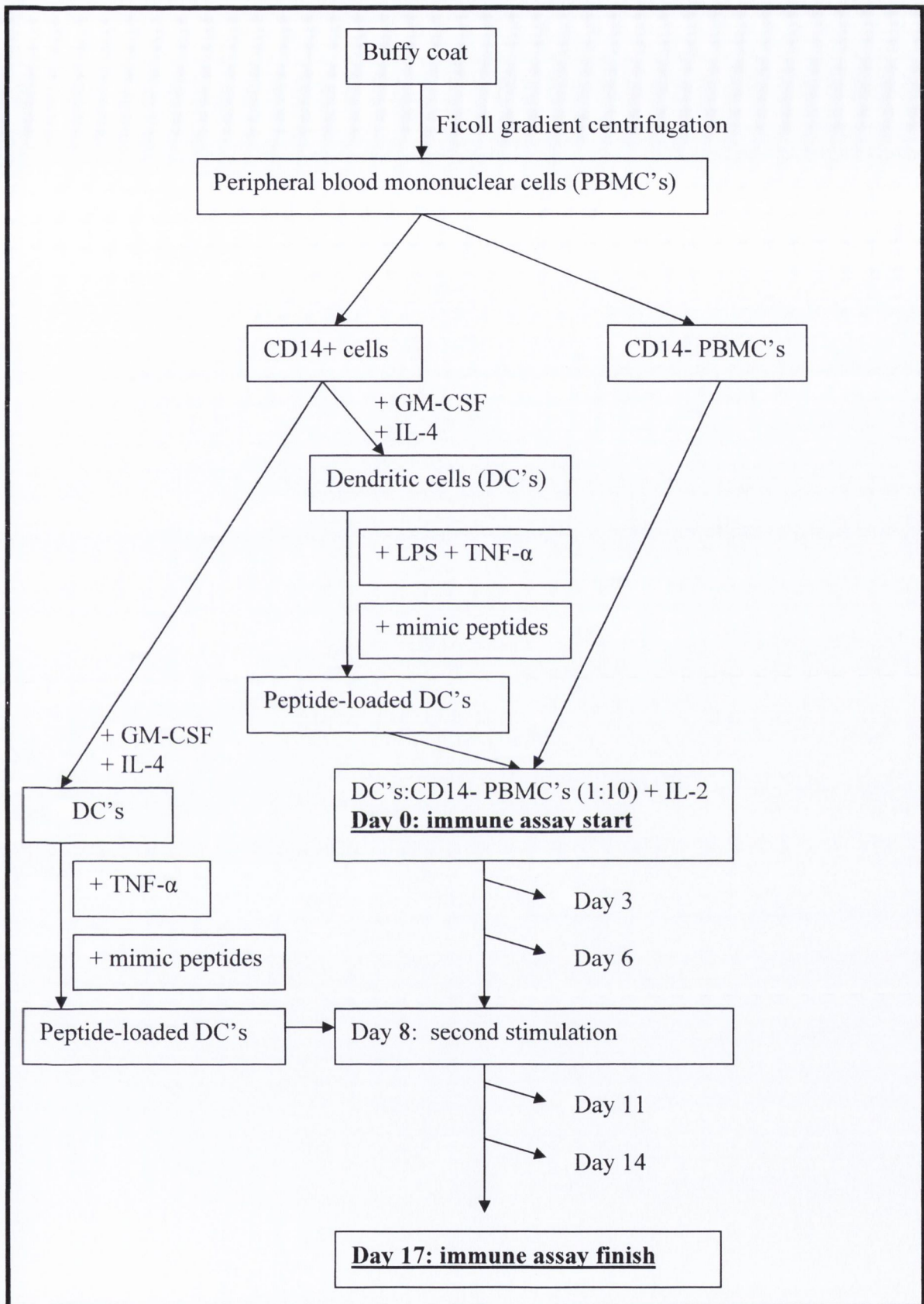
FIG. 5.5 Outline of the immune assay procedure.
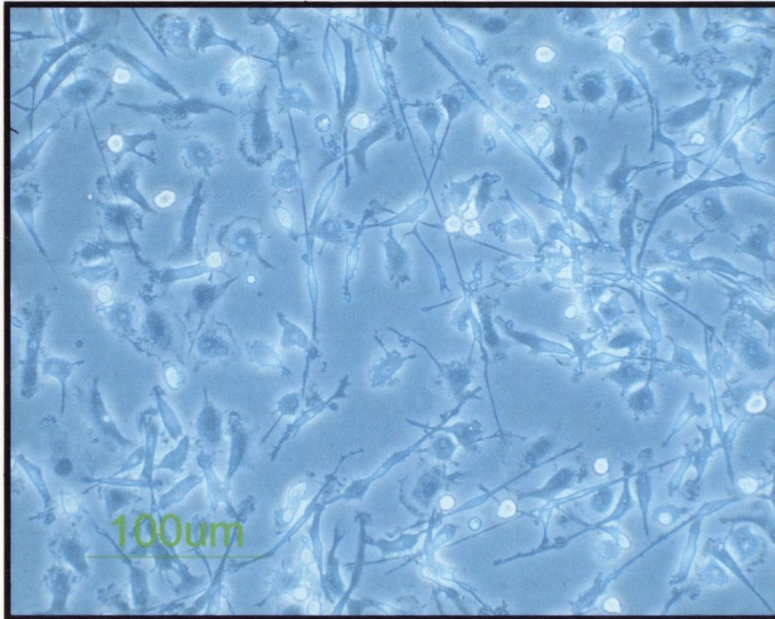
FIG.5.6 Photo of differentiated DC's.

Fully differentiated DC's showing presence of characteristic dendrites. Photos taken under phase contrast (Phase 1) on an E400 inverted microscope. Magnification is 200X.
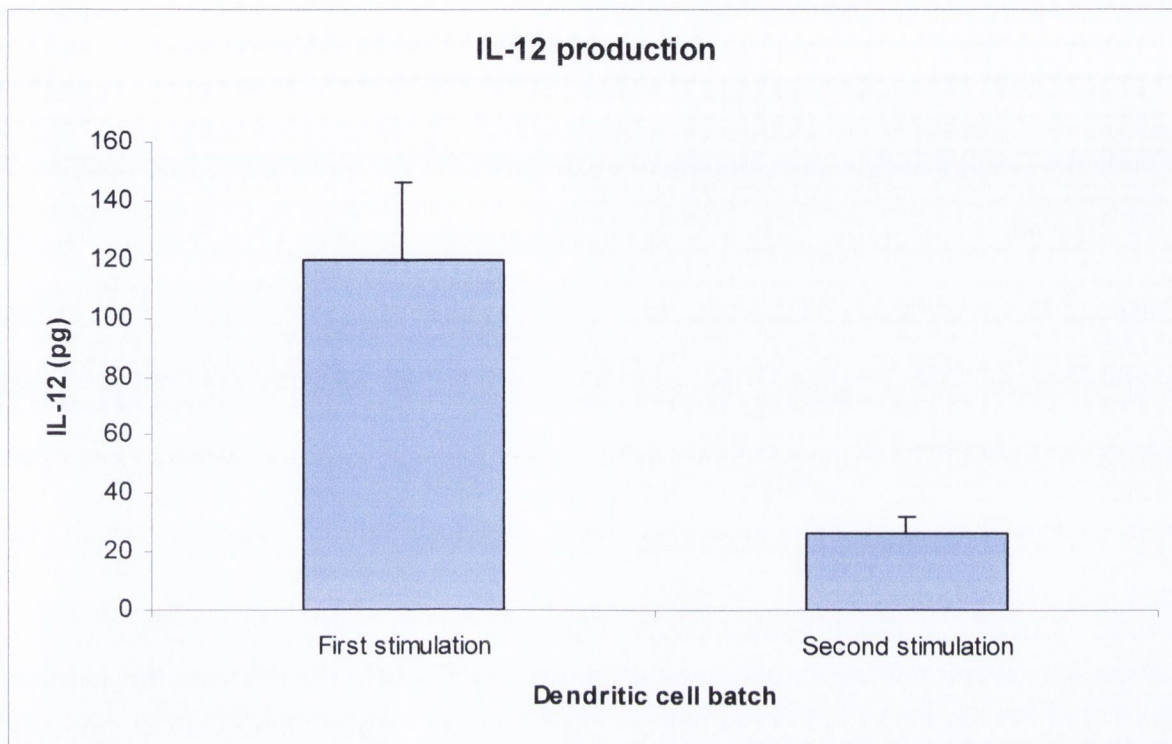
FIG. 5.7 Levels of IL-12 produced by the two batches of DC's. Concentrations were determined by ELISA against an IL-12 standard curve. Values represent triplicate samples. Error bars indicate standard deviation.

5.2.6.3 Interferon-γ assays to measure CD8+ T cell responses.

Dendritic cells have the ability to activate both CD4+ and CD8+ T cell responses and both of these responses can be very useful in generating immune activity against a given tumour either by antibody-mediated activity or cytotoxic T cell activity, respectively. Cytotoxic T cell activity can be monitored by detecting levels of interferon-γ production. The ability of the mimotope-loaded DC's to induce cytotoxic T cell activity was measured by detecting levels of interferon-γ production at 2-3 day intervals. Two negative controls were also included; DC's alone (no peptide) and DC's loaded with WHK peptide (WHKTSQPPRLIF) previously shown to be a poor immune activator (Arnaiz et al., 2006). The levels of interferon-γ production following mimotope-induced activation are shown in FIG. 5.8.

A high level of interferon-γ production can initially be seen following the addition of the first batch of DC's. This effect appeared to be present in all samples and is likely to have resulted from the use of LPS in DC maturation. This global effect of LPS has been observed in previous experiments in this lab (James TC and Bond U, unpublished data and (Arnaiz et al., 2006). However this effect was markedly reduced by day 8. From day 8 onwards, two of the mimic peptides, TNT and LAP, showed a consistently higher level of interferon-γ production compared to the controls. The level of interferon-γ production generated for each mimotope was compared to the no peptide control at each respective time point and using a student t-test the P values were determined which are listed in Table 5.8. Both TNT and LAP induction were statistically significant (listed in red in Table 5.8). In addition, the effect of the LSS mimic peptide was also statistically significant but only on day 11.

163
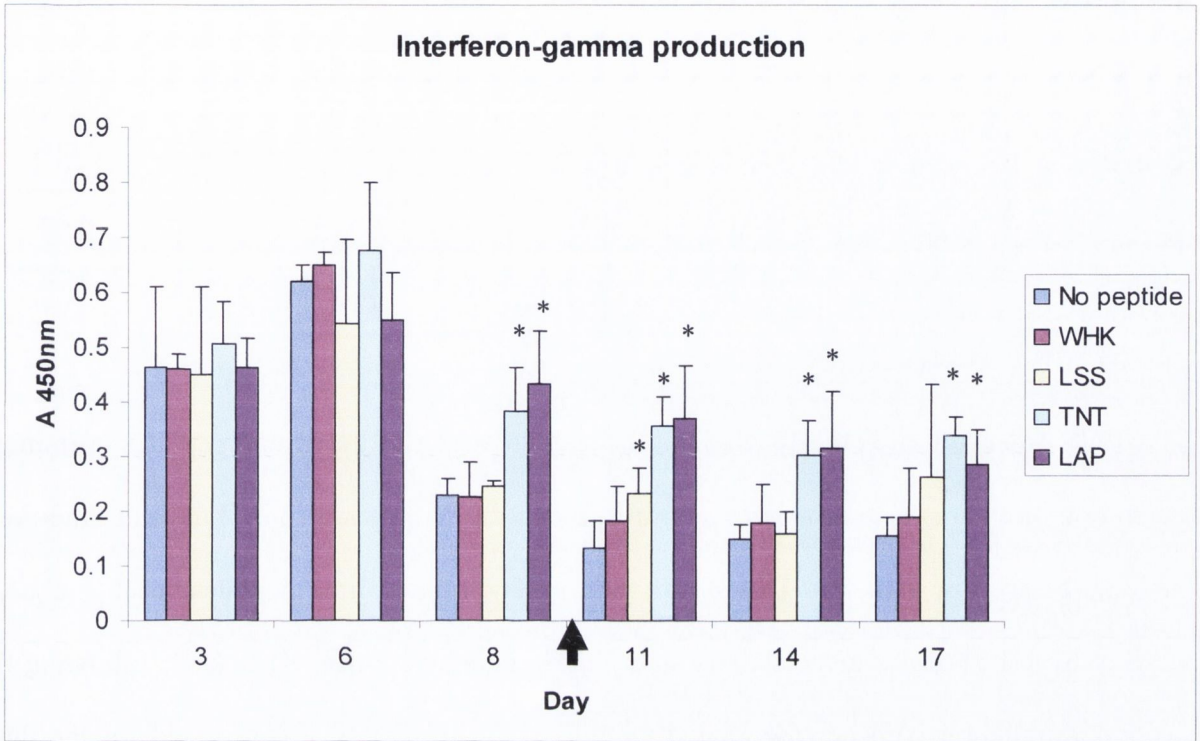
FIG. 5.8 Levels of interferon-γ produced by T cells in response to peptide-loaded DC's.

Values are representative of triplicate samples. Standard deviation is indicated. Legend

indicates the peptides loaded on the DC's. Arrow indicates the second round of stimulation

with peptide-loaded DC's. * indicates statistical significance (see Table 5.8 for P values).

Table 5.8 Statistical significance (P values) of mimotope-induced interferon-γ production.

Day / Mimic	3	6	8	11	14	17
WHK	0.5	0.17	0.45	0.12	0.19	0.22
LSS	0.5	0.2	0.2	0.01	0.28	0.19
TNT	0.3	0.28	0.04	0.004	0.007	0.008
LAP	0.5	0.21	0.02	0.007	0.03	0.02

In order to more closely examine the specific effect of the mimic peptides in immune activation, the data was normalized with respect to the no peptide control at each time-point and can be seen in FIG. 5.9. This shows that by day 8 two mimic peptides, TNT and LAP, display over 1.75-times more activity than the no peptide control. At day 11, following the second stimulation with peptide-loaded DC's, a peak of activity was detected for the three mimic peptides. Both TNT and LAP showed a nearly 3-fold increase in interferon-γ production over the controls, whereas LSS showed a nearly 2-fold increase. This would suggest that the second batch of DC's caused an increase in the immune response, possibly due to the clonal expansion of antigen-specific activated T cells. The effect caused by LSS proved to be significant only at this point, whereas the activity of both TNT and LAP continued to be significantly high for the duration of the experiment (consistently approximately 2-fold higher than controls). In contrast the WHK peptide showed little to no activity during the experiment, consistent with previous data (Arnaiz et al., 2006).
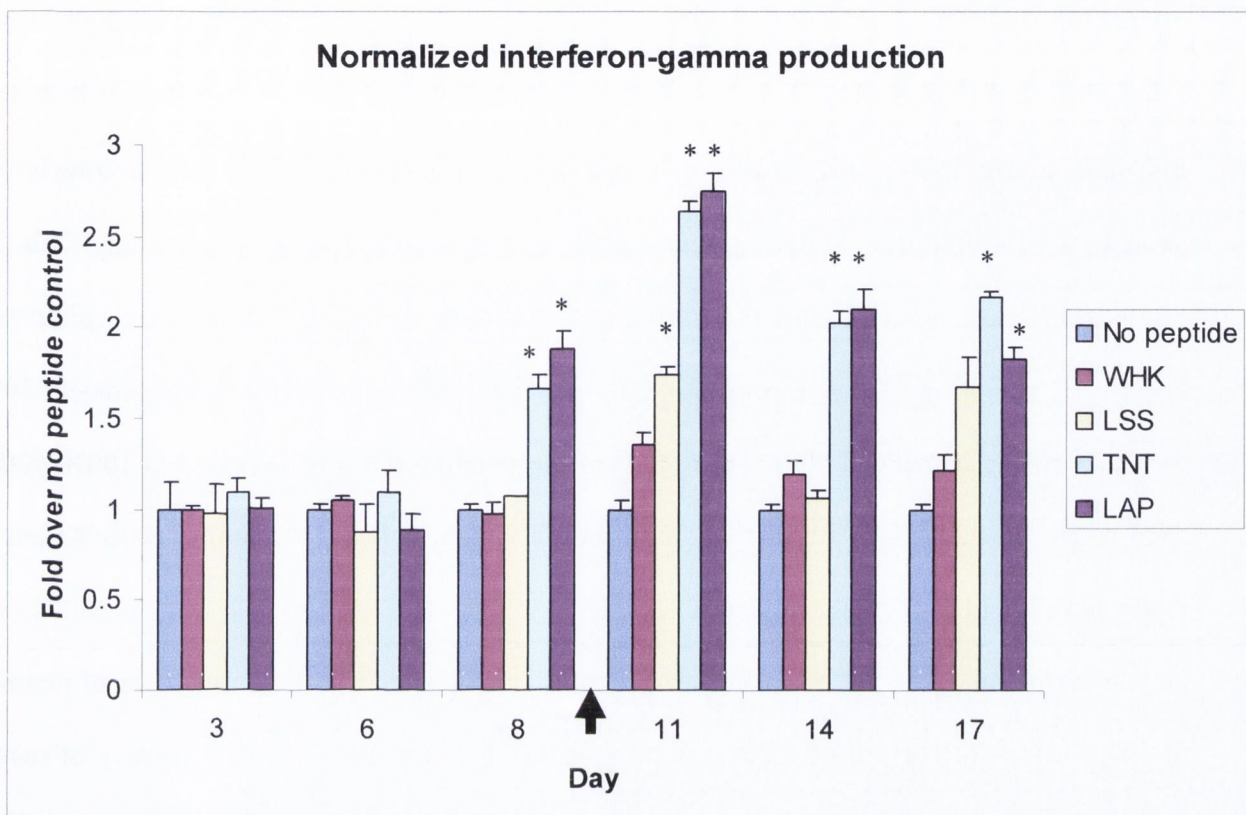
FIG. 5.9 Specific immune stimulatory activity of the mimic peptides.

Levels of interferon-γ produced were normalized to the respective no peptide control. Values are representative of triplicate samples. Standard deviation is indicated. Legend indicates the peptides loaded on the DC's. * indicates statistical significance (see Table 5.8 for P values). Arrow indicates the second round of stimulation with peptide-loaded DC's.

5.3 Discussion.

The aim of this work was to use the HSP70-PC recognizer peptides (AIP, SQE and cISTc) identified in the previous chapter to generate putative tumour antigen mimotopes using mirror image phage display. This was performed using two phage peptide display libraries, PhD-C7C and PhD-12, with the aim of comparing the effectiveness of the two libraries in the generation of mimotopes. Despite the insert loss experienced during the bio-panning with the PhD-C7C library, a set of enriched mimic peptides were identified. The first of which was LSSPVTY which was derived from the SQE recognizer. It was present in approximately 30% of phage clones sequenced after four rounds of bio-panning but this increased to 100% in the final round. In addition a number of small motifs which included the amino acids K and S were also evident in several sequences.

Bio-panning of the AIP recognizer peptide also resulted in the enrichment of peptide motifs. Strong enrichment of peptide sequences was hampered by a high frequency of insert loss during the experiment. Despite this, a number of recurring motifs were detected. The most abundant sequences were LQTPYRA and SNASIKA. These peptides were independently eluted with two different peptides (cSTLc and AIP) which share a common LNV motif, suggesting that this tripeptide motif may be important for binding to these two peptides. In addition two other motifs; TXYR and SXAXXK were observed.

Bio-panning of the cISTc recognizer peptide showed less enrichment after four rounds when compared to AIP and SQE. However notable sequence enrichment occurred after the total eight rounds. One sequence, TNTLSNN was present in 80% of clones sequenced. The only noticeable homology with sequences in round four is that of a dipeptide SN motif. The other final round sequence identified was LAPNQAA and it shared a PXQA motif with a peptide seen in round 4. The reason for the delay in sequence enrichment in this bio-panning

167

experiment is unclear, however it may have been affected by the smaller size and cyclic nature of the cISTc peptide. This indicates that more rounds of bio-panning are required when smaller peptides are used as the target.

Bio-panning with the PhD-12 phage library showed strong sequence enrichment in each experiment after just four rounds of selection. It was also interesting to observe that not one peptide insert was lost from the phage during this experiment, which is in stark contrast to the PhD-C7C. As the frequency of insert loss appears to increase per round during bio-panning with the PhD-C7C library, one explanation could be that there is an evolutionary disadvantage of expressing a foreign disulfide-constrained peptide on the phage surface. This may lead to spontaneous loss of the genetic information and phage without an insert may replicate at a much faster rate and ultimately out-compete those with an insert. The presence of a linear peptide on the phage surface may not exert the same kind of evolutionary stress, however the exact cause of this phenomenon remains to be seen. This observation doesn't appear to be reported in the literature, though specific bio-panning details are often not fully documented. In addition, there are not many documented cases of bio-panning experiments that were extended to the same number of rounds performed in this study.

One sequence, SVSVGMKPSPRP, was the most heavily enriched sequence in both the SQE and cISTc recognizer bio-panning experiments using the linear PhD-12 library. As SQE and cISTc were both identified by their ability to bind HSP70-PC's derived from MDA-MB-231 cells, it is theoretically possible that they could bind a similar target protein. However, in the previous chapter, the SQE and cISTc peptides showed differential binding to HSP70-PC's, cellular proteins and whole cells. Interestingly this exact sequence was previously identified in independent experiments in this lab as a putative tumour antigen mimic peptide derived from two different HSP70-PC recognizer peptides; NNYDDISLRARP and IERPLHESVLAT (Arnaiz et al., 2006).

The appearance of SVSVGMKPSPRP in numerous other different bio-panning experiments raises speculation about its specificity. It has previously been identified as binding to human cerebrospinal fluid antibodies and mouse monoclonal antibodies against lipo-oligosaccharide of *Neisseria* (Menendez and Scott, 2005), non-small cell lung carcinoma cells (Chang et al., 2009) and phosphatidyl serine (Deutscher, 2010). Perhaps the most notable identification is that by Lee et al (Lee et al., 2007) who identified the exact same sequence and documented specific *in vivo* homing of this peptide to human lung and oral tumour vasculature in xenograft models. In addition they coupled the peptide to liposomal doxorubicin and documented therapeutic efficacy. They propose that this peptide is a good candidate for clinical development. However due to the extremely diverse range of documented targets for this peptide, its clinical uses may be limited.

One other 12-mer peptide, KSLSRHDHIHHH, was also heavily enriched during the AIP and cISTc bio-panning experiments with the PhD-12 library. This sequence appears to be novel and it's possible that the AIP and cISTc peptides bind to a common target as they were both independently isolated by their ability to bind HSP70-PC's from the same cell line. The SCCHYSSQLTPS sequence was also uniquely identified in the cISTc bio-panning and could reflect a target specific to the cISTc peptide.

Due to time constraints only three mimic peptides (LSS, TNT and LAP) were chosen for further characterization and development but the novel 12-mer sequences and other constrained 7-mers identified here remain candidates for future development and analysis. Homology of these three mimic peptides to known proteins was examined using BLASTP in order to gain insight into their potential origins. The most significant hit with LSS was with a serine protease, whereas TNT showed the most homology to a protein involved in protein kinase activity and LAP had homology to a transcriptional repressor. However as mimotopes are very short sequences and are often conformational mimics of tumour antigens, it is not

169

possible to gain a confirmed identification using bio-informatics. It is interesting to note that the three mimic peptides are all neutral hydrophobic peptides, which corresponds with the type of peptides known to be preferentially bound by HSP70 (Flynn et al., 1991). As HSP70 is believed to transport peptides for presentation by MHC Class I, these mimic peptides fit the criteria for cell surface presentation.

The three lead mimic peptide sequences were chosen for synthesis and their cognate peptides were designed with a small C-terminal GG spacer. Each of the three mimic peptides showed specific interaction with their respective recognizer peptide as determined by incubating biotin-tagged SQE and cISTc with mimic peptide-coated magnetic beads. SQE showed 1.3-fold binding to LSS over unlinked beads and no binding to a control peptide. The cISTc recognizer showed over 4-fold more binding to TNT, 1.3-fold binding to LAP and no binding to a control peptide when compared to unlinked beads. As the mimic peptides demonstrated specific binding to their respective peptide, their ability to stimulate immune responses was examined.

Monocyte-derived DC's pulsed with each of the three mimic peptides showed activation of autologous T cells as determined by interferon-γ production. Both TNT and LAP showed a significant level of activity by day 8. Following a second stimulation with peptide-pulsed DC's a peak of significant T cell activity was seen for all three mimic peptides but not for the control peptide. This increase in T cell activity would be consistent with the clonal expansion of peptide-specific T cells. The effect of LSS appeared to decrease after this point, however both TNT and LAP caused a sustained increase in T cell activity.

The ability of the mimic peptides to stimulate T cell immune responses validates their definition as true mimotopes. The two strongest mimotopes were TNT and LAP, both of which were derived from the cISTc peptide. Future work should examine the ability of these mimotopes to stimulate immune responses using a larger number of human samples. This

170

could be followed by examination of the ability of the activated T cells to specifically kill tumour cells firstly *in vitro*, and subsequently in xenograft models.

Autologous vaccines hold promise for the future and the recent approval of Provenge, a vaccine based on DC presentation of prostatic acid phosphatase (PAP) for treatment of prostate cancer, is an indication of this. The approach described here could lead to two possible autologous cancer immunotherapies. Firstly the DC's could be matured, pulsed *ex vivo* with appropriate mimotopes and re-administered to the patient and secondly a portion of DC's could be used to activate T cells *ex vivo* allowing for clonal expansion and subsequent re-administration. Pre-conditioning of cancer patients for immunotherapy is currently coming into focus where, for example, chemotherapy is used to deplete Tregs prior to adoptive transfer of activated T cells or DC's, thereby allowing for a potent immune response (Mondino et al., 2010). In addition, DC's are excellent stimulators of the immune response and *ex vivo* maturation ensures that the DC's are driving immunity rather than tolerance when subsequently re-administered.

The overall result of this work was the generation of three novel breast tumour mimotopes; LSS, TNT and LAP, which have the ability to stimulate human immune responses *in vitro*. This early stage work provides indications that these mimotopes may be useful for future clinical use but warrant further investigation. In addition, the generation of the three mimotopes also validates the hypothesis that *in vitro* mirror image phage display can identify true mimotopes and thus this strategy can be applied further in the future for the generation of more potentially novel tumour mimotopes.

Chapter 6:

General discussion

The first aim of this project was to identify novel biomarkers that could preferentially or differentially bind breast tumour cells using phage-peptide display technology. Firstly, bio-panning was carried out on live breast cells *in vitro* which led to the identification of a number of highly selected peptides. A second approach combined *in vivo* and *in vitro* bio-panning with the aim of identifying peptides with tumour-homing abilities. A small set of peptides were reproducibly identified from these two bio-panning approaches, which had high affinity for the target cells but unfortunately did not demonstrate any tumour or tissue specificity. These results show that it was difficult to distinguish between the surface of tumour and non-tumour cells using whole cell bio-panning. The vast array of shared normal proteins on the cell surface is likely to contribute to the difficulty in identifying tumour antigens, especially if they are expressed at a lower level than other potentially abundant normal cell proteins. Stringent and repeated subtraction steps on multiple types of normal cells prior to each round of whole cell bio-panning on tumour cells or the use of isogenic tumour and non-tumour cells, may assist in the selection of a tumour-specific biomarker in future experimentation using the whole cell bio-panning approach.

It was also interesting to observe that the use of *in vivo* bio-panning did not contribute to the discovery of tumour specific biomarkers in this study. Indeed the same peptides were isolated in the *in vitro* bio-panning experiments, suggesting that *in vitro* experiments can reflect results achieved with *in vivo* studies. This would make a case for *in vitro* studies which would spare the use of animals, in addition to the time and expense associated with animal work.

The use of fluorescence to examine peptide specificity proved to be limited in its value. Fluorescent cell staining did provide an indication of an interaction between peptides and cells but this interaction was not quantifiable. Fluorescent cell staining showed no obvious differences between the binding affinities of the peptides, yet flow cytometry and

173

ELISA's showed measurable differences between the peptides tested. Fluorescent tissue staining was also problematic as tissue auto-fluorescence and photo-bleaching made it extremely difficult to assess the distribution of peptide staining in tissue samples. The use of the more conventional chemical dyes, such as DAB, proved to more reliable and provides clearer staining patterns with the benefit of long-term preservation of stained tissue samples.

The second strategy for the identification of novel tumour biomarkers involved bio-panning a group of purified cellular proteins known to chaperone tumour antigens (HSP70-PC's) when purified from tumour cells. In this case, phage-displayed peptides were selected based on their binding to the antigens present in tumour cell-derived HSP70-PC's. This led to the identification of a set of novel cysteine flanked 7-mer peptides termed "HSP70-PC recognizer peptides". Several of these peptides shared homology with previously identified 12-mer HSP70-PC recognizer peptides, demonstrating that the strategy of bio-panning tumour-derived HSP70-PC's can produce reproducible results. The HSP70-PC recognizer peptides bound to HSP70-PC's in a separate binding assay, however use of techniques such as surface plasmon resonance would improve the sensitivity of these peptide-protein binding assays.

One of the newly identified HSP70-PC recognizer peptides, cISTc, was tested for specificity on patient tumour tissues and appeared to localize in the same areas as HSP70 in two breast tumour samples but this was less evident in other tumour tissues. The difference between the distribution of cellular staining between cISTc and HSP70 indicates that cISTc may potentially be useful as a breast tumour biomarker. It also suggests that HSP70 present in other organ tissues and tumours may be associated with different antigens. The distribution of the cISTc peptide in a larger set of tissue samples including normal breast tissues, in addition to other matched tumour and normal organ tissues, could provide definitive indications of the specificity and potential use of this peptide as a breast tumour biomarker or homing molecule.

The distribution pattern of HSP70 within patient tumour tissues was in itself interesting. Usually considered a ubiquitous protein, its over-expression in many tumours is placing HSP70 in the limelight as a potential tumour biomarker. Aberrant expression of members of the HSP70 family of proteins on tumour cell surfaces is being increasingly detected in several cancers and so examination of HSP70 distribution within patient tumours may become a useful diagnostic tool. Indeed there were interesting patterns of staining in the small sample set examined in this study.

Identification of the cellular binding target of the cISTc peptide would also provide invaluable information regarding the nature of the target tumour antigen. Protein pull-down experiments performed here provided some interesting results as to the potential binding partner, which included GRP78, a member of the HSP70 family of proteins. Drawbacks of the approach include the need for high quantities of cellular proteins, in addition to the fact that the exact identity of the target protein can be masked by the presence of a complex of proteins pulled down by the peptide. Therefore future work could employ cDNA expression libraries to try and identify the specific target protein and this could be subsequently confirmed by protein expression and knock-down studies. The results from these experiments indicate that bio-panning of tumour-derived HSP70-PC's is a more successful approach in the identification of specific tumour biomarkers than whole cell bio-panning.

Three HSP70-PC recognizer peptides were used in the generation of putative tumour antigen mimic peptides using "mirror-image phage display". This technique aims to generate mimic peptides without prior knowledge of the tumour antigen and without the requirement of monoclonal antibodies. The hypothesis is that peptides capable of binding the HSP70-PC recognizer peptides could be structural mimics of the original antigens. Two phage libraries were used during mimic peptide development; the PhD-C7C phage library, which was used throughout this study, and the PhD-12 library. Bio-panning with the PhD-C7C phage library

175

led to the identification of mimic peptides which demonstrated more target specificity than peptides identified with the PhD-12 library. However there were some drawbacks associated with the PhD-C7C library which included loss of peptide inserts from the phage in successive rounds of bio-panning, coupled with the need for an increased number of bio-panning rounds to identify enriched peptide sequences. It was also discovered that bio-panning using smaller peptides as a target requires more rounds of selection to obtain sequence enrichment. Despite these drawbacks a number of putative cysteine flanked 7-mer mimic peptides were identified and three were tested for their ability to stimulate human immune responses.

Human monocyte-derived DC's loaded with the mimic peptides; TNT, LAP and LSS, were capable of activating autologous T cells *in vitro*. This demonstrated that the newly identified mimic peptides were true "mimotopes" capable of stimulating human immune responses. Therefore this cost-effective mirror image phage display technique could be useful for the future identification of more novel tumour mimotopes. Future work could examine the immuno-stimulatory ability of the mimotopes using cells from a larger range of healthy individuals and also cancer patients, in addition to analyzing the ability of any activated immune cells to target and kill tumour cells *in vitro*. Both mimotopes and DC's have demonstrated low toxicity in early clinical trials, therefore if positive results are achieved with a comprehensive set of further *in vitro* immune assays, they may be suitable candidates for use in a phase I clinical trial for the treatment and prevention of breast cancer. As DC's can stimulate both B and T cell responses, patient immune responses to mimotope-pulsed DC's could be measured by the presence of antigen-specific antibodies and T cells. DC-vaccine efficacy can be evaluated by measurement of antigen-specific immune activity, reduction of tumour burden or increases in disease-free survival in cancer patients.

In summary, the overall results of this project were;

- The identification of peptides with the potential for use as breast tumour biomarkers or breast tumour-homing molecules.

- The generation of breast tumour mimotopes which warrant further investigation for possible use in future cancer immunotherapy.

- The validation of mirror-image phage display with tumour-derived HSP70-PC's as a technique for identifying novel tumour mimotopes.

References

Aina, O., Liu, R., Sutcliffe, J., Marik, J., Pan, C., and Lam, K. (2007). From combinatorial chemistry to cancer-targeting peptides. Molecular pharmaceutics *4*, 631-651.

Akalu, A., Roth, J., Caunt, M., Policarpio, D., Liebes, L., and Brooks, P. (2007). Inhibition of angiogenesis and tumor metastasis by targeting a matrix immobilized cryptic extracellular matrix epitope in laminin. Cancer research *67*, 4353-63.

Alessi, P., Ebbinghaus, C., and Neri, D. (2004). Molecular targeting of angiogenesis. Biochimica et Biophysica Acta (BBA) - Reviews on Cancer *1654*, 39-49.

Altschul, S.F., Madden, T.L., Schaffer, A.A., Zhang, J., Zhang, Z., Miller, W., and Lipman, D.J. (1997). Gapped BLAST and PSI-BLAST: a new generation of protein database search programs. Nucl. Acids Res. *25*, 3389-3402.

Anand, P., Kunnumakkara, A.B., Sundaram, C., Harikumar, K.B., Tharakan, S.T., Lai, O.S., Sung, B., and Aggarwal, B.B. (2008). Cancer is a preventable disease that requires major lifestyle changes. Pharm Res *25*, 2097-2116.

Anderson, K.S. (2009). Tumor vaccines for breast cancer. Cancer Invest *27*, 361-368.

Apostolopoulos, V., Pietersz, G.A., Tsibanis, A., Tsikkinis, A., Drakaki, H., Loveland, B.E., Piddlesden, S.J., Plebanski, M., Pouniotis, D.S., Alexis, M.N., *et al.* (2006). Pilot phase III immunotherapy study in early-stage breast cancer patients using oxidized mannan-MUC1 [ISRCTN71711835]. Breast Cancer Res *8*, R27.

Arap, W., Kolonin, M., Trepel, M., Lahdenranta, J., Cardó-Vila, M., Giordano, R., Mintz, P., Ardelt, P., Yao, V., and Vidal, C. (2002). Steps toward mapping the human vasculature by phage display. Nature medicine *8*, 121-127.

179

Arnaiz, B., Madrigal-Estebas, L., Todryk, S., James, T., Doherty, D., and Bond, U. (2006). A novel method to identify and characterise peptide mimotopes of heat shock protein 70-associated antigens. Journal of Immune Based Therapies and Vaccines *4*, 2.

Barth, R.J., Jr., Fischer, D.A., Wallace, P.K., Channon, J.Y., Noelle, R., Gui, J., and Ernstoff, M.S. (2010). A randomized trial of ex vivo CD40L activation of a DC vaccine in colorectal cancer patients: tumor-specific immune responses are associated with improved survival. Clin Cancer Res *16*, 5548-5556.

Battey, J., Moulding, C., Taub, R., Murphy, W., Stewart, T., Potter, H., Lenoir, G., and Leder, P. (1983). The human c-myc oncogene: Structural consequences of translocation into the igh locus in Burkitt lymphoma. Cell *34*, 779-787.

Brenner, M.K., and Heslop, H.E. (2010). Adoptive T cell therapy of cancer. Current Opinion in Immunology *22*, 251-257.

Calderwood, S.K. (2010). Heat shock proteins in breast cancer progression–A suitable case for treatment? International Journal of Hyperthermia *26*, 681-685.

Cartellieri, M., Bachmann, M., Feldmann, A., Bippes, C., Stamova, S., Wehner, R., Temme, A., and Schmitz, M. (2010). Chimeric antigen receptor-engineered T cells for immunotherapy of cancer. J Biomed Biotechnol *2010*, 956304.

Chang, D.-K., Lin, C.-T., Wu, C.-H., and Wu, H.-C. (2009). A Novel Peptide Enhances Therapeutic Efficacy of Liposomal Anti-Cancer Drugs in Mice Models of Human Lung Cancer. PLoS ONE *4*, e4171.

Chen, T., and Cao, X. (2010). Stress for maintaining memory: HSP70 as a mobile messenger for innate and adaptive immunity. European Journal of Immunology *40*, 1541-1544.

Chen, Y.-T., Scanlan, M.J., Sahin, U., Türeci, Ö., Gure, A.O., Tsang, S., Williamson, B., Stockert, E., Pfreundschuh, M., and Old, L.J. (1997). A testicular antigen aberrantly expressed in human cancers detected by autologous antibody screening. Proceedings of the National Academy of Sciences *94*, 1914-1918.

Cheng, W., and Allen, T. (2010). The use of single chain Fv as targeting agents for immunoliposomes: an update on immunoliposomal drugs for cancer treatment. Expert Opinion on Drug Delivery *7*, 461-478.

Classon, M., and Harlow, E. (2002). The retinoblastoma tumour suppressor in development and cancer. Nat Rev Cancer *2*, 910-917.

Croce, C.M. (2008). Oncogenes and Cancer. New England Journal of Medicine *358*, 502-511.

Danielczyk, A., Stahn, R., Faulstich, D., Löffler, A., Märten, A., Karsten, U., and Goletz, S. (2006). PankoMab: a potent new generation anti-tumour MUC1 antibody. Cancer Immunology, Immunotherapy *55*, 1337-1347.

de Cerio, A.L.-D., Zabalegui, N., Rodriguez-Calvillo, M., Inoges, S., and Bendandi, M. (2007). Anti-idiotype antibodies in cancer treatment. Oncogene *26*, 3594-3602.

de Martel, C., and Franceschi, S. (2009). Infections and cancer: Established associations and new hypotheses. Critical Reviews in Oncology/Hematology *70*, 183-194.

Desmetz, C., Cortijo, C., Mangé, A., and Solassol, J. (2009). Humoral response to cancer as a tool for biomarker discovery. Journal of Proteomics *72*, 982-988.

Deutscher, S.L. (2010). Phage display in molecular imaging and diagnosis of cancer. Chem Rev *110*, 3196-3211.

Ding, L., Ellis, M.J., Li, S., Larson, D.E., Chen, K., Wallis, J.W., Harris, C.C., McLellan, M.D., Fulton, R.S., Fulton, L.L., *et al.* (2010). Genome remodelling in a basal-like breast cancer metastasis and xenograft. Nature *464*, 999-1005.

Dunn, G.P., Koebel, C.M., and Schreiber, R.D. (2006). Interferons, immunity and cancer immunoediting. Nat Rev Immunol *6*, 836-848.

Dunn, G.P., Old, L.J., and Schreiber, R.D. (2004). The three Es of cancer immunoediting. Annu Rev Immunol *22*, 329-360.

Eton, O., Ross, M., East, M., Mansfield, P., Papadopoulos, N., Ellerhorst, J., Bedikian, A., and Lee, J. (2010). Autologous tumor-derived heat-shock protein peptide complex-96 (HSPPC-96) in patients with metastatic melanoma. Journal of Translational Medicine *8*, 9.

Evans, C.G., Chang, L., and Gestwicki, J.E. (2010). Heat shock protein 70 (hsp70) as an emerging drug target. J Med Chem *53*, 4585-4602.

Finn, O.J. (2008). Cancer Immunology. New England Journal of Medicine *358*, 2704-2715.

Flynn, G.C., Pohl, J., Flocco, M.T., and Rothman, J.E. (1991). Peptide-binding specificity of the molecular chaperone BiP. Nature *353*, 726-730.

Fong, L., and Engleman, E.G. (2000). Dendritic cells in cancer immunotherapy. Annu Rev Immunol *18*, 245-273.

Foon, K.A., and Bhattacharya-Chatterjee, M. (2001). Are Solid Tumor Anti-Idiotype Vaccines Ready for Prime Time? Clinical Cancer Research *7*, 1112-1115.

Galluzzi, L., Giordanetto, F., and Kroemer, G. (2009). Targeting HSP70 for Cancer Therapy. Molecular Cell *36*, 176-177.

Gonzalez, V., and Hurley, L.H. (2010). The c-MYC NHE III(1): function and regulation. Annu Rev Pharmacol Toxicol *50*, 111-129.

Green, D.R., and Kroemer, G. (2009). Cytoplasmic functions of the tumour suppressor p53. Nature *458*, 1127-1130.

Higano, C.S., Schellhammer, P.F., Small, E.J., Burch, P.A., Nemunaitis, J., Yuh, L., Provost, N., and Frohlich, M.W. (2009). Integrated data from 2 randomized, double-blind, placebo-controlled, phase 3 trials of active cellular immunotherapy with sipuleucel-T in advanced prostate cancer. Cancer *115*, 3670-3679.

Hudson, M.E., Pozdnyakova, I., Haines, K., Mor, G., and Snyder, M. (2007). Identification of differentially expressed proteins in ovarian cancer using high-density protein microarrays. Proceedings of the National Academy of Sciences *104*, 17494-17499.

Hunder, N.N., Wallen, H., Cao, J., Hendricks, D.W., Reilly, J.Z., Rodmyre, R., Jungbluth, A., Gnjatic, S., Thompson, J.A., and Yee, C. (2008). Treatment of Metastatic Melanoma with Autologous CD4+ T Cells against NY-ESO-1. New England Journal of Medicine *358*, 2698-2703.

Jakobsen, C.G., Rasmussen, N., Laenkholm, A.-V., and Ditzel, H.J. (2007). Phage Display–Derived Human Monoclonal Antibodies Isolated by Binding to the Surface of Live Primary Breast Cancer Cells Recognize GRP78. Cancer research *67*, 9507-9517.

183

Jerne, N.K. (1974). Towards a network theory of the immune system. Ann Immunol (Paris) *125C*, 373-389.

Jiang, B., Liu, W., Qu, H., Meng, L., Song, S., Ouyang, T., and Shou, C. (2005). A Novel Peptide Isolated from a Phage Display Peptide Library with Trastuzumab Can Mimic Antigen Epitope of HER-2. Journal of Biological Chemistry *280*, 4656-4662.

Kamal, M., Shaaban, A., Zhang, L., Walker, C., Gray, S., Thakker, N., Toomes, C., Speirs, V., and Bell, S. (2010). Loss of CSMD1 expression is associated with high tumour grade and poor survival in invasive ductal breast carcinoma. Breast Cancer Research and Treatment *121*, 555-563.

Kim, Y., Lillo, A.M., Steiniger, S.C.J., Liu, Y., Ballatore, C., Anichini, A., Mortarini, R., Kaufmann, G.F., Zhou, B., Felding-Habermann, B., and Janda, K.D. (2006). Targeting Heat Shock Proteins on Cancer Cells: Selection, Characterization, and Cell-Penetrating Properties of a Peptidic GRP78 Ligand†. Biochemistry *45*, 9434-9444.

Knittelfelder, R., Riemer, A.B., and Jensen-Jarolim, E. (2009). Mimotope vaccination – from allergy to cancer. Expert Opinion on Biological Therapy *9*, 493-506.

Krag, D., Shukla, G., Shen, G., Pero, S., Ashikaga, T., Fuller, S., Weaver, D., Burdette-Radoux, S., and Thomas, C. (2006). Selection of tumor-binding ligands in cancer patients with phage display libraries. Cancer research *66*, 7724-7733.

Kruser, T.J., and Wheeler, D.L. (2010). Mechanisms of resistance to HER family targeting antibodies. Experimental Cell Research *316*, 1083-1100.

Laakkonen, P., Åkerman, M.E., Biliran, H., Yang, M., Ferrer, F., Karpanen, T., Hoffman, R.M., and Ruoslahti, E. (2004). Antitumor activity of a homing peptide that targets tumor lymphatics and tumor cells. PNAS *101*, 9381-9386.

Laakkonen, P., and Vuorinen, K. (2010). Homing peptides as targeted delivery vehicles. Integr Biol (Camb) *2*, 326-337.

Lee, A.S. (2007). GRP78 Induction in Cancer: Therapeutic and Prognostic Implications. Cancer research *67*, 3496-3499.

Lee, S., Xie, J., and Chen, X. (2010). Peptide-Based Probes for Targeted Molecular Imaging. Biochemistry *49*, 1364-1376.

Lee, T.Y., Lin, C.T., Kuo, S.Y., Chang, D.K., and Wu, H.C. (2007). Peptide-mediated targeting to tumor blood vessels of lung cancer for drug delivery. Cancer Res *67*, 10958-10965.

Lemmel, C., and Stevanovic, S. (2003). The use of HPLC-MS in T-cell epitope identification. Methods *29*, 248-259.

Levey, D. (2008). Outlining the Gap Between Preclinical Models and Clinical Situation. In Cancer Vaccines: Challenges and Opportunities in Translation, A. Bot, Obrocea, M., ed. (Informa HealthCare).

Liu, L., Wang, S., Shan, B., Sang, M., Liu, S., and Wang, G. (2010). Advances in viral-vector systemic cytokine gene therapy against cancer. Vaccine *28*, 3883-3887.

Lu, B., and Finn, O.J. (2007). T-cell death and cancer immune tolerance. Cell Death Differ *15*, 70-79.

185

MacDonald, T.J., Stewart, C.F., Kocak, M., Goldman, S., Ellenbogen, R.G., Phillips, P., Lafond, D., Poussaint, T.Y., Kieran, M.W., Boyett, J.M., and Kun, L.E. (2008). Phase I Clinical Trial of Cilengitide in Children With Refractory Brain Tumors: Pediatric Brain Tumor Consortium Study PBTC-012. Journal of Clinical Oncology *26*, 919-924.

McCormick, A.A., Reddy, S., Reinl, S.J., Cameron, T.I., Czerwinkski, D.K., Vojdani, F., Hanley, K.M., Garger, S.J., White, E.L., Novak, J., *et al.* (2008). Plant-produced idiotype vaccines for the treatment of non-Hodgkin's lymphoma: Safety and immunogenicity in a phase I clinical study. Proceedings of the National Academy of Sciences *105*, 10131-10136.

Menendez, A., and Scott, J.K. (2005). The nature of target-unrelated peptides recovered in the screening of phage-displayed random peptide libraries with antibodies. Anal Biochem *336*, 145-157.

Mittendorf, E.A., Peoples, G.E., and Singletary, S.E. (2007). Breast cancer vaccines. Cancer *110*, 1677-1686.

Mocellin, S., Mandruzzato, S., Bronte, V., Lise, M., and Nitti, D. (2004). Part I: Vaccines for solid tumours. The Lancet Oncology *5*, 681-689.

Moelans, C.B., de Weger, R.A., Monsuur, H.N., Vijzelaar, R., and van Diest, P.J. (2010). Molecular profiling of invasive breast cancer by multiplex ligation-dependent probe amplification-based copy number analysis of tumor suppressor and oncogenes. Mod Pathol *23*, 1029-1039.

Mondino, A., Dardalhon, V., Michelini, R.H., Loisel-Meyer, S., and Taylor, N. (2010). Redirecting the immune response: role of adoptive T cell therapy. Hum Gene Ther *21*, 533-541.

NCRI (2009). Cancer mortality 2006. In Cancer in Ireland 1994-2007 (National Cancer Registry Ireland).

O'Day, E., and Lal, A. (2010). MicroRNAs and their target gene networks in breast cancer. Breast Cancer Research *12*, 201.

O'Donovan, P.J., and Livingston, D.M. (2010). BRCA1 and BRCA2: breast/ovarian cancer susceptibility gene products and participants in DNA double-strand break repair. Carcinogenesis *31*, 961-967.

O'Neill, D., and Bhardwaj, N. (2005). Exploiting dendritic cells for active immunotherapy of cancer and chronic infection. Methods Mol Med *109*, 1-18.

Pagano, J.S., Blaser, M., Buendia, M.-A., Damania, B., Khalili, K., Raab-Traub, N., and Roizman, B. (2004). Infectious agents and cancer: criteria for a causal relation. Seminars in Cancer Biology *14*, 453-471.

Palucka, A.K., Ueno, H., Fay, J.W., and Banchereau, J. (2010). LPS-activated dendritic cell vaccine in combination with immunomodulatory dose of cytoxan in patients with stage IV melanoma: Phase I/IIa clinical trial. J Clin Oncol (Meeting Abstracts) *28*, TPS313-.

Pasqualini, R., Arap, W., and McDonald, D.M. (2002). Probing the structural and molecular diversity of tumor vasculature. Trends in Molecular Medicine *8*, 563-571.

Pasqualini, R., and Ruoslahti, E. (1996). Organ targeting In vivo using phage display peptide libraries. Nature *380*, 364-366.

187

Patel, L.R., and Simons, J.W. (2010). GM-CSF Gene-Transduced Prostate Cancer Vaccines: GVAX. In Drug Management of Prostate Cancer, W.D. Figg, C.H. Chau, and E.J. Small, eds. (Springer New York), pp. 329-342.

Patil, R., Clifton, G.T., Holmes, J.P., Amin, A., Carmichael, M.G., Gates, J.D., Benavides, L.H., Hueman, M.T., Ponniah, S., and Peoples, G.E. (2010). Clinical and Immunologic Responses of HLA-A3+ Breast Cancer Patients Vaccinated with the HER2/neu-Derived Peptide Vaccine, E75, in a Phase I/II Clinical Trial. Journal of the American College of Surgeons *210*, 140-147.

Pejawar-Gaddy, S., and Finn, O.J. (2008). Cancer vaccines: Accomplishments and challenges. Critical Reviews in Oncology/Hematology *67*, 93-102.

Perales, M.-A., Yuan, J., Powel, S., Gallardo, H.F., Rasalan, T.S., Gonzalez, C., Manukian, G., Wang, J., Zhang, Y., Chapman, P.B., *et al.* (2008). Phase I/II Study of GM-CSF DNA as an Adjuvant for a Multipeptide Cancer Vaccine in Patients With Advanced Melanoma. Mol Ther *16*, 2022-2029.

Perosa, F., Favoino, E., Vicenti, C., Merchionne, F., and Dammacco, F. (2007). Identification of an Antigenic and Immunogenic Motif Expressed by Two 7-Mer Rituximab-Specific Cyclic Peptide Mimotopes: Implication for Peptide-Based Active Immunotherapy. J Immunol *179*, 7967-7974.

Pleasance, E.D., Cheetham, R.K., Stephens, P.J., McBride, D.J., Humphray, S.J., Greenman, C.D., Varela, I., Lin, M.-L., Ordóñez, G.R., Bignell, G.R., *et al.* (2009). A comprehensive catalogue of somatic mutations from a human cancer genome. Nature *463*, 191-6.

Przepiorka, D., and Srivastava, P.K. (1998). Heat shock protein-peptide complexes as immunotherapy for human cancer. Molecular Medicine Today *4*, 478-484.

Raina, D., Ahmad, R., Joshi, M.D., Yin, L., Wu, Z., Kawano, T., Vasir, B., Avigan, D., Kharbanda, S., and Kufe, D. (2009). Direct Targeting of the Mucin 1 Oncoprotein Blocks Survival and Tumorigenicity of Human Breast Carcinoma Cells. Cancer research *69*, 5133-5141.

Rammensee, H., Bachmann, J., Emmerich, N.P., Bachor, O.A., and Stevanovic, S. (1999). SYFPEITHI: database for MHC ligands and peptide motifs. Immunogenetics *50*, 213-219.

Rasmussen, U., Schreiber, V., Schultz, H., Mischler, F., and Schughart, K. (2002). Tumor cell-targeting by phage-displayed peptides. Cancer gene therapy *9*, 606-12.

Reichardt, V.L., Brossart, P., and Kanz, L. (2004). Dendritic cells in vaccination therapies of human malignant disease. Blood Rev *18*, 235-243.

Renkvist, N., Castelli, C., Robbins, P.F., and Parmiani, G. (2001). A listing of human tumor antigens recognized by T cells. Cancer Immunology, Immunotherapy *50*, 3-15.

Reuschenbach, M., von Knebel Doeberitz, M., and Wentzensen, N. (2009). A systematic review of humoral immune responses against tumor antigens. Cancer Immunology, Immunotherapy *58*, 1535-1544.

Riemer, A.B., and Jensen-Jarolim, E. (2007). Mimotope vaccines: Epitope mimics induce anti-cancer antibodies. Immunology Letters *113*, 1-5.

Riemer, A.B., Klinger, M., Wagner, S., Bernhaus, A., Mazzucchelli, L., Pehamberger, H., Scheiner, O., Zielinski, C.C., and Jensen-Jarolim, E. (2004). Generation of Peptide Mimics of the Epitope Recognized by Trastuzumab on the Oncogenic Protein Her-2/neu. J Immunol *173*, 394-401.

Ruoslahti, E. (2002). Drug targeting to specific vascular sites. Drug Discovery Today *7*, 1138-1143.

Sabbatini, P., Berek, J.S., Casado, A., Cwiertka, K., Pinter, T., Pluzanska, A., Scambia, G., Pujade-Lauraine, E., Vermorken, J.B., and Pfisterer, J. (2010). Abagovomab maintenance therapy in patients with epithelial ovarian cancer after complete response (CR) post-first-line chemotherapy (FLCT): Preliminary results of the randomized, double-blind, placebo-controlled, multicenter MIMOSA trial. J Clin Oncol (Meeting Abstracts) *28*, 5036-.

Santoro, A., Pressiani, T., Citterio, G., Rossoni, G., Donadoni, G., Pozzi, F., Rimassa, L., Personeni, N., Bozzarelli, S., Colombi, S., *et al.* (2010). Activity and safety of NGR-hTNF, a selective vascular-targeting agent, in previously treated patients with advanced hepatocellular carcinoma. Br J Cancer *103*, 837-844.

Schliemann, C., and Neri, D. (2007). Antibody-based targeting of the tumor vasculature. Biochimica et Biophysica Acta (BBA) - Reviews on Cancer *1776*, 175-192.

Schlotter, C., Vogt, U., Allgayer, H., and Brandt, B. (2008). Molecular targeted therapies for breast cancer treatment. Breast Cancer Research *10*, 211.

Schreiber, R.D. (2005). Cancer vaccines 2004 opening address: the molecular and cellular basis of cancer immunosurveillance and immunoediting. Cancer Immun *5 Suppl 1*, 1.

Schroter, S., Minev, B. (2008). Peptide-Based Active Immunotherapy in Cancer. In Cancer Vaccines: Challenges and Opportunities in Translation, A. Bot, Obrocea, M., ed. (Informa HealthCare).

Sergeeva, A., Kolonin, M.G., Molldrem, J.J., Pasqualini, R., and Arap, W. (2006). Display technologies: Application for the discovery of drug and gene delivery agents. Advanced Drug Delivery Reviews *58*, 1622-1654.

Shadidi, M., and Sioud, M. (2003). Selective targeting of cancer cells using synthetic peptides. Drug resistance updates: reviews and commentaries in antimicrobial and anticancer chemotherapy *6*, 363.

Sharma, S., Tammela, J., Wang, X., Arnouk, H., Driscoll, D., Mhawech-Fauceglia, P., Lele, S., Kazim, A.L., and Odunsi, K. (2007). Characterization of a Putative Ovarian Oncogene, Elongation Factor 1α, Isolated by Panning a Synthetic Phage Display Single-Chain Variable Fragment Library with Cultured Human Ovarian Cancer Cells. Clinical Cancer Research *13*, 5889-5896.

Shi, L., Sings, H.L., Bryan, J.T., Wang, B., Wang, Y., Mach, H., Kosinski, M., Washabaugh, M.W., Sitrin, R., and Barr, E. (2007). GARDASIL[reg]: Prophylactic Human Papillomavirus Vaccine Development - From Bench Top to Bed-side. Clin Pharmacol Ther *81*, 259-264.

Shiku, H., Takahashi, T., Resnick, L.A., Oettgen, H.F., and Old, L.J. (1977). Cell surface antigens of human malignant melanoma. III. Recognition of autoantibodies with unusual characteristics. The Journal of Experimental Medicine *145*, 784-789.

Silvera, D., Formenti, S.C., and Schneider, R.J. (2010). Translational control in cancer. Nat Rev Cancer *10*, 254-266.

191

Simons, J.W., and Sacks, N. (2006). Granulocyte-macrophage colony-stimulating factor-transduced allogeneic cancer cellular immunotherapy: The GVAX® vaccine for prostate cancer. Urologic Oncology: Seminars and Original Investigations *24*, 419-424.

Smith, G.P. (1985). Filamentous fusion phage: Novel expression vectors that display cloned antigens on the virion surface. Science *228*, 1315-1317.

Soruri, A., and Zwirner, J. (2005). Dendritic cells: limited potential in immunotherapy. The International Journal of Biochemistry & Cell Biology *37*, 241-245.

Srinivasan, R. (2008). Therapeutic and Prophylactic Cancer Vaccines: Emerging Perspectives from Allogeneic and Infectious Disease Vaccines. In Cancer Vaccines: Challenges and Opportunities in Translation, A. Bot, Obrocea, M., ed. (Informa HealthCare).

Srivastava, P. (2002). Interaction of heat shock proteins with peptides and antigen presenting cells: chaperoning of the innate and adaptive immune responses. Annu Rev Immunol *20*, 395-425.

Srivastava, P.K. (1997). Purification of Heat Shock Protein-Peptide Complexes for Use in Vaccination against Cancers and Intracellular Pathogens. Methods *12*, 165-171.

Srivastava, P.K., Callahan, M.K., and Mauri, M.M. (2009). Treating human cancers with heat shock protein-peptide complexes: the road ahead. Expert Opinion on Biological Therapy *9*, 179-186.

Srivastava, P.K., Menoret, A., Basu, S., Binder, R.J., and McQuade, K.L. (1998). Heat shock proteins come of age: primitive functions acquire new roles in an adaptive world. Immunity *8*, 657-665.

Staneloudi, C., Smith, K.A., Hudson, R., Malatesti, N., Savoie, H., Boyle, R.W., and Greenman, J. (2007). Development and characterization of novel photosensitizer : scFv conjugates for use in photodynamic therapy of cancer. Immunology *120*, 512-517.

Steinman, R.M., and Banchereau, J. (2007). Taking dendritic cells into medicine. Nature *449*, 419-426.

Stevenson, F.K., Ottensmeier, C.H., and Rice, J. (2010). DNA vaccines against cancer come of age. Current Opinion in Immunology *22*, 264-270.

Tamura, Y., Peng, P., Liu, K., Daou, M., and Srivastava, P.K. (1997). Immunotherapy of Tumors with Autologous Tumor-Derived Heat Shock Protein Preparations. Science *278*, 117-120.

Tan, H.T., Low, J., Lim, S.G., and Chung, M.C.M. (2009). Serum autoantibodies as biomarkers for early cancer detection. FEBS Journal *276*, 6880-6904.

Taylor, C., Hershman, D., Shah, N., Suciu-Foca, N., Petrylak, D.P., Taub, R., Vahdat, L., Cheng, B., Pegram, M., Knutson, K.L., and Clynes, R. (2007). Augmented HER-2–Specific Immunity during Treatment with Trastuzumab and Chemotherapy. Clinical Cancer Research *13*, 5133-5143.

Trepel, M., Arap, W., and Pasqualini, R. (2002). In vivo phage display and vascular heterogeneity: implications for targeted medicine. Current Opinion in Chemical Biology *6*, 399-404.

van der Bruggen, P., Traversari, C., Chomez, P., Lurquin, C., De Plaen, E., Van den Eynde, B., Knuth, A., and Boon, T. (1991). A gene encoding an antigen recognized by cytolytic T lymphocytes on a human melanoma. Science *254*, 1643-1647.

Weiner, L.M., Dhodapkar, M.V., and Ferrone, S. (2009). Monoclonal antibodies for cancer immunotherapy. The Lancet *373*, 1033-1040.

Welcker, M., and Clurman, B.E. (2008). FBW7 ubiquitin ligase: a tumour suppressor at the crossroads of cell division, growth and differentiation. Nat Rev Cancer *8*, 83-93.

WHO (2009). Global burden of cancer. In Fact sheet No. 297 (World Health Organization).

Wu, A.M., and Senter, P.D. (2005). Arming antibodies: prospects and challenges for immunoconjugates. Nat Biotech *23*, 1137-1146.

Yee, C., Thompson, J.A., Byrd, D., Riddell, S.R., Roche, P., Celis, E., and Greenberg, P.D. (2002). Adoptive T cell therapy using antigen-specific CD8+ T cell clones for the treatment of patients with metastatic melanoma: In vivo persistence, migration, and antitumor effect of transferred T cells. Proceedings of the National Academy of Sciences of the United States of America *99*, 16168-16173.

Zhang, L., Giraudo, E., Hoffman, J.A., Hanahan, D., and Ruoslahti, E. (2006). Lymphatic Zip Codes in Premalignant Lesions and Tumors. Cancer research *66*, 5696-5706.

Zhang, L., Pan, X., and Hershey, J.W.B. (2007). Individual Overexpression of Five Subunits of Human Translation Initiation Factor eIF3 Promotes Malignant Transformation of Immortal Fibroblast Cells. Journal of Biological Chemistry *282*, 5790-5800.